X-LINKED CHARCOT-MARIE-TOOTH NEUROPATHY: MUTATION AND HAPLOTYPE ANALYSES

by

İrem Akat

B.S., Molecular Biology and Genetics, Boğaziçi University, 2007

Submitted to the Institute for Graduate Studies in
Science and Engineering in partial fulfillment of
the requirements for the degree of
Master of Science

Graduate Program in Molecular Biology and Genetics
Boğaziçi University
2009

For my mother Şükran Akat,
No one has ever been given more loving and
unconditional support than I have been given by you

ACKNOWLEDGEMENTS

I would like to express my sincere gratitude to Associate Professor Esra Battaloglu for her invaluable guidance and help during the preparation of this thesis. I would like to mention her supportive attitude and unlimited encouragement during my study. I would also like to thank my thesis committe members Professor Hande Caglayan and Professor Yesim Parman for giving their time to evaluate my work and their valuable advices.

I would like to express my special thanks to Professor Garth Nicholson and Dr. Marina Kennerson for giving me the opportunity to be a part of Anzac Research Institute and making me fell like one of their own students. I would also like to mention their invaluable trust, encouragement, guidance, patience and inspiration. I would also like to express my sincere gratitude to Endeavour Awards, Australian Scholarships for providing support to study in Australia.

A special thank to my friends in CMT laboratory; Duygu Daglıkoca and Burcak Ozes for helping and advising me whenever I needed. I would like to extend my thanks to all my friends in MBG expecially, Melek Aslı Kayserili, Ibrahim Barıs, Cigdem Atay, Neslihan Zohrap, Mahmutcan Hız, Gamze Kuser, Yeliz Yılmaz Sert, and Funda Ejder.

Love, kisses and gratitude to my friends in Northcort Neuroscience laboratory; Megan Brewer, Rabia Chaudhry, Kelly Williams, Jennifer Solski, Shu Yang, Alexander Drew, Shannon Chu, Shajjia Razi, Sadaf Warraich and Obaid Albulym for making my great Sydney experience even more greater and creating a lovely working environment for me.

So much love and thanks to Hamdi Kul, for his insane understanding, continuing moral support and providing worth of inspiration. I know nothing would be possible without him.

Last, but not the least, I would like to give an ocean of thanks to my family and my awesome sister Gizem Akat for their incomparable love and support.

ABSTRACT

X-LINKED CHARCOT-MARIE-TOOTH NEUROPATHY: MUTATION AND HAPLOTYPE ANALYSES

Charcot-Marie-Tooth disease is the most common peripheral neuropathy with a prevalence of 17-40 per 100.000 individuals. X-linked Charcot-Marie-Tooth (CMTX) disease accounts for up to 15% of all CMT cases. There are five known loci for CMTX (CMTX1, CMTX2, CMTX3, CMTX5 and Cowchock Syndrome). To date only genes for CMTX1 (*GJB1/Cx32*) and CMTX5 (*PRPS1*) have been identified.

In this study, 23 CMT families and 72 isolated CMT cases were analyzed. A combination of SSCP, high resolution melting analysis and sequencing was used to screen the cohort for *GJB1/Cx32* mutations. In ten patients, nine different mutations, two of which were novel, have been identified. The incidence of *Cx32* mutations in our cohort was found to be 10%.

Ten families were selected for haplotype analysis according to clinical criteria and pedigree analysis. After exclusion of *PRPS1* mutations in these families, we investigated linkage to CMTX2, CMTX3 and CMTX4 loci. The analyses revealed linkage to CMTX2 in two, CMTX3 in one, and to CMTX4 in one other family. *PRPS2* gene was screened as a candidate gene in two CMTX2 families. The patients tested negative for causative mutations but two common polymorphisms were identified. Linkage to known X-linked recessive loci was excluded in six families.

This study is the first on X-linked recessive CMT in Turkish population. It is important to show further evidence for the involvement of previously identified X-linked recessive CMT loci. The families excluded for all known loci reveals further genetic heterogeneity of X-linked CMT.

ÖZET

X'E BAĞLI KALITIM GÖSTEREN CHARCOT-MARIE-TOOTH HASTALARINDA MUTASYON VE HAPLOTİP ANALİZİ

Her 100.000 kişiden 17-40 aralığında görülebilen Charcot-Marie-Tooth hastalığı en yaygın herediter periferik nöropatidir. X'e bağlı kalıtım gösteren Charcot-Marie-Tooth hastalığı (CMTX) CMT vakalarının yaklaşık %15'ini kapsar. Beş kromozom bölgesi CMTX hastalığı ile ilişkilendirilmiştir (CMTX1, CMTX2, CMTX3, CMTX5 and Cowchock Sendromu). Bügüne kadar sadece CMTX1 (*Cx32*) ve CMTX5'e (*PRPS1*) neden olan genler belirlenmiştir.

Bu tez kapsamında, 23 CMT ailesinde ve 72 izole CMT olgusunda hastalığın genetik temeli araştırılmıştır. Hasta grubunda PCR-SSCP, yüksek çözünürlüklü erime analizi ve DNA dizileme yöntemleri kullanılarak Cx32 geninde mutasyon taraması yapılmıştır. Çalışmada, on hastada ikisi yeni, yedisi önceden bildirilmiş, dokuz farklı mutasyon tanımlanmıştır. *Cx32* mutasyonların CMTX hastalarımızda görülme sıklığı %10 olarak saptanmıştır.

Klinik bulgular ve aile ağacı incelemesi sonucu, 23 CMT ailesinden 10'u haplotip analizi için şeçilmiştir. Bu ailelerde PRPS1 geninde mutasyon taraması ardından, CMTX2, CMTX3 ve CMTX4 bölgeleri için haplotip analizi çalışmaları gerçekleştirilmiştir. Çalışma sonucunda iki ailede CMTX2, bir ailede CMTX3 ve bir diğerinde de CMTX4 bölgesine bağlantı tanımlanmıştır. CMTX2 haplotipi gösteren iki ailede aday gen olarak belirlenen PRPS2 geninde mutasyon taraması yapılmıştır. Bu gende bilinen iki polimorfizm dışında hastalığa neden olabilecek bir nukleotit değişimi gözlenmemiştir. Altı ailede X'e bağlı çekinik CMT bölgelerinin hastalıktan sorumlu olmadığı belirlenmiştir.

Bu çalışma, ülkemizde X'e bağlı çekinik CMT hastalarında yapılan ilk araştırma olması açısından önemlidir. Ayrıca daha önceden tanımlanmış X'e bağlı çekinik CMT bölgelerinin varlığına destek veriler elde edilmiş olması açısından değerlidir. Bilinen tüm bölgelere bağlantının dışlandığı aileler hastalığın genetik heterojenliğinin bilinenden daha fazla olduğunu kanıtlamıştır.

TABLE OF CONTENTS

LIST OF FIGURES

LIST OF TABLES

LIST OF ABBREVIATIONS

A	Adenine
C	Cytosine
G	Guanine
H	Histidine
I	Isoleucine
L	Leucine
M	Methionine
Q	Glutamine
R	Arginine
T	Thymine
V	Valine
W	Tryptophan
X	Stop codon
Y	Tyrosine

AD	Autosomal dominant
APS	Ammonium peroxodisulphate
AR	Autosomal recessive
Arg	Arginine
ATP	Adenosine triphosphate
bp	Base pair
cM	Centimorgan
CMAP	Compound muscle action potential
CMT	Charcot-Marie-Tooth
CMTX	X-Linked Charcot-Marie-Tooth Disease
CNS	Central Nervous System
Cx32	Connexin 32
DMSO	Dimethylsulphoxide
DNA	Deoxyribonucleic acid
dNTP	Deoxyribo Nucleotide Tri-Phosphate

EDTA	Ethylenediaminetetraacetate
EST	Expressed Sequence Tags
EtBr	Ethidium bromide
Glu	Glutamic acid
HNPP	Hereditary neuropathy with liability to pressure palsies
Mb	Megabase
MBP	Myelin basic protein
min	Minute
MITE	Mariner insect transposon-like element
MPZ	Myelin protein zero
mRNA	Messenger ribonucleic acid
NCV	Nerve conduction velocity
OD_{260}	Optical density at 260 nm
PCR	Polymerase chain reaction
PLP	Proteolipid protein
PMP22	Peripheral myelin protein 22
PNS	Peripheral Nervous System
P0	Protein zero
PRPS1	Phosphoribosyl pyrophosphate synthetase gene
PRPS2	Phosphoribosyl pyrophosphate synthetase two
RFLP	Restriction fragment length polymorphism
RCS	Rosenberg and Chutorian Sydrome
rcf	Relative centrifugal force
SDS	Sodium dodecyl sulphate
SSCP	Single stranded conformation polymorphism
TAE	Tris-acetate-EDTA
TBE	Tris-borate-EDTA
TE	Tris-EDTA
TEMED	N, N, N, N’-Tetramethylethylenediamine
W	Watt
UTR	Untranslated region

1. INTRODUCTION

Charcot-Marie-Tooth disease (CMT), also known as hereditary motor and sensory neuropathy (HSMN) is the most common inherited peripheral neuropathy, with a prevalence of 17-40 per 100.000 individuals (Barisic *et al.,* 2007). Up to date, CMT is associated with more than 40 loci and 36 causative genes (http://www.molgen.ua.ac.be/CMTMutations/). The disease was firstly described in 1886 by three scientist Charcot and Marie from France and independently Tooth from England, and the name given after them (Charcot and Marie, 1886 and Tooth, 1886).

The main clinical features of CMT are slowly progressive distal muscle weakness, atrophy that initially affects the small foot muscles, peroneal muscles and often later affecting the upper extremities. In addition, foot deformities like *pes cavus*, steppage gait, distal sensory loss and loss of tendon jerks were found. (Harding and Thomas, 1980; Kuhlenbäumer *et al.*, 2002; Young and Suter, 2003) (Figure 1.1). Different clinical features can be seen in different subtypes. Disease is usually progressive, but it rarely causes wheelchair dependence (Young and Suter, 2003).

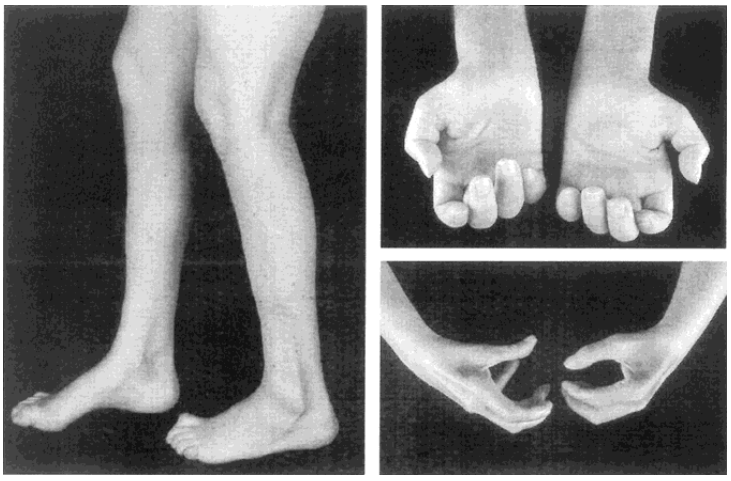

Figure 1.1. Lower and upper extremities of a patient with Charcot-Marie-Tooth disease showing muscle atrophy in the lower legs, feet and hand-muscles
(Kuhlenbäumer *et al*., 2002)

According to clinical, electrophysiological and histopathological features CMT is subdivided into two main groups; demyelinating and axonal. If the primary defect occurs in the myelin or myelinating Schwann cells, the disease is considered as demyelinating with slowed nerve conduction velocities (NCV). The neuropathy is called as axonal if the primary defect occurs in the axon of a nerve with normal or slightly normal NCVs but reduced compound muscle action potential, CMAP (Dyck *et al*., 1993).

However, identification of new genes responsible for CMT and data from genotype/phenotype correlation revised this classical division. Some of these genes are expressed both in Schwann cells and axons. Axons and Schwann cells are intensively interacting with each other and pathological signs of myelinating and axonal neuropathies often appear mixed and interconnected (Maier *et al*., 2002). Even within the same subtype, the phenotypic expression of the disease can be heterogeneous. Therefore it becomes difficult to differentiate the primary defect and distinguish these two subtypes.

Further division of these subtypes can be done according to the inheritance pattern and the results of molecular genetic investigations. Inheritance pattern can be autosomal dominant (AD), autosomal recessive (AR), X-linked dominant, or X-linked recessive.

Myelin is a lipid and protein rich structure that insulates axons and decreases the dispersion of the electrical current while it is transmitted through the axon. By this way, it increases the axonal conduction velocity in neurons. (Rummler *et al.*, 2004). It is formed by the spiral wrapping of the axons by myelinating oligodendrocytes in the central nervous system (CNS) and Schwann cells in the peripheral nervous system (PNS) (Bronstein, 2000). Major structural myelin proteins are proteolipid protein (PLP) and myelin basic protein (MBP) in the CNS; and protein zero (PO), MBP and peripheral myelin protein-22 kD (PMP-22) in the PNS.

During development of the peripheral nervous system, Schwann cell precursors migrate out from the neural crest and contact with the peripheral axons (le Douarin and Dupin, 1993). This immature Schwann cells further differentiate into myelinating or non-myelinating Schwann cells (Figure 1.2). Schwann cells that associate with an axon become myelinating Schwann cells and initiate myelin specific gene expression by turning

on the genes encoding the major myelin proteins and modify the cytoskeleton (Webster, 1993, Scherer 1997(A) and Kombolzt *et al.*, 2000). Schwann cells wrap around the axon until the axon is tightly covered with membrane (Figure 1.3). Schwann cells that can not contact with an axon becomes non-myelinating Schwann cell (Jessen *et al.*, 1990).

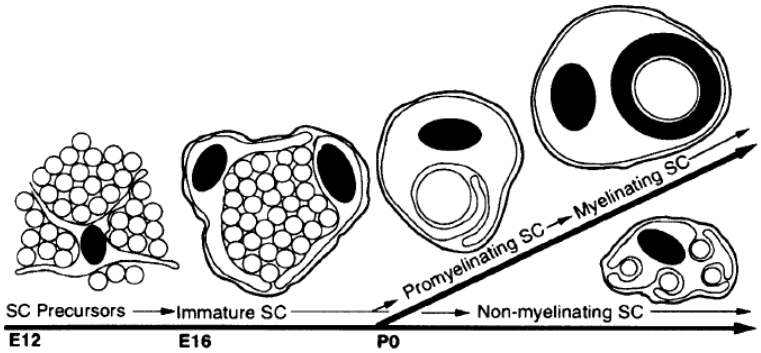

Figure 1.2. Schematic representation of rat Schwann cell differentiation in peripheral nerves. E12= Embriyonic day 12, E 16= Embriyonic day 16, P0= day of birth (Scherer, 1997)

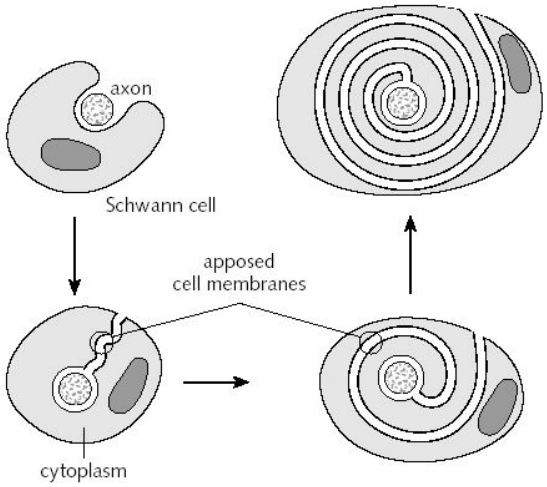

Figure 1.3. Myelination of an axon in peripheral nervous system (Modified from Answers.com)

During maturation, myelin becomes compacted by the elimination of most of the cytoplasm in the wrapping processes. Along the myelinated nerve fibers there are nodes of Ranvier at the intervals. These small non-myelinated intervals are rich in voltage-gated sodium channels and necessary for rapid saltatory conduction. Therefore Schwann cells

also determine the distribution of ion channels and support the maintenance of axons and the survival of neurons during development and regeneration Edgar and Garbern, 2004; Poliak and Peles, 2003).

After myelination, Schwann cell-axon interaction remains important for the maintenance and support of the axon. If a nerve is cut and separate a Schwann cell from the axons, degeneration occurs by a process called Wallerian degeneration. During Wallerian degeneration Schwann cells turn off the major myelin protein coding genes. (Scherer and Salzer, 2001).

According to the defective gene and the type of mutations, either Schwann cells or neurons will be affected that disturbs Schwann cell–axon interaction and leads to axonal atrophy and disability (Suter and Scherer, 2003). Also mutations in axonal transport gene are involved in the axonal degeneration. Especially peripheral neurons are more sensitive to axonal transport damages since they extend over long distances (Suter and Scherer, 2003; Niemann *et al.*, 2006).

If the primary defect is in the myelin, it is called as the demyelination subtype that is called CMT1 if inherited autosomal dominantly or CMT4 if inherited autosomal recessively. If the disease occurs because of axonal degeneration it is referred as CMT2. CMT2 can be inherited in both autosomal dominant and autosomal recessive way. The third subtype, in which both demyelination and axonal degeneration can be observed, is called as dominant intermediate CMT (DI-CMT) if it is inherited autosomal dominantly, or CMTX if it is inherited by X-linked inheritance.

1.1. Charcot-Marie-Tooth Disease Type 1 (CMT1)

CMT type 1 (CMT1), is the most common type of CMT (Dyck, 1984) and constitutes 70% of all CMT cases (Nelis *et al*., 1996; Wise *et al*., 1993). The main clinical features of CMT1 are the markedly reduced nerve conduction velocities (NCV) that is usually smaller than 38 m/s and onion bulb formations on biopsy samples (Figure 1.4) (Baxter *et al*., 2002). There are various genes identified up to date which are responsible for autosomal dominant demyelinating CMT1.

CMT1A is associated with the duplication of the peripheral myelin protein 22 (*PMP22*) gene located on the chromosome 17p11.2-p12 (Raeymaekers *et al.*, 1989; Vance *et al.*, 1989; Timmerman *et al.*, 1992; Matsunami *et al.*, 1992; Patel *et al.*, 1992). Although 70% of the patients carry *PMP22* duplication, point mutations were identified less frequently (Valentijn *et al.*, 1992 and Roa *et al.*, 1993). PMP22 protein is important in myelination and regulation of cell growth and differentiation (Martini & Schachner, 1997; Adlkofer *et al.*, 1997). Deletion of the PMP22 gene results in a disease called Hereditary neuropathy with liability to pressure palsies (HNPP) making it allelic to CMT1A (Adlkofer *et al.*,1997). Point mutations in the PMP22 gene have also been identified resulting in HNPP.

CMT1B is caused by mutations in myelin protein zero gene (*MPZ* or *P0*) located on chromosome 1q22– q23 (Hayasaka *et al.*, 1993). Mutations in the *MPZ* gene account for less than 5% of all CMT1 cases (Nelis *et al.*, 1996). MPZ is the major protein in peripheral myelin and act as an adhesion molecule that connects myelin lamellae (Martini & Schachner, 1997).

CMT1C is associated with the mutations in the lipopolysaccharide-induced tumor necrosis factor (*LITAF*) gene on chromosome 16p13.1- p12.3. The LITAF (also known as SIMPLE) protein is important in protein degradation pathways including the degradation of the PMP22 protein (Street *et al.*, 2003).

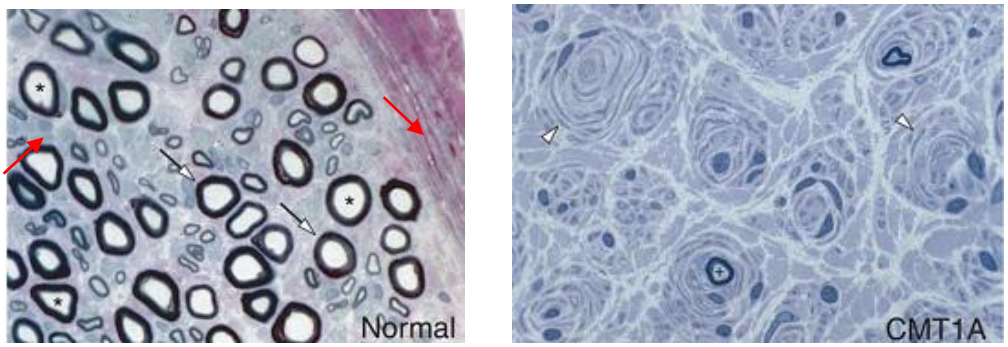

(a) (b)

Figure 1.4. Histopathological examination of a sural nerve (a) in a normal individual and (b) in a CMT1A patient. Arrows indicate myelinated fibers; asterisks show axons on a nerve cross-section. Red arrows show onion-bulb formations (Young and Suter, 2003)

Mutations in the early growth response element 2 gene (*EGR2*) gene on chromosome 10q21.1– q22.1 is associated with CMT1D, which accounts for less than 1% of all CMT cases (Warner *et al.*, 1998). EGR2 protein is a transcription factor that regulates the expression of myelin genes (Topilko *et al.*, 1994; Nagarajan *et al.*, 2001), and found to have a role in cell proliferation (Joseph *et al.*, 1988).

CMT1F is mapped to the neurofilament light chain gene (*NEFL*) on chromosome 8q21 that plays a role in the neurofilament organization and axonal transport. Mutations in the same gene can also associate with autosomal dominant axonal CMT (CMT2E) (Mersiyanova *et al.*, 2000).

1.2. Charcot-Marie-Tooth Disease Type 2 (CMT2)

CMT type 2 (CMT2) is the axonal form of the disease and occurs less frequently than CMT1, being responsible for about 20% of all CMT patients (Barisic *et al.*, 2008). It is characterized by normal or slightly reduced NCVs (usually bigger than 38m/s) and the reduced compound muscle action potentials (CMAP) (Dyck *et al*., 1993). Clinical features are similar with CMT1, however nerve biopsies show thinly myelinated fibers, chronic axonal atrophy and regeneration. In CMT2 primary injury occurs in axons and degeneration of myelin sheaths observed later by Wallerian degeneration mechanism rather than demyelination (Griffin and Hoffman 1993, Scherer and Salzer 2001).

CMT2A is associated with mutations in the mitofusin 2 gene (*MFN2*) located on chromosome 1p36 which is a large dynamin-like GTPase (Bradbury, 2004). MFN2 located in the outer mitochondrial membrane and unfunctional protein may result in insufficient transport between mitochondria and extended axons of peripheral nerves. A mutation in the kinesin motor protein 1B gene (*KIF1B*) was found in one Japanese CMT2A family, but no futher mutations in this gene found in any other families so far (Zhao *et al.*, 2001).

CMT2B is caused by the mutations in the RAS-associated GTP-binding protein gene (*RAB7*) on chromosome 3q13–q22 (Kwon *et al.*, 1995; Verhoeven *et al.*, 2003). RAB7 regulates the intracellular membrane trafficking and late endocytic pathway (Feng

et al., 1995). CMT2C is linked to chromosome 12q23–q24, but the gene has not been identified yet (Dyck *et al.*, 1994). CMT2D is caused by mutations in the glycyl-tRNA synthetase gene (*GARS*) which is a housekeeping gene that has an important role in translation (Sivacumar *et al.*, 2005). CMT2E is associated with the neurofilament light chain gene (*NEFL*) which disrupts neurofilament organization and axonal transport when mutated (De Jonghe *et al.*, 2001). CMT2F results from mutations in the gene that codes for heat shock protein B1 (HSPB1, also called HSP27) (Evgrafov *et al.*, 2004; Ismailov *et al.*, 2001). CMT2G has been linked to the chromosomal locus at 12p12–13.3 (Nelis *et al.*, 2004). CMT2H and CMT2K are linked to *GDAP1* gene mutations at chromosome 8q13–q21.1. *GDAP1* gene mutations can cause both axonal recessive CMT (CMT2H/K) and demyelinating recessive CMT (CMT4A) (Cuesta *et al.*, 2002; Baxter *et al.*, 2002). CMT2I and CMT2J are associated with *MPZ* gene mutations which is also responsible from CMT1B (Marrosu *et al.*, 1998; De Jonghe *et al.*, 1999). CMT2L is identified in a large Chinese family and suggested to result from mutations in heat shock protein 22 (*HSPB8/22*) on chromosome 12q24.3 (Tang *et al.*, 2004)

There are also autosomal recessively inherited forms of axonal CMT (AR-CMT2) which are very rare neuropathies. There are several genes and loci associated with AR-CMT (Bouhouche *et al.*, 1999; Barhoumi *et al.*, 2001; Rautenstrauss *et al.*, 2005; Cuesta *et al.*, 2002; Birouk *et al.*, 2003).

1.3. Charcot-Marie-Tooth Disease Type 4 (CMT4)

CMT4 is a demyelinating CMT with autosomal recessive inheritance (Kuhlenbaumer *et al*., 2002). Clinical features are similar to CMT1 and it is genetically heterogeneous like the other forms of the disease. Up to date three loci and seven genes were associated with CMT4. CMT4A is associated with mutations in *GDAP1* gene (Ben Othmane *et al.*, 1993; Bertorini *et al.*, 2004). Mutations in the myotubularin-related protein 2 gene (*MTMR2*) that codes for a tyrosine phosphatase are referred as CMT4B1 (Bolino *et al.*, 2000) and mutations in the myotubularin related protein 13 gene (MTMR13) are known as CMT4B2 (Azzedine *et al.*, 2003). CMT4D, CMT4E, CMT4F and CMT4J are associated with N-myc downstream-regulated gene 1 (NDRG1); EGR2

gene, periaxin gene (*PRX*) and the factor induced gene *FIG4* (*KIAA0274*), respectively (Kalaydjieva *et al.*, 1996; Warner *et al.*, 1998; Delague *et al.*,2000; Chow *et al.*, 2007). The genes responsible for CMT4G and CMT4H are not known yet (Gabreels-Festen *et al.*, 1999; Thomas *et al.*, 2001; De Sandre-Giovannoli *et al.*, 2005).

1.4. Intermediate Dominant Charcot-Marie-Tooth Disease (DI-CMT)

Clinical features of dominant intermediate CMT are similar to both demyelinating and axonal CMT with median motor nerve conduction velocities (NCV) range from 25 to 45 m/s. Several loci have been linked to DI-CMT. Mutations in dynamin 2 (DNM2) (Zuchner *et al.*, 2005), tyrosyl-tRNA synthetase (*YARS)* (Jordanova *et al.*, 2006), and *MPZ* (Mastaglia *et al.*, 1999) were related to DI-CMT. It is also linked to chromosome 10q24.1–q25.1, but the causative gene for this subtype is unknown (Verhoeven *et al.*, 2001).

1.5. X-Linked Charcot-Marie-Tooth Disease (CMTX)

X-linked Charcot–Marie–Tooth disease (CMTX) is the second most common form of CMT (Dubourg *et al.*, 2001; Kleopa & Scherer, 2002). Nerve conduction velocities of CMTX patients are only moderately reduced, generally between 30-40 m/s for males and between 40-50 m/s for females (Nicholson and Nash, 1993). In addition, there is less evidence of demyelination and more signs of axonal degeneration in biopsies of CMTX patients (Sander *et al.*, 1998). This is why it is called as ‘intermediate subtype’ between CMT1 and CMT2. Clinical features of CMTX can be variable. Age of onset is usually delayed to late childhood or third decade, but there are cases of infantile onset.

CMTX1 is dominantly inherited and affected males have moderate to severe symptoms, whereas heterozygous females are usually mildly affected. The clinical features of female carriers can be variable because of random X-chromosome inactivation (Scherer *et al.*, 1998). CMTX2, CMTX3, CMTX4 and CMTX5 are X-linked recessive disorders, therefore female carriers are mostly asymptomatic. The dominant form CMTX1 accounts for nearly 90% of all CMTX cases, while recessive forms are responsible from the remaining 10% (Ressot and Bruzzone, 2000).

1.5.1. CMTX1

In 1986, Fischbeck *et al.* identified four families having an X-linked neuropathy, all four families showed the same linkage pattern to a region near the centromere of the X chromosome on Xq13.1 (Fischbeck *et al.*, 1986). Mutation analysis on the same families and four different families identified seven different mutations in the coding region of the Cx32 gene which codes for the connexin protein (Bergoffen *et al.*, 1993). Six of them were missense mutations and one of them is a frameshift mutation which results in a premature stop codon.

Connexins are membrane-spanning proteins that form gap junction channels which transfer ions and small molecules from cell to cell (Kumar *et al.*, 1996). Six connexin subunits form a connexon molecule which is a hemichannel. These hemichannels interact with their counterparts in neighboring cells to form complete intercellular gap junction channels (Figure 1.5).

Gap junctions enable the interaction between adjacent cells by regulating the passage of small metabolites and inorganic ions in most animal tissues. They provide intercellular passage of small molecules up to about 1000 daltons (Bone *et al.*, 1997), and are thought to have diverse functions, including the propagation of electrical signals, growth control, and cellular differentiation. These intracellular interactions are very important for the coordinated cellular activity and tissue homeostasis. (Loewenstein, 1981; Bruzzone *et al.*, 1996).

Mutations in connexin genes found to be responsible for a wide spectrum of hereditary diseases in humans. Mutations in the gap junction protein connexin 26 (Cx26) gene were found to be responsible for non-syndromic deafness in humans (Kelsell *et al.*, 1997). Human connexin 31 gene mutations (GJB3) are responsible for erythrokeratodermia or deafness (Richard *et al.*, 1998; Xia *et al.*, 1998). In addition, mutations in human connexin 46 or 50 gene cause hereditary cataracts (Mackay *et al.*, 1999; Shiels *et al.*, 1998). It was also shown that deletion of connexin 37 leads to infertility in female mice (Simon *et al.*, 1997); connexin 43 knockout mice die of cardiopulmonary anomalies shortly after birth (Reaume *et al.*, 1995) and deletion of

connexin 40 in mice leads to cardiac conduction abnormalities (Kirchhoff *et al.*, 1998; Simon *et al.*, 1998)

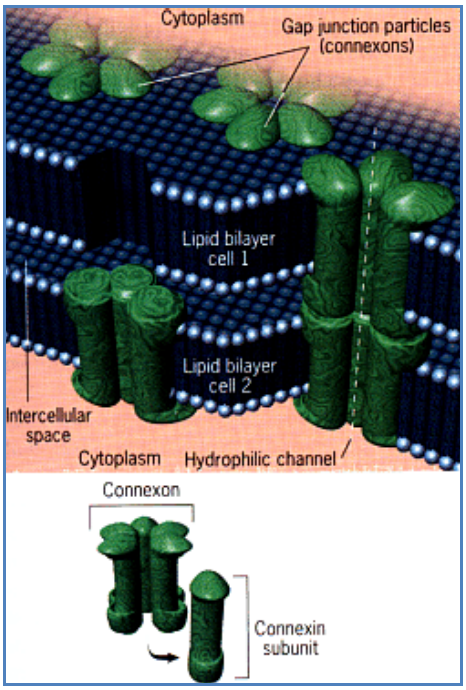

Figure 1.5. Gap junction formation from two hemichannels

Cx32 is highly expressed in myelinating Schwann cells and it is regulated in parallel with other myelin genes (Scherer *et al.*, 1995). Northern blot analysis showed that expression of the Cx32 gene in peripheral nerves is greater than any other tissues (Bergoffen *et al.*, 1993). Cx32 also found to be expressed in oligodendrocytes in central nervous system (Scherer *et al.*, 1997(B)). In CNS myelin Cx45 is also expressed (Dermietzel *et al.*, 1997; Kunzelmann *et al.*, 1997) that may compensate for the absence of Cx32.

In a peripheral nerve, Cx32 found to be localized in the paranodal regions, and Schmidt-Lanterman incisures of myelinating Schwann cells forming gap junctions between adjacent layers of the myelin sheath (Figure 1.6) (Bergoffen *et al.*,1993; Scherer *et al.*, 1995). This system could provide fast communication between the outer myelin layers and axons (Nelis *et al.*, 1999b). After association of Cx32 gene with X-linked CMT, the importance of Schmidt-Lanterman incisures and the paranodal regions were

understood. Altered activity of gap junctions at the paranodes and incisures, disrupt the interaction between the myelin sheets and the axons as well as Schwann cells.

Cx32 protein has four transmembrane segments, two extracellular loops, and three cytoplasmic domains (Figure.1.7) (Bennett *et al.*, 1991). The amino acid sequence is highly conserved among species, especially in the extracellular and transmembrane domains. Third transmembrane domain forms the gap junction's pore, which is between aminoacids at positions 139 and 142 (Milks *et al.*, 1988; Bone *et al.*, 1997). A mutation in those residues is important for distrupting and blocking the channel activity. N-terminal domain brings the polypeptide chain to the endoplasmic reticulum (Falk *et al.*, 1994) and together with the first transmembrane domains have a role in the voltage gating. Extracellular loops are responsible from the hemichannel interaction (Dahl *et al.*, 1992) and the intracellular loop and C-terminal domain determine the pH gating (Bruzzone *et al.*, 1996).

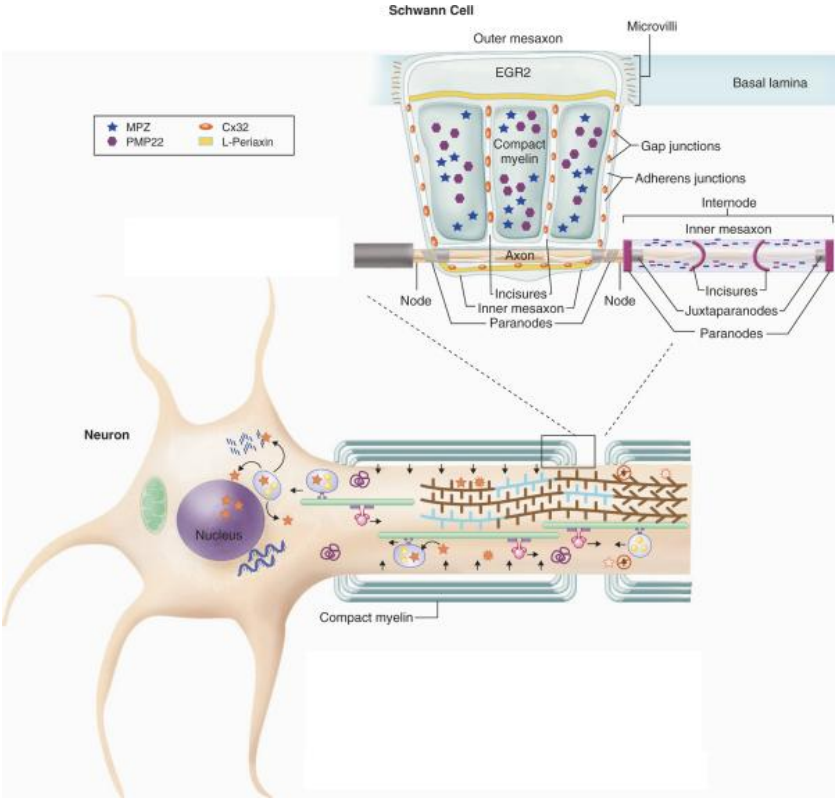

Figure 1.6. Schematic view of an axon in PNS with its myelinating Schwann cell. The location of Cx32, MPZ, PMP22 and L-Periaxin proteins on the myelin sheat is given in different colors which are explained on the box in left.
(modified from Goldman: Cecil Medicine)

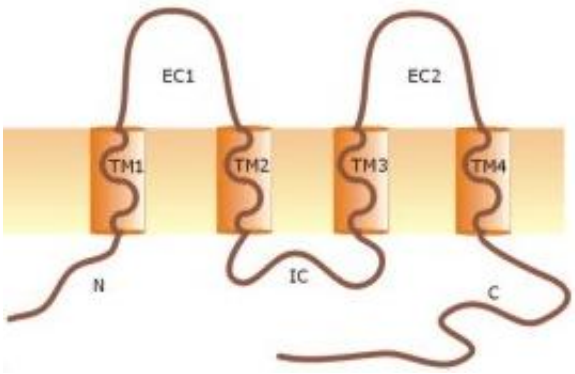

Figure 1.7. Schematic representation of Cx32 protein

More than 240 different mutations have been identified in CMTX1 patients up to date. Types of mutations are variable like missense, nonsense, deletions, insertions, and frame-shift mutations. Mutations are distributed throughout the entire coding region without any specific clustering. The largest number of mutations was seen in the transmembrane domains and only a few mutations were identified in the middle cytoplasmic loop (Ressot and Bruzzone, 2000).

To understand the effects of mutations, functional studies were performed by using micro-injection of low molecular weight fluorescent tracer compounds and measuring the diffusion through connexin channels (Balice-Gordon *et al.*, 1998). The majority of the mutations tested can not form functional channels because the defective protein were either retained in intracellular compartments or can not assemble with the neighbouring hemichannel or can not have proper gating mechanisms (Abrams *et al.*, 2000; Ressot and Bruzzone, 2000; Yum *et al.*, 2002).

1.5.2. CMTX2

Several X-linked recessive families having Charcot-Marie-Tooth disease have been reported in the literature (Erwin 1944; Fryns *et al.*, 1980; Fischbeck *et al.*, 1986 and lonasescu *et al.*, 1991). Males can be moderately to severely effected but female heterozygotes don't show any clinical and functional disabilities. Slightly decreased nerve

conduction velocities can be seen in some carrier females (Fryns *et al.*, 1980) due to random X-chromosome inactivation.

Linkage analyses for whole X chromosome markers were done for a family showing X-linked mode of inheritance and having infantile onset, atrophy with weakness of the lower limbs, areflexia, *pes cavus*, and mental retardation (2 of 5 patients) (Ionasescu *et al.*, 1991). Electrophysiological findings of the family showed both demyelination and axonal involvement in all affected patients. Obligate carrier females had normal electrophysiological findings. Using thirty X chromosome DNA probes, detecting restriction fragment length polymorphisms, a linkage to Xp22.2 markers DXS143-DXS16- DXS43 was identified with a maximum lod score of 3.48 at DXS16 (Ionasescu *et al.*, 1991). No further linkage or data was found about this subtype of CMT later, and the gene responsible for CMTX2 is still unknown.

1.5.3. CMTX3

CMTX3 is another X-linked recessive form of CMT disease. It is first described in two American families with later onset (10 to 14 years), distal atrophy with weakness, and normal intelligence. Obligate carrier females showed no signs of the disease. In one of the families affected males showed spasticity and pyramidal signs. Linkage analyses for these two families using RFLP markers revealed linkage to a 31.2 Mb interval at the region Xq26 (Ionasescu *et al.*, 1991).

After a decade, a second linkage to this locus was identified in a large New Zealand/United Kingdom (NZ/UK) family with 11 affected males and 14 asymptomatic female carriers (Huttner *et al.*, 2006). Affected individuals of this family also showed the typical symptoms with decreased nerve conduction velocities and reduced CMAPs. However spasticity and pyramidal signs were not found in any of the affected males as well as any other additional symptoms. Linkage analysis for this family using 35 microsatellite markers narrowed the region to a 3.72 Mb interval on Xq26.3-q27.1 (Huttner *et al.*, 2006).

Lastly, the disease in a large Australian X-linked CMT family, showing the same phenotype with the previous families without spasticity or pyramidal signs, was linked to CMTX3 loci (Brewer *et al.*, 2008). Re-analysis of one of the original American families with these two additional families showed that they shared the same disease haplotype in the distal portion of the disease haplotype (Figure 1.8). Comparison of this haplotype with the normal population provided statistically significant data that sharing this haplotype is not a random association ($p<0.0001$). The shared haplotype between the affected individuals was identical by descent. This shows these three families have a common ancestor and the disease is caused by a founder mutation (Brewer *et al.*, 2008). This new data further narrowed the disease locus to a 2.5 Mb interval.

This 2.5 Mb interval contains 15 annotated genes and and 18 expressed sequence tag (EST) clusters (UCSC Genome Browser, Human Mar. 06 Assembly). Coding region and exon-intron boundaries of LDOC1 gene was excluded. (Huttner *et al.*, 2006). Ten from the remaining 14 genes (RP1177G6.2, CDR1,SPANXB2, SPANXC, SPANXA2, SPANXA1, BC042039, SPANXE, MAGEC2, and SPANXN4) were further excluded (Brewer *et al.*, 2008). No pathogenic mutation was identified up to date, after screening of the remaining 4 genes. Thus EST clusters should also be checked for novel transcripts. The causative gene for CMTX3 will be a novel undescribed gene. (Brewer et al,, 2008).

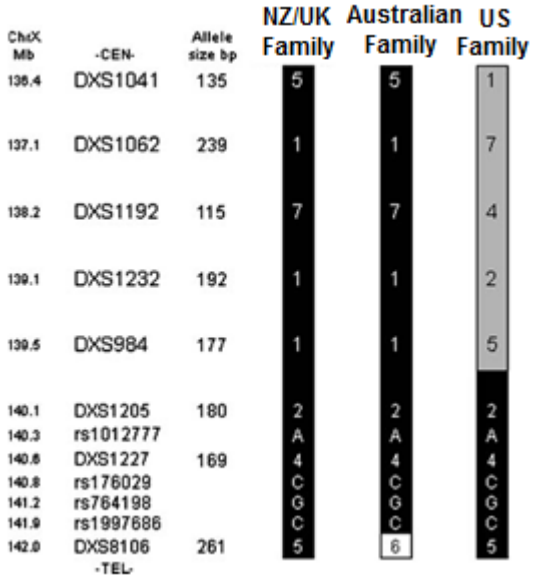

Figure 1.8. Comparison of haplotypes for three CMTX3 families. Black bar shows the haplotype shared by all families (Brewer *et al.*, 2008)

1.5.4. CMTX4 (Cowchock Syndrome)

An unusual form of slowly progressive X-linked recessive CMT was identified in a three generation Pennsylvania family of Italian origin (Cowchock *et al.,* 1985). Like the other X-linked recessive CMTs severity in males were variable and female carriers were asymptomatic. The family included seven affected males and three obligate carrier females. Five of the seven affected males had deafness and three of these five showed mental retardation or social development delay (Cowchock *et al.*, 1985).

Linkage analysis was done for the same family by using random polymorphic X chromosome DNA markers (Fischbeck *et al.*, 1986). After finding close linkage to PGK locus, this gene was screened and excluded for this family (Fischbeck *et al.*, 1986). Further analysis of this family with additional 19 macrosatellite markers covering approximately 76 cM region revealed a significant linkage to the region Xq24-q26 (Priest *et al.*, 1995). This refined 11 cM interval flanked by the markers DXS425 and HPRT proved that this family has both genetically and clinically distinct type of CMT. However the defective gene responsible for this type of CMT has not been identified yet.

1.5.5. CMTX5

CMTX5 is described in a Korean family showing a rare symptom triad of sensorineural hearing loss, progressive visual impairment and peripheral neuropathy. (Kim *et al.*, 2005). This family had five affected male patients and six obligate female carriers. Male patients showed mixed features of segmental demyelination and axonal loss. The symptom triad observed in CMTX5 was also reported in Rosenberg-Chutorian syndrome (RCS) (Rosenberg and Chutorian, 1967). This suggests that CMTX5 and RCS are allelic disorders and have the same causative gene.

X-chromosome wide linkage analysis using 48 STR markers mapped the disease to the region Xq21.32–24. Additional markers were used for fine mapping of the region and the disease gene was localized into a 15.2 cM interval between the markers DXS990 and DXS8067 (Kim *et al.*, 2005). This region contains more than 170 candidate genes (USCS genome browser). Screening the candidate genes that are expressed in the inner ear

according to the cochlear expression database revealed a mutation in phosphoribosyl pyrophosphate synthetase gene (PRPS1) (Kim *et al.,* 2007). Screening of the RCS patients for PRPS1 gene identified another mutation and confirmed X-linked recessive inheritance in this family (Kim *et al.,* 2007). No other mutations were identified after these two families which suggests that the causative gene for CMTX5 (PRPS1) specifically leads to a unique symptom triad.

PRPS1 is the major isoform of the human phosphoribosyl pyrophosphate (PRPP) synthetase gene family (Taira *et al.,* 1989). Protein sequence of PRPS1 is highly conserved across different species from zebrafish to human. PRPS1 is an enzyme that catalyzes the synthesis of PRPP substrate and which has a role in biosynthesis of purines and pyrimidines, from ATP and Rib-5-P. Functional studies showed decreased PRPS enzyme activity in affected CMTX5 patients compared with the normal family members and unrelated control individuals (Kim *et al.,* 2007).

Identification of *PRPS1* gene responsible from CMTX5 is the first case for an inherited peripheral neuropathy to be result from a decreased activity of a metabolic enzyme critical for purine metabolism and nucleotide biosynthesis (Kim *et al.,* 2007).

2. AIM OF THE STUDY

The aim of this study is to investigate the molecular basis of CMT in a cohort of 23 families with suspected X-linked inheritance and 72 isolated cases. The study includes screening of known genes and loci for CMTX and we target to identify families linked to a known CMTX locus that can be helpful for the identification of causative genes in future studies.

More specifically, we aim;

- to screen the genes *Cx32* (CMTX1) and *PRPS1* (CMTX5) to identify causative mutations and achieve molecular diagnosis; and to compare the reliability of two different mutation screening methods; Single Strand Conformation Polymorphism (SSCP) and High Resolution Melting Analysis (HRM).
- to perform haplotype analysis to test linkage to CMTX2, CMTX3, and CMTX4 loci in familial CMTX cases.

3. MATERIALS

3.1. Subjects

Peripheral blood samples of Turkish CMT patients and their family members analyzed in this study were provided by Department of Neurology, Istanbul Medical School, İstanbul University. Informed consent was obtained from all family members and the study was approved by Ethics Review Committees of participating institution.

3.2. Chemicals

All solid and liquid chemicals used in this study were purchased from Merck (Germany), Sigma (USA), Riedel de-Häen (Germany) and Carlo Erba (Germany), unless stated otherwise in the text.

3.3. Fine Chemicals

Fine Chemicals used in this study are given in details in the below sections.

3.3.1. Enzymes

Taq DNA Polymerases used in Boğaziçi University were purchased from Fermentas (MBI Fermentas, Lithuania). The restriction enzyme MspI and AciI were purchased from (MBI Fermentas, Lithuania).

Chromo AT Taq DNA Polymerases and *Perpetual Taq* DNA Polymerases used in microsatellite analysis performed in Anzac Research Institute were purchased from Vivantis (*Vivantis, Australia*). HRM mixes used in High Resolution Melting Analysis were purchased from Trend-Bio (Australia).

3.3.2. Oligonucleotide Primers

The primers used in the PCR-SSCP analysis were synthesized by Operon (USA), and Integrated DNA technologies (Leuven, Belgium). The primers designed for High Resolution Melting Analysis were synthesized by Sigma (Australia). The primers used for microsatellite analysis were synthesized by Invitrogen (Australia) and all the forward primers were 5'-FAM-labelled.

The sequence of primer sets and PCR conditions used for amplification of different genes and loci are given in Table 3.1 through Table 3.8.

Table 3.1. Sequences of the primers used for exon amplification of *Cx32* gene for PCR-SSCP Analysis

Exon	Primer (F/R*)	Primer Sequence (5'→3')	Product Size (bp)	Annealing Temp. (°C)
Exon 1	Cx32-1F	TGAGGCAGGATGAACTGGACAGGT	306	59
	Cx32-1R	TTGCTGGTGAGCCACGTGCATGGC		
	Cx32-2F	ATCTCCCATGTGCGGCTGTGGTCC	432	63
	Cx32-2R	GATGATGAGGTACACCACCT		
	Cx32-3F	CGTCTTCATGCTAGCTGCCTCTGG	304	60
	Cx32-3R	TGGCAGGTTGCCTGGTATGT		

* F: Forward primer, R: Reverse primer

Table 3.2. Sequences of the primers used for exon amplification of *Cx32* gene for HRM Analysis

Exon	Primer (F/R)	Primer Sequence (5'→3')	Product Size (bp)	Annealing Temp(°C)
Exon 1	Cx32AM1F	TGTTTTGCAGGTGTGAATGAG	349	68
	Cx32AM1R	AGCCGTAGCATTTTCTTCTCT		
	Cx32AM2F	TGCACGTGGCTCACCAGCAA	347	68
	Cx32AM2R	CTCGGCCACATTGAGGATGAT		
	Cx32AM3F	CCGTCTTCACCGTCTTCATGCTA	316	68
	Cx32AM3R	GATGGGAGGTTGCCTGGTAT		

Table 3.3. Sequences of the primers used for exon amplification of *PRPS1* gene for PCR-SSCP Analysis

Exon	Primer (F/R)	Primer Sequence (5'→3')	Product Size (bp)	Annealing Temp. (°C)
Exon 1	PRPS1-1F	ATTGAGTCTGTGGCCGACTT	244	63
	PRPS1-1R	GGGCAGGTGAGGTCTAGTCA		
Exon 2	PRPS1-2F	ATGGATATGGAGGGCTGACA	299	65
	PRPS1-2R	CAAGTGCTCCTGCTTCCTCT		
Exon 3	PRPS1-3F	TTCTTTCCTCCCCTCCATTT	164	56
	PRPS1-3R	TCCTCCCACCTTTCAAACAC		
Exon 4	PRPS1-4F	TGAAGCAAAACTGATCCAGC	195	59
	PRPS1-4R	TCCCAGTACATTGGGAACAA		
Exon 5	PRPS1-5F	GAACACGCTCTGTTTTGCAG	286	62
	PRPS1-5R	GGTTCCAAAAGGAATCAGCA		
Exon 6	PRPS1-6F	TGGAAGCCTAAGCAGGCTAAT	273	64
	PRPS1-6R	TTTGCACAAATCTCATCCTCA		
Exon 7	PRPS1-7F	GGCCAGTCATCTCTGACCAT	257	65
	PRPS1-7R	AAGCTACACTGGAGCAAGCC		

Table 3.4. Sequences of the primers used for exon amplification of *PRPS1* gene for HRM Analysis

Exon	Primer (F/R)	Primer Sequence (5'→3')	Product Size (bp)	Annealing Temp. (°C)
Exon 1	1-1F	GAGCTACACCGAGGACCAAAC	256	66.5
	1-1R	TATTCGGCATCCTGGCCAACT		
	1-2F	CCGTGATCGCTTAGTGGAGT	200	66.5
	1-2R	CAGGTGAGGTCTAGTCAGGGT		
Exon 2	2F	GGGCTGACAGTACAGTGGTTT	282	63
	2R	CTCCTGCTTCCTCTGCTCAA		

Table 3.4. Sequences of the primers used for exon amplification of *PRPS1* gene for HRM Analysis (continued)

Exon	Primer (F/R)	Primer Sequence (5'→3')	Product Size (bp)	Annealing Temp. (°C)
Exon 3	3F	AGTAGGTACACAATAAATAGTTTCTTGAGT	233	63
	3R	TCCTCCCACCTTTCAAACAC		
Exon 4	4F	TGGAAGAGAAGGAAAGTGAAGCAA	210	66.5
	4R	CCCAGTACATTGGGAACAATACTA		
Exon 5	5F	ACACATACATATGAACACGCTC	244	67.5
	5R	TTTCCTTCTAACTACCAGCCC		
Exon 6	6F	CTGCAATGACAAGTAAGATGAATCC	265	67.5
	6R	AGTAACCACCTCCTAAACACTTAGAAA		
Exon 7	7F	GCCAGTCATCTCTGACCATATGATAGT	200	67.5
	7R	GAAACAAGGGTGGGGTGGATTT		

Table 3.5. Sequences of the primers used for the amplification of microsatellite markers at the CMTX2 locus

Marker	Primer (F/R)	Primer Sequence (5'→3')	Product Size (bp)	Annealing Temp. (°C)
DXS8051	DXS8051-F*	ACCAGAAATGAGCGATTATTG	145-175	Touchdown cycle
	DXS8051-R	TTTTTGAACTAAGAACCTGGAG		
DXS7108	DXS7108-F*	GCTAAAATAGATGCTCAATATAATG	236-256	Touchdown cycle
	DXS7108-R	GAGGTTTTCAGAACTGCAA		
DXS1224	DXS1224-F*	CTTCAAGCCTACAAAATCTGG	157-169	Touchdown cycle
	DXS1224-R	TGGGTGGCAACACTCACT		
DXS8022	DXS8022-F*	CTGTCACAGAAGTCCCATTTTA	160-188	Touchdown cycle
	DXS8022-R	GGAAACTAATGCAGCATGTC		
DXS8108	DXS8108-F*	AGAGTAGGTCTTAAATGTTTTCACG	127-151	Touchdown cycle
	DXS8108-R	TGTATAACGAGATGTTTTGATATGT		
DXS987	DXS987-F*	GTTGAGATAATGAGGCCAGT	200-224	Touchdown cycle
	DXS987-R	ACNTTAAAAGCCTGGTTCTTCTAAA		

* Forward Primers are 5′-FAM fluorescence labeled.

Table 3.6. Sequences of the primers used for the amplification of microsatellite markers in CMTX3 locus

Marker	Primer (F/R)	Primer Sequence (5'→3')	Product Size (bp)	Annealing Temp. (°C)
DXS1041*	DXS1041F	GTCCTCTTGGAACATGAGAA	120-176	Touchdown cycle
	DXS1041R	CGAACAATTATGGGTTGTCT		
DXS1062*	DXS1062F	GAGATGTGTGACCTTGAGCACT	222-248	Touchdown cycle
	DXS1062R	GTTGCCTGTTAAGCACTTTGAATC		
DXS1192*	DXS1192F	GTTGCCAACTGCTGGAACG	121-137	Touchdown cycle
	DXS1192R	TGTGGTGCAGGGAAGCC		
DXS1232*	DXS1232F	ACCAACAGCCTAATAATGC	163-199	52
	DXS1232R	AGAGATGGGAGCAGCA		
DXS984*	DXS984F	TTTCTGTCTGCCAAGTGTTT	154-184	55
	DXS984R	TACTGNGCCCTACTCCATTC		
DXS1205*	DXS1205F	CCTACGCATGTGGCTC	184-198	55
	DXS1205R	ATTAATGGCTTAGAGTACTTTTCA		
DXS1227*	DXS1227F	AGAGGTCCGAGTCTTCCAC	174-186	55
	DXS1227R	ATAAGGGTTTACTCCCCCAA		
DXS8106*	DXS8106F	CTTGCACTTGCTGTGG	260-286	Touchdown cycle
	DXS8106R	AGCTGTAGAGTTGAGGAATG		

* used by Brewer *et al.*, 2007

Table 3.7. Sequences of the primers used for the amplification of Microsatellite Markers in CMTX4 locus

Marker	Primer (F/R)	Primer Sequence (5'→3')	Product Size (bp)	Annealing Temp.(°C)
DXS8057	DXS8057F	GGGGTAATATGCAGCCTC	202-258	Touchdown cycle
	DXS8057R	AGCCACCATGCCTAGC		
DXS1047	DXS1047F	CCGGCTACAAGTGATGTCTA	196-210	Touchdown cycle
	DXS1047R	CCTAGGTAACATAGTGAGACCTTG		
DXS8068	DXS8068F	ACTTAGCATAATGTCCTCCAG	233-245	Touchdown cycle
	DXS8068R	CCTCTGTAAAGAACCTGCAC		

Table 3.8. Sequences of the primers used for exon amplification of *PRPS2* gene for HRM Analysis

Exon	Primer (F/R)	Primer Sequence (5'→3')	Product Size (bp)	Annealing Temp. (°C)
Exon 1	PRPS2-1F	CCGCTCTTCCTCCCTCTCTG	346	65
	PRPS2-1R	AGCGCTCTCCCTAGCCC		
Exon 2	PRPS2-2F	AATATGCTTGGATATTAACCG	262	63
	PRPS2-2R	CCCACAGCAGGTTTCTA		
Exon 3	PRPS2-3F	GGAATCTAACAGTATCCATCTTT	206	63
	PRPS2-3R	ATTTAATTTAACAGACTTGATTTAACC		
Exon 4	PRPS2-4F	CAACATGACACTCACTTCTC	181	63
	PRPS2-4R	AAATCTGCAAGGTGTAGC		
Exon 5	PRPS2-5F	GCGAGATCTCTAGTTGACTGTATG	275	63
	PRPS2-5R	TTTCCCTTTCCTAGTGAGAAGTCCTAA		
Exon 6	PRPS2-6F	AGTATTCCAAGAATATTTGCATACCCT	257	63
	PRPS2-6R	TAGGTGCCTGGCTGCTT		
Exon 7a	PRPS2-7aF	TCCTGCTTCCCTTCTCC	311	62
	PRPS2-7aR	GGAAAGAAATGATCTTGAGCTTTAG		
Exon 7b	PRPS2-7bF	GCATCAGATCTTTGTATATGCTAAGATT	263	62
	PRPS2-7bR	ACCTTTGGCAACCTCGAA		
Exon 7c	PRPS2-7cF	TTCATTGTGGAAGTCATAGT	261	59
	PRPS2-7cR	GTCCAAATTAAGCACAGTAAC		
Exon 7d	PRPS2-7dF	TTTTTTTTGGATAACTCAGTTTCA	346	59
	PRPS2-7dR	TATATCCTTTTTAAAAATCTGAGATCA		
Exon 7e	PRPS2-7eF	AGCCTAAGAATGTATAGAGCTAGT	349	59
	PRPS2-7eR	CAGTAGAATTGGACAGGACC		
Exon 7f	PRPS2-7fF	GTGGAAACTTAAGTGAGACC	350	62
	PRPS2-7fR	AAACATATTACTCCACAATGATAC		

3.3.3. DNA Size Markers

The size markers used in this study were 100-bp DNA ladder with a range of 100-1000 bp (Fermentas, Lithuania) or Hyperladder IV (Bioline, USA).

3.3.4. Other Fine Chemicals

QIAquick PCR Purification Kit was purchased from Qiagen (Germany). Jet Quick PCR Purification Kit used after HRM analysis was purchased from Genomed, (Germany).

3.4. Buffers and Solutions

3.4.1. DNA Extraction from Peripheral Blood

Cell Lysis Buffer	:	155 mM NH_4Cl 10 mM $KHCO_3$ 1 mM Na_2EDTA (pH 7.4)
Nuclei Lysis Buffer	:	10 mM Tris-HCl (pH 8.0) 400 mM NaCl 2 mM Na_2EDTA (pH 7.4)
Sodiumdodecylsulphate	:	10% SDS (w/v) (pH 7.2)
Proteinase K	:	20 mg/ml
TE Buffer	:	20 mM Tris-HCl (pH 8.0) 0.1 mM Na_2EDTA (pH 8.0)
5 M NaCl solution	:	292.2 g NaCl in 1 l dH_2O

3.4.2. Polymerase Chain Reaction (PCR)

10 X $MgCl_2$ Free Buffer	:	100 mM Tris-HCl 500 mM KCl (pH 9.1 at 20°C) (Fermentas, Lithuania and; Vivantis, Australia)
Magnesium Chloride ($MgCl_2$)	:	25 mM $MgCl_2$ (Fermentas, Lithuania and Vivantis, Australia)
10X PCR Enhancer	:	10X PCR Enhancer Solution (Invitrogen)
Deoxyribonucleotide Triphosphates (dNTPs)	:	100 mM of each dNTP (Fermentas, Lithuania and Bioline, USA)

3.4.3. Agarose Gel Electrophoresis

10 X TBE Buffer (Tris-Borate-EDTA Buffer)	:	0.89 M Tris-Base 0.89 M Boric Acid 20 mM Na_2EDTA (pH 8.3)
25X TAE Buffer (Tris-Acetate-EDTA Buffer)	:	1M Tris-acetate 25 mM EDTA (pH 8)
1 or 2% Agarose Gel	:	1 or 2% Agarose (w/v) (Basica LE or Vivantis) in 0.5 X TBE Buffer or TAE Buffer
Ethidium Bromide	:	10 mg/ml
10 X Loading Buffer	:	2.5 mg/ml Bromophenol Blue 1% SDS (w/v) in 2 ml glycerol

3.4.4. Polyacrylamide Gel Electrophoresis

10 X TBE Buffer	:	0.89 M Tris-Base 0.89 M Boric Acid 20 mM Na_2EDTA (pH 8.3)
30 % Acrylamide Stock (29:1)	:	29% Acrylamide (w/w) 1% N, N'-methylenebisacrylamide (w/w)
8 % Non-Denaturing Gel	:	8% Acrylamide Stock (39:1) (v/v) 0.6X TBE Buffer (pH 8.3)
Ammoniumpersulfate	:	1% APS (w/v)
10X Denaturing Buffer	:	95% Formamide (w/v) 20 mM EDTA 0.05% Xylene Cyanol (w/v) 0.05% Bromophenol Blue (w/v)

3.4.5. Silver Staining

Buffer A	:	10% Ethanol (v/v) 0.5% Glacial Acetic Acid (v/v)
Buffer B	:	0.1% $AgNO_3$ in dH_2O (w/v)
Buffer C	:	1.5% NaOH (w/v) 0.01% $NaBH_4$ (w/v) 0.015% Formaldehyde (v/v)
Buffer D	:	0.75% Na_2CO_3 (w/v)

3.5. Equipment

Automated DNA Sequencing and Microsatellite Size Fractionation using the ABI 3100 Genetic Analyser were performed by outsourced facilities Australian Cancer Research Foundation Facility, Garvan Institute of Medical Research and Sydney University Prince Alfred Molecular Analysis Centre (SUPAMAC)

High Resolution Melting (HRM) analysis were performed at Anzac Research Institute, Northcott Neuroscience Center, NSW, Australia by using Eppendorf Master Cycler and 9700 Thermal Cycler (Applied Biosystems) for PCR amplification and Idaho Technology Light Scanner for melting analysis.

All other experiments were performed using facilities of the Department of Molecular Biology and Genetics at Boğaziçi University (Istanbul, Turkey). The equipments used were as follows;

Autoclave	:	Model MAC-601 (Eyela, Japan)
Balances	:	Electronic Balance Model VA124 (Gec Avery, UK) Electronic Balance Model CC081 (Gec Avery, UK)
Centrifuges	:	Centrifuge 5415C (Eppendorf, Germany) Universal 16R (Hettich, Germany)
Deep Freezers	:	-20°C (Bosch, Germany) -70°C (GFL, Germany)
Documentation System	:	GelDoc Documentation System (Bio-Rad, USA)

Electrophoretic Equipments	:	Horizon 58, Model 200 (BRL, USA) Sequi-Gen Sequencing Cell (Bio-Rad,USA) DGGE System Model # DGGE-200 (C.B.S. Scientific Co., USA) Horizon 1020, Model H1 (BRL, USA) PROTEAN Vertical electrophoresis System (Bio-Rad, USA)
Incubators	:	Shake'n'Stack (Hybaid, UK) Oven EN400 (Nuve, Turkey)
Magnetic Stirrer	:	Chiltern Hotplate Magnetic Stirrer, HS31 (UK)
Ovens	:	Microwave Oven (Vestel, Turkey)
Power Supplies	:	Power Pac Model 3000 (Bio-Rad, USA) PSU 400/200 (Scie-Plus, UK)
Refrigerator	:	+4°C (Arçelik, Turkey)
Spectrophotometer	:	NanoDrop ND-1000 (NanoDrop, USA)
Thermal Cyclers	:	Icycler (Bio-Rad, USA) Mycycler (Bio-Rad, USA) Light-Cycler 1.5 (Roche, Germany)
Vortex	:	Nuvemix (Nuve, Turkey)
Water Purification System System	:	WA-TECH Ultra Pure water Purification (WA-TECH, Germany)

4. METHODS

4.1. DNA Extraction from Peripheral Blood

Ten ml blood samples were collected in tubes containing K_3EDTA to prevent coagulation. Tubes were stored at 4 ˚C until DNA extraction. The blood samples were transferred into sterile 50ml centrifuge Falcon tubes and thirty ml ice-cold red blood cell (RBC) lysis buffer is added. The samples were then left at 4 ˚C for 20 minutes to lyse the erythrocyte membranes. For collecting the leukocyte nuclei, the lysed solution was centrifuged at 1732 relative centrifugal force (rcf), at 4 ˚C for 10 min. The supernatant was discarded and the pellet was resuspended in 10 ml RBC lysis buffer by vortexing. The resuspension was centrifuged again at 1732 rcf, at 4 ˚C for an additional 10 minutes. The supernatant was discarded and the nuclei pellet was resuspended in three ml nuclei lysis buffer by vortexing. Storage of nuclei at -20 ^{0}C or -70^{0}C was possible at this stage. Then 30 µl Proteinase K (Section 3.4.1) and 50 µl of 10% SDS (w/v) were added and the samples were incubated at 37 ºC overnight or 56 ºC for three hours to degrade the cellular proteins. Afterwards, 10ml of 2.5 M NaCl was added and the mixture was shaken vigorously. The samples were centrifuged at 1732 rcf at room temperature for 20 min. The supernatant was taken into a new 50 ml Falcon tube and two volumes of absolute ethanol were added to precipitate the DNA. The DNA was spooled and transferred to a sterile 1.5 ml eppendorf tube. After air drying of the DNA pellet to evaporate ethanol, 200-500 µl of Tris-EDTA (TE) buffer (Section 3.5.1) was added and the samples were left overnight at room temperature to dissolve completely.

4.2. Quantitative Analysis of Extracted DNA

The concentration of the genomic DNA was measured by using the Nanodrop ND-1000 spectrophotometer, according to the optical density at 260 nm. The measurement was done based on the fact that 50 µg of double stranded DNA has an absorbance of 1.0 at 260nm. The purity of the DNA checked by A_{260}/A_{280} ratio which should be between 1.8-2.

4.3. Mutation Analysis

Ninety five CMT patients, which were found to be negative for CMT1A duplication, *PMP22* and *MPZ* point mutations in previous studies, were screened for *Cx32* and *PRPS1* gene mutations by using both PCR-SSCP and High Resolution Melting Analysis and subsequent DNA sequencing.

4.3.1. Mutation Analysis of *GJB1/Cx32* and *PRPS1* Genes by Using PCR-SSCP

PCR-SSCP method is based on the fact that under non-denaturing conditions, single stranded DNA fragments forms unique conformations according to their primary sequences (Orita *et al.*, 1989; Hayashi, 1992), Therefore even a single base change can result in a conformational change that can be detected by polyacrylamide gel electrophoresis.

4.3.1.1.Polymerase Chain Reaction (PCR). The coding exon of *Cx32* gene was amplified in three overlapping fragments using the primers described (Table 3.1). The primers for the coding region of *PRPS1* gene were designed by using the web-based software; Primer 3 (http://seqtool.sdsc.edu) (Table 3.3).

PCR reactions were performed in a volume of 25 µl containing 200 ng DNA, 2.5 µl of 10X polymerase buffer, 2.0 mM $MgCl_2$, 0.2 mM dNTPs, 0.4 mM of each primer and 1U of *Taq* polymerase (Fermentas). The PCR program on Icycler^{TM} (BioRad) thermal cycler was as follows: an initial denaturation step at 95ºC for 5 min, followed by 35 cycles of 30 s at 95ºC, 30 s at annealing temperature, 30 s at 72ºC, a final elongation at 72°C for 5 min, and cooling at 15°C for 1 min. PCR products (5µl) were size fractionated on 2% (w/v) agarose gels to check for correct amplicon size.

4.3.1.2.Single Strand Conformation Polymorphism (SSCP). The PCR products were run on 8% (v/v) acrylamide gels with or without glycerol to detect the different migration patterns. The 20 cm-20 cm and 22 cm-20 cm glass plates were cleaned to remove dust and oily fingerprints to prevent any interference. One mm spacers were placed on two edges of the glass plates and they were stabilized by clamps.

Acrylamide gel (8% v/v) were prepared in a total volume of 60 ml containing 16 ml of 30% (29:1 acrylamide- N, N'-methlene-bis-acrylamide); 7.2 ml of 5 X TBE buffer and dH_20. Lastly, 600 µl of 10 per cent ammonium per sulfate (APS) and 60 µl of TEMED were added and the solution was poured between the two plates. A plastic comb was placed to the upper part of the gel and the gel was left for at least 1 h at room temperature for polymerization.

For electrophoresis PCR products were mixed with denaturing loading dye (Section 3.5.4) in 1:1 ratio. Samples were denatured at 94˚C for 5 min and chilled on ice for an additional 5 min. Denatured samples (7µl) were loaded on the gel. The gel was run in 0.6 X TBE buffer generally at 110 Volts for 18 hours.

4.3.1.3.Silver Staining. DNA fragments, separated on the gel, were visualized by silver-staining method. The gel was incubated with Buffer A (Section 3.5.5) for 3 min. to fix the DNA. After the removal of Buffer A, the gel was treated with Buffer B (Section 3.5.5), a silver nitrate solution for 10 min. The gel was washed with dH_2O and incubated in freshly prepared Buffer C (Section 3.5.5) until the bands become visible. At last, the gel was placed in Buffer D (Section 3.5.5) for 5 min. to terminate the color reaction. The gel was transferred into a transparent folder and sealed.

When an abnormal migration pattern was detected, the patient's genomic DNA was amplified again by the same set of primers; and both forward and reverse strands were sequenced.

4.3.2. Mutation Analysis of *Cx32, PRPS1* and *PRPS2* Genes Using High Resolution Melting (HRM) Analysis

HRM analysis is based on the melting of the DNA double helix that has been amplified in the presence of a saturating fluorescence double-stranded DNA binding dye. As DNA becomes single stranded, the dye is released and the fluorescence signal decreases, the differences in the florescent data can be plotted vs. temperature change. Melting behaviour of an amplicon depend on the sequence, GC content, length, and heterozygosity of the amplicon.

All primers used in HRM Analysis were designed by Light Scanner Primer Design Software (Idaho Techology) to amplify the coding sequences and intron-exon boundaries of the *Cx32, PRPS1* and *PRPS2* genes.

The coding region of *Cx32* gene was divided into 3 overlapping amplicons and the first coding exon of *PRPS1* gene divided into two amplicons. Sequences of primers and annealing temperatures for *Cx32* and *PRPS1* were given in the Tables 3.2. and 3.4 respectively.

To facilitate heteroduplex formation, DNAs from hemizygous males were mixed with a male wild-type DNA (1:1 w/w) prior to PCR amplification. Samples were analyzed in duplicate to minimize false positive results. PCR reactions were performed in a reaction of 10 µL containing 10 ng DNA, 4 µl 10X HRM master mix (Trend-Bio), 1X PCR Enhancer (Invitrogen) and 4 pmol primers; except for the amplification of Exon 3 of *PRPS1* gene in which 0.25 pmol of each primer was used. PCR was performed on Mastercycler (Eppendorf) with an initial denaturation of 5 min at 95°C, followed by 35 cycles of 30 s at 95°C, 30 s at annealing temperature, and 40 s at 68°C, with a final extension of 5 min at 68°C.

For family P224 and P727 that are found to have a CMTX2 haplotype, coding sequences and intron-exon boundaries of *PRPS2* gene were screened as a candidate causative gene for CMTX2. Primers and annealing temperatures are given in Table 3.8.

PRPS2 gene amplicons (Figure 4.1) were amplified in a reaction containing 10 ng DNA, 5 µl 10X HRM mix (Trend-Bio), and 4 pmol primers, except for Exon1 and Exon7a in which 1.5 µl and 1 µl 10X PCR Enhancer (Invitrogen) were added, respectively. PCR was performed on Mastercycler (Eppendorf) using the same cycling profile as the *Cx32* and *PRPS1* genes.

After amplification, melting analysis was performed on 96-well LightScanner (Idaho Technology) and melting-curves were analyzed by using LightScanner Software (version 1.0.1.524) as previously described (Kennerson *et al.,* 2007). Samples showing aberrant melting curves were sequenced afterwards.

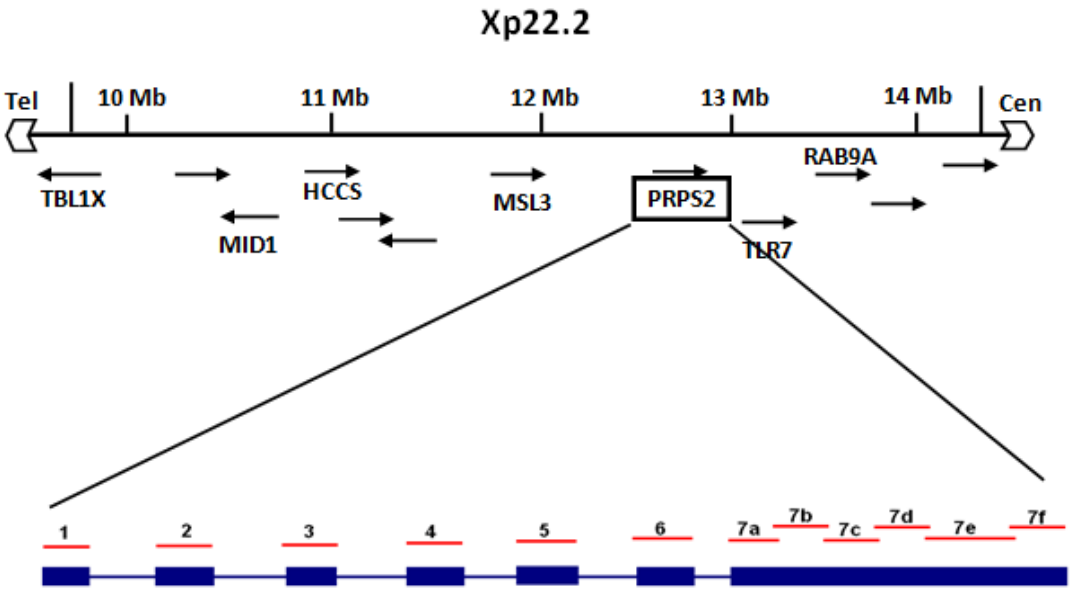

Figure 4.1. Candidate genes in CMTX2 region Xp22.2 and amplicons used to amplify seven coding exons of *PRPS2* gene

4.3.3. DNA Sequence Analysis

PCR products were purified using the Qiagen PCR purification kit (Qiagen). After purification samples were send to Iontek (Istanbul, Turkey) to be sequenced with an automated sequencer ABI 3700 PRISM (Applied Biosystems). PCR products used in HRM analysis were purified by JetQuick PCR Purification Kit (Genomed) according to the manufacturer's instructions. PCR products were mixed with forward and reverse primers and sequenced by Sydney University Prince Alfred Molecular Analysis Centre (SUPAMAC) using ABI 3730 sequencer or by ACRF facility of the Garvan Institute of Medical Research using BigDye Terminator Cycle Sequencing protocols.

The sequences were analyzed and aligned using SeqMan software (DNASTAR) and the UCSC Genome Browser. DNA sequence variants were cross referenced using the Inherited Peripheral Neuropathies Mutation Database (IPNMD) (http://www.molgen.ua.ac.be/CMTMutations) or CHIP Bioinformatics Tool, SNPPer (http://snpper.chip.org).

4.3.4. Restriction Endonuclease Analysis

For the validation of mutations, restriction analysis was performed with an appropriate enzyme for the DNA samples of the patient, available family members and normal control samples. These variations either produced a new restriction enzyme site or abolished a previously existing one. Exons containing the sequence variations were amplified using suitable primer sets. Ten µl of PCR product was digested with 3U of restriction enzyme and 2 µl of its suitable buffer in a total volume of 20 µl reaction. The samples were incubated at 37°C overnight. The digestion products were run on 2% agarose gel and stained by ethidium bromide to visualize DNA.

4.4. Haplotype Analysis

Ten multi-generation families suitable for haplotypes analysis were selected for the study according to specific clinical criteria, and pedigree analysis (Table 4.1). These families were analyzed to identify linkage to the CMTX2, CMTX3 and CMTX4 (Cowchock Syndrome) loci.

Table 4.1. Clinical data of the index patients

	Affected Members	**Severity**		**Age of onset**	**Median NCVs**	**Additional Features**
		Mobility	**Upper limbs**			
P155	2 brothers	Confined to wheelchair	Distal & proximal weakness	2nd decade	23m/s	Pes cavus Cerebeller dysfunction
P158	3 brothers Mother	Abnormal	Normal	2nd decade	31m/s	Pes cavus Sensory ataxia
P192	3 brothers	Confined to wheelchair	Distal weakness	1st decade	NA	Pes cavus Scoliosis Sensory ataxia
P224	2 brothers	Abnormal	Normal	3rd decade	46m/s	Pes cavus
P381	2 brothers	Confined to wheelchair	NA	NA	NA	NA
P408	2 brothers	Normal	Distal weakness	3rd decade	25m/s	Pes cavus Tremor Deafness Cerebellar dys. Bilateral cataract

Table 4.1. Clinical data of the index patients (continued)

	Affected Members	**Severity**		**Age of onset**	**Median NCVs**	**Additional Features**
		Mobility	**Upper limbs**			
P444	2 sisters 2 brothers a daughter a son	Abnormal	Distal weakness	1st decade	50m/s	NA
P470	2 brothers	Abnormal	Distal weakness	>40 years	38.8m/s	Pes cavus Sensory ataxia
P683	5 siblings mother	Abnormal	Distal weakness	NA	45.2m/s	Pes cavus Tremor Deafness
P727	2 cousins	Abnormal	Distal weakness	2nd decade	30m/s	Sensory loss

Families were genotyped for CMTX2, CMTX3 and CMTX4 loci using the microsatelite markers shown in Figure 4.2. The sequence of primers and annealing temperatures used in the amplification of microsatellite markers are given in Table 3.5, 3.6 and 3.7.

Microsatellite markers were amplified in 10 µl reactions using the master mixes given in Table 4.2. PCR was performed on either a 9700 thermocycler (Applied Biosystems) or a MasterCycler (Eppendorf) with a Touchdown cycle (an initial denaturation of 5 min at 95°C, followed by 10 cycles of 30 s at 95°C, 30 s at 65°C, and 40 s at 68°C, followed by 25 cycles of 30 s at 95°C, and 30 s 55°C) or with an initial denaturation of 5 min at 95°C, followed by 35 cycles of 30 s at 95°C, 30 s at annealing temperature, and 40 s at 68°C, with a final extension of 5 min at 68°C. Amplified markers were sent to the Australian Cancer Research Foundation Facility, Garvan Institute of Medical Research (NSW, Australia), for size fractionation using the GeneScan LIZ 600 size standard. Haplotypes were analyzed using Genemarker v1.5 software and pedigrees constructed using Cyrillic2.0 software.

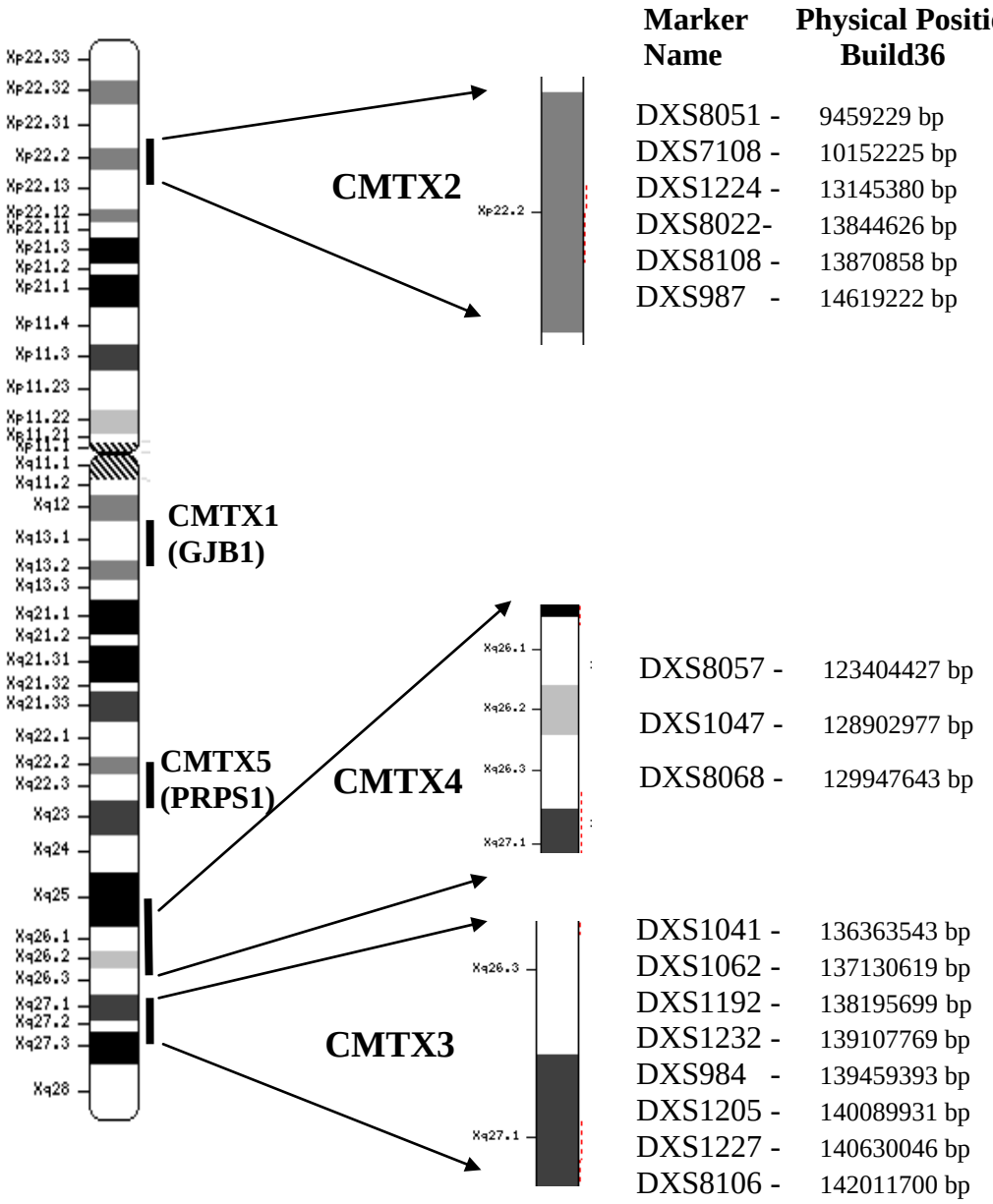

Figure 4.2. Ideogram of human X chromosome showing the physical map and genetic location of microsatellite markers used in this study for haplotype analysis

Table 4.2. Master mix used in the amplification of microsatellite marker

Master Mix	1	2	3
DNA	10 ng	10 ng	10 ng
10X Buffer	1 µl	1 µl	1 µl
$MgCl_2$	1.5 mM	1.5 mM	1.5 mM
dNTP	2.5 mM	0.5 mM	0.5 mM
Primers	0.4 mM	0.5 mM	0.4 mM
PCR Enhancer	-	1X	-
Taq polymerase	1U Perpetual Taq Polymerase	0.5U Chromo At Taq Polymerase	1U Chromo At Taq Polymerase

Master mix 1,2 and 3 used in the amplification of CMTX2, CMTX3 and CMTX4 macrosatellite markers respectively.

5. RESULTS

The molecular basis of X-linked Charcot-Marie-Tooth Disease (CMTX) was investigated in 95 unrelated CMT patients. Twenty three of the patients had a family history whereas 72 were isolated cases. CMT1A duplication, *PMP22* and *MPZ* point mutations were excluded in all of the patients in previous studies.

Upon exclusion of *Cx32* and *PRPS1* gene mutations in this cohort, haplotype analyses for CMTX2, CMTX3 and CMTX4 (Cowchock Syndrome) loci were performed in 10 selected multi-generational families, with a possible X-linked inheritance. Families showing a CMTX2 haplotype were screened for mutations in a high priority candidate gene *PRPS2*.

5.1. Mutation Analysis

The known CMTX genes *Cx32* and *PRPS1*; and the high priority candidate gene for CMTX2 (*PRPS2*) were screened for pathogenic mutations.

5.1.1. Mutation Analysis of *Cx32* Gene

Mutational analysis of *Cx32* gene (NM_001097642) was performed using a combination of Single Strand Conformation Polymorphism (SSCP), High Resolution Melting Analysis (HRM) and sequencing techniques. The nomenclature used for variations were established upon the Human Genome Variation Society website (http://www.hgvs.org/mutnomen/recs.html#general). Mutations are designated based on numbering of the A in the ATG translation initiation site as +1.

5.1.1.1.SSCP Analysis. Mutation screening performed by SSCP analysis was followed by sequencing sense and antisense strands of the individuals that show band shifts on SSCP gel. Altered migration patterns were observed in eight patients and sequencing results showed eight different mutations. Seven were missense mutations and one was a nonsense mutation.

Aberrant migration pattern was observed in fragment 1 of *Cx32* for patient P31 and sequencing results revealed a hemizygous missense mutation c.271G>A (V91M) which was previously reported by Ananth *et al.*, 1999 (Figure 5.1a and 5.1b).

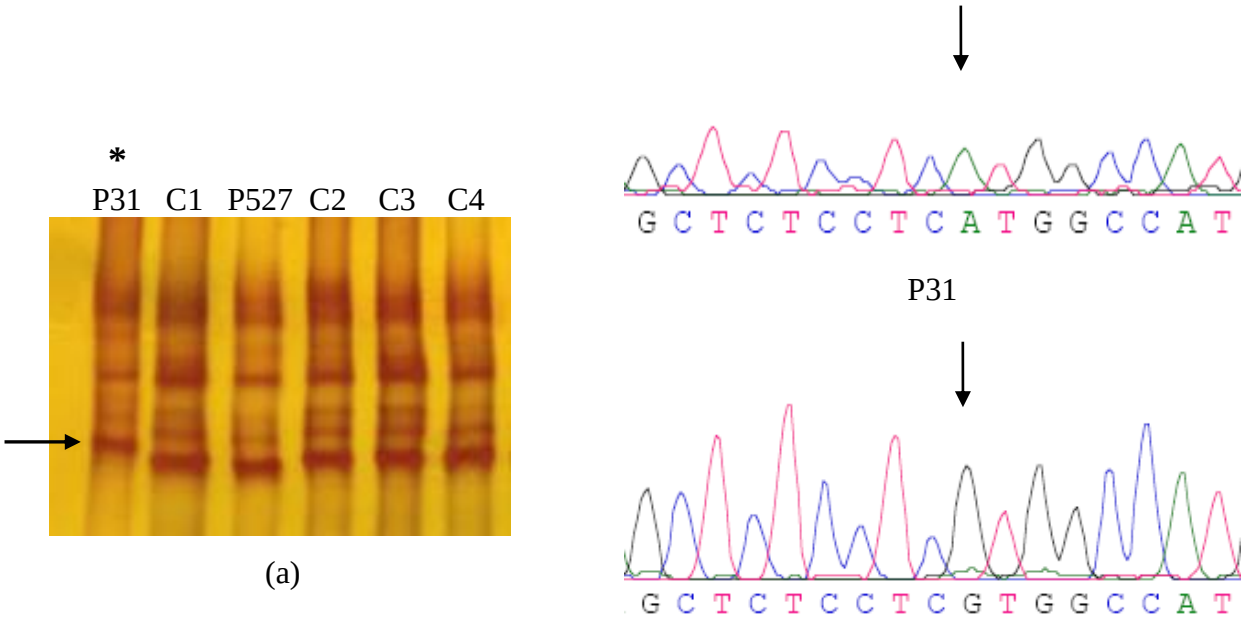

(a)

(b)

Figure 5.1.(a) 8% SSCP gel showing an altered migration pattern for patient P31

(b) chromatogram showing the c.271G>A alteration and the normal sequence.

A different migration pattern was detected in patient P280 in the SSCP gel for fragment 1 of *Cx32* gene and sequencing results showed a hemizygous missense mutation c.224G>A (R75Q) which was previously described by Tan *et al.*, 1996 (Figure 5.2a and 5.2b).

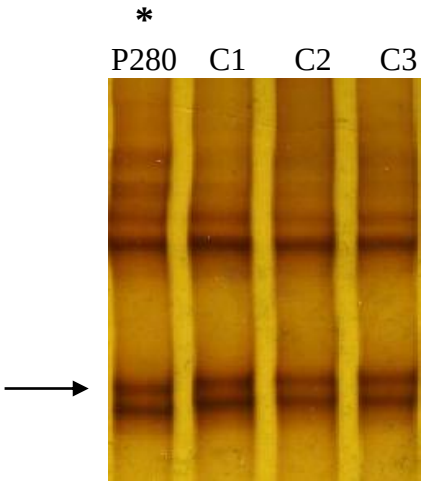

(a)

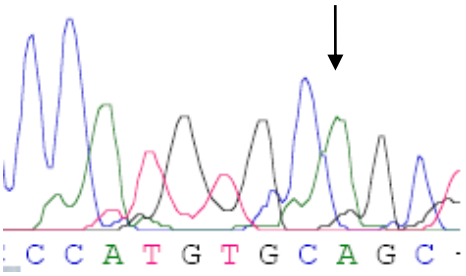

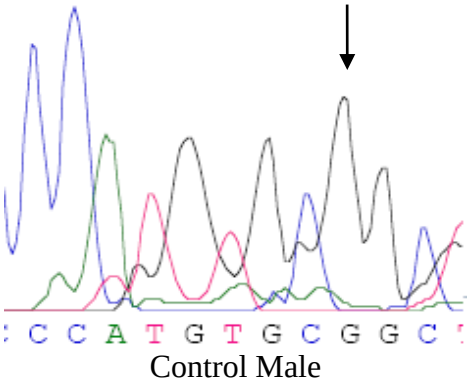

(b)

Figure 5.2 (a) 8% SSCP gel showing altered migration pattern for patient P280 (b) chromatograms showing the c.224G>A alteration and the control sequence

Patient P527 showed an aberrant migration band in the SSCP gel (Figure 5.3a) and sequencing results showed a novel c.379A>C (I127L) change. (Figure 5.3b). It is unlikely that this is a common polymorphism since 25 healthy individuals did not show the same migration pattern on SSCP analysis and the amino acid substitution occurs at a highly conserved residue (Figure 5.3c).

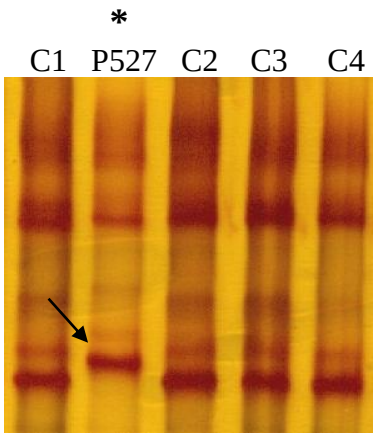

(a)

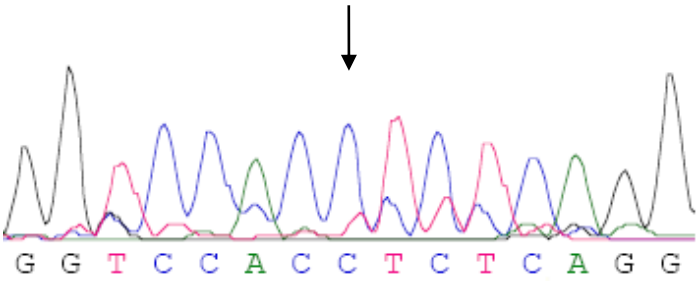

P527

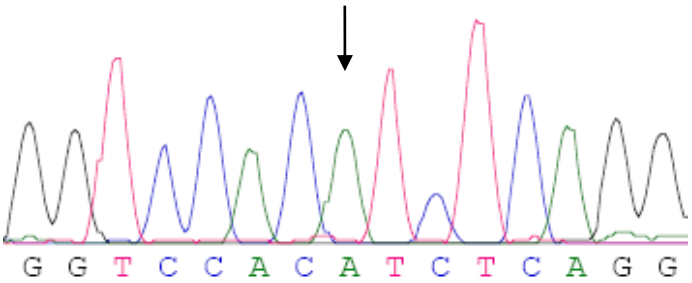

Normal male

(b)

p.I127L

Human	K	R	H	K	V	H	I	S	G	T	L
Mouse	K	R	H	K	V	H	I	S	G	T	L
Rat	K	R	H	K	V	H	I	S	G	T	L
Rabbit	K	S	Q	K	V	R	I	E	G	S	L
Dog	K	R	H	K	V	H	I	S	G	T	L
Armadillo	K	R	H	K	V	H	I	S	G	T	L
Elephant	K	R	H	K	V	H	I	S	G	T	L
Opossum	K	R	H	K	V	H	I	S	G	T	L
Chicken	K	K	H	K	M	R	I	A	G	S	L
X_tropicalis	K	K	H	K	V	K	I	S	G	T	L
Tetraodon	K	D	R	K	M	H	I	T	G	P	L

(c)

Figure 5.3.(a) 8% SSCP gel showing altered migration pattern for patient P527
(b) chromatograms showing the c.379A>C alteration and control sequences
(c) Alignment analysis of the p.I127L mutation in the *Cx32* gene in different species. Position 127 is shown in red box.

A different migration pattern was also observed in fragment 1 for patient P550 and sequencing results showed a hemizygous missense mutation c.43C>T (R15W) which was previously described by Nelis *et al.*, 1996 (Figure 5.4a and 5.4b). The sequence change destroys a restriction site for MspI which digests the 306bp PCR amplicon into 51bp and

255bp products in wild type individuals. For the verification of the mutation, MspI restriction digestion was performed in 25 healthy individuals. The 306 bp product was not observed in any control individuals (Figure 5.4c).

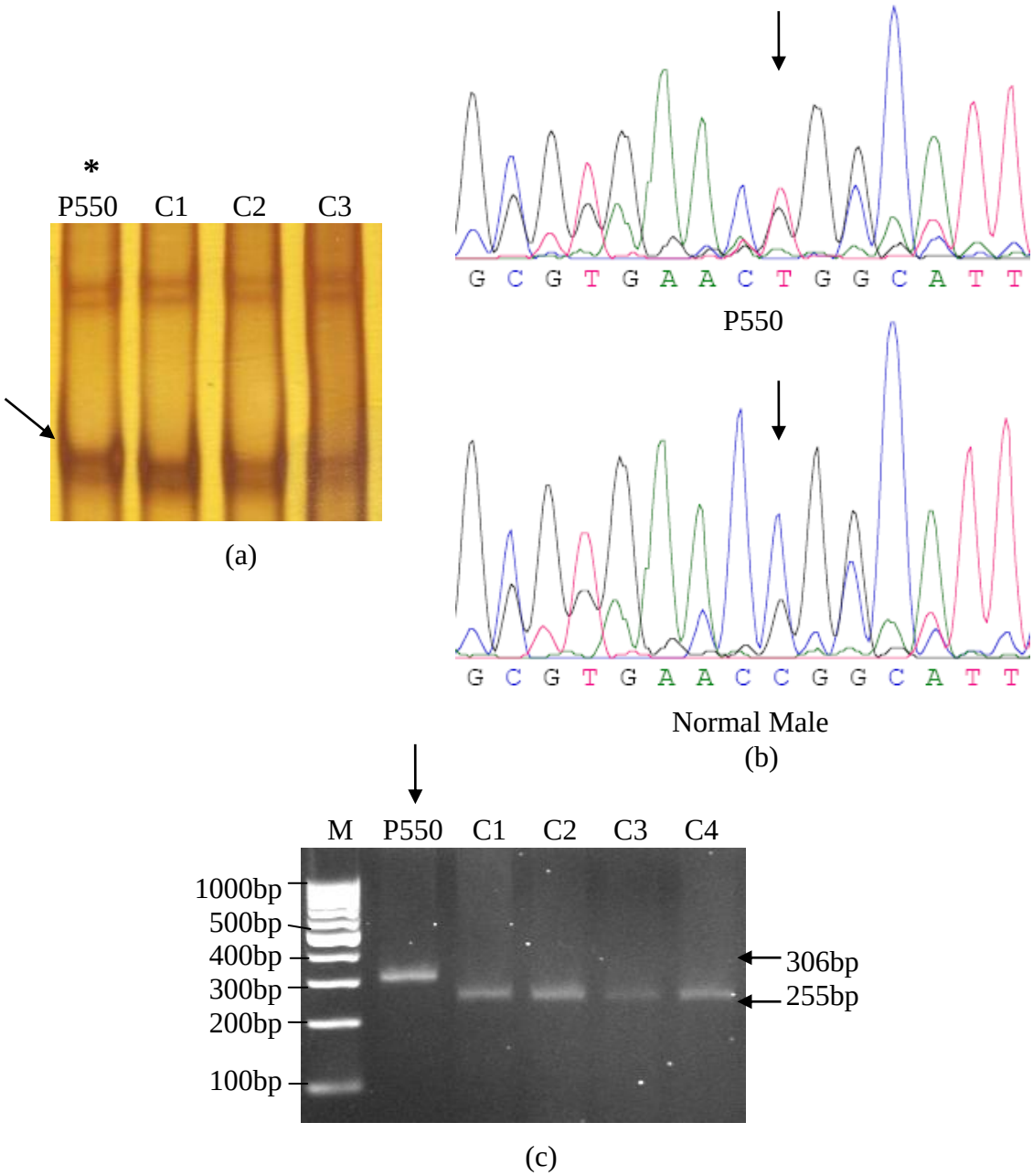

Figure 5.4 (a) 8% SSCP gel showing altered migration pattern for patient P550 (b) chromatograms showing the c.43C>T alteration and control sequence (c) MspI restriction digestion indicating the uncut 306bp PCR product in the patient vs 255bp products in the controls (51bp product can not be seen in the picture)

An aberant migration pattern was detected in fragment 2 of *Cx32* gene for patient P560 (Figure 5.5a) and sequencing results showed a hemizygous missense mutation c.283G>A (V95M) which was previously described by Bone *et al.*, 1995 (Figure 5.5b).

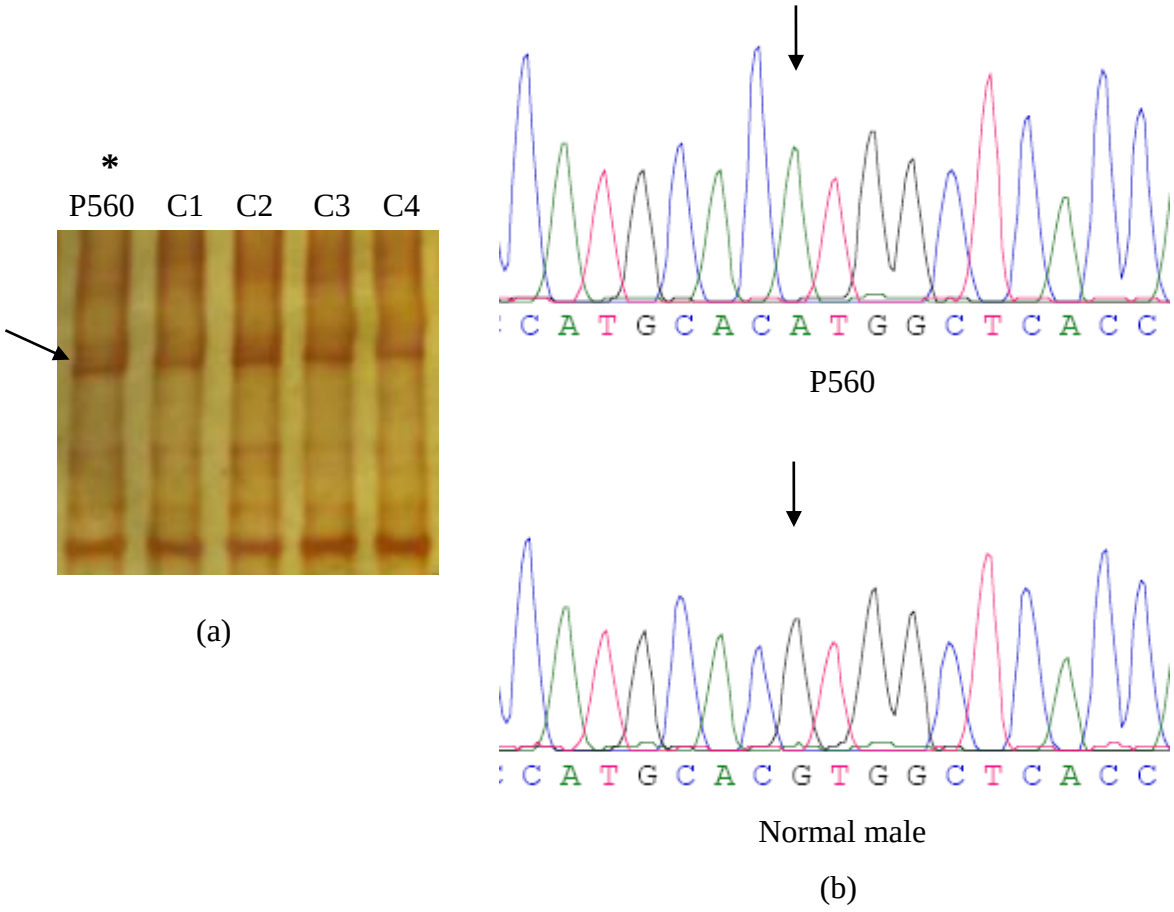

Figure 5.5. (a) 8% SSCP gels showing altered migration pattern for patient P560 (b) chromatograms showing the c.283G>A change and control sequence

A different migration pattern was detected in the SSCP analysis of patient P571 for fragment 3 of *Cx32* gene and sequencing results showed a novel hemizygous nonsense mutation c.763C>T (Q255X) which causes a premature stop codon. (Figure 5.6a and 5.6b). SSCP analysis was performed with an additional 25 healthy control individuals, the same pattern was not observed in any of the control individuals that suggests the change is not a common polymorphism. In addition, glutamine in the position of the amino acid change is a highly conserved residue in closely related species to human. (Figure 5.6c).

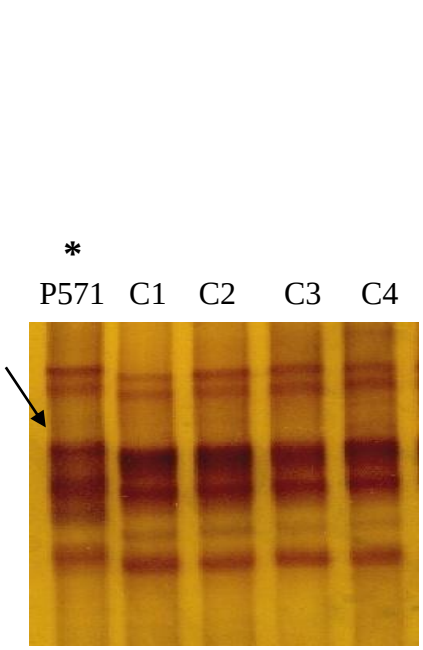

(a)

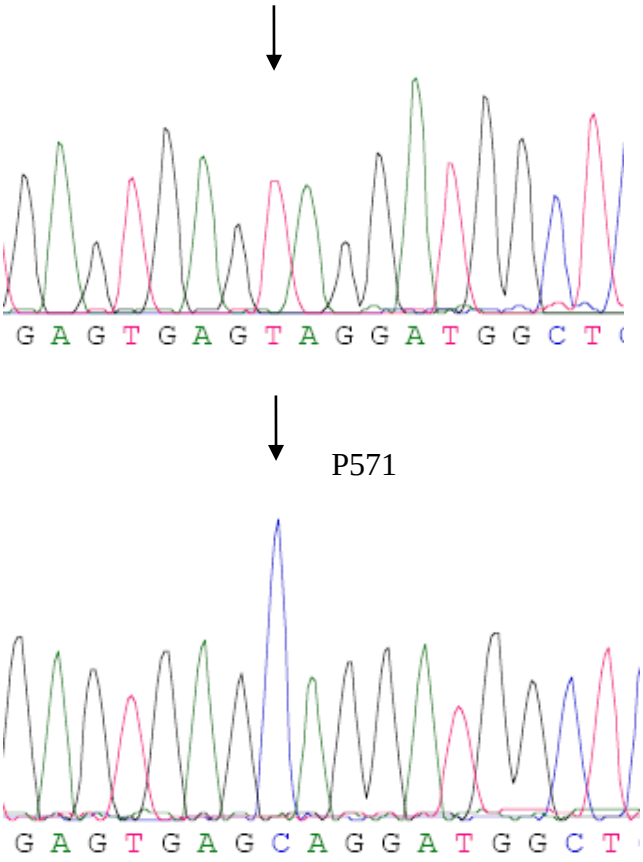

Normal male

(b)

p.Q255X

human	N	K	L	L	S	E	Q	D	G	S	L	K	D	I	L	R	R	S	P	G	T	G	A	G	L
mouse	N	K	L	L	S	E	Q	D	G	S	L	K	D	I	L	R	R	S	P	G	T	G	A	G	L
rat	N	K	L	L	S	E	Q	D	G	S	L	K	D	I	L	R	R	S	P	G	T	G	A	G	L
rabbit	D	K	L	L	S	E	Q	D	G	S	L	K	D	I	L	L	L	S	P	G	T	G	A	G	L
dog	N	K	L	L	S	E	Q	D	G	S	L	K	D	I	L	R	R	S	P	G	T	G	A	G	L
armadillo	N	K	L	L	S	E	Q	D	G	S	L	K	D	I	L	R	R	S	P	G	T	G	A	G	L
elephant	N	K	L	L	S	E	Q	D	G	S	L	K	D	I	L	R	R	S	P	G	T	G	A	G	L
opossum	N	K	L	L	S	D	Q	D	G	S	L	K	D	I	L	R	R	S	P	G	T	G	A	G	L
chicken	N	Q	L	L	S	E	Q	D	G	S	L	K	D	M	L	R	R	N	P	G	-	-	-	-	L

(c)

Figure 5.6. (a) 8% SSCP gel showing altered migration pattern for patient P571 (b) chromatograms showing the c.763C>T alteration and control sequence. (c) Alignment analysis of the p.Q255X mutation in the *Cx32* gene in different species. Position 255 is shown in red box

Patient P579-1 showed an aberrant migration pattern in fragment 2 of *Cx32* gene, and sequencing results revealed a c.298C>T (H100Y) alteration in hemizygous state (Figure 5.7a and 5.7b). Since his female cousin was showing the same symptoms her DNA sample was also sequenced and she was found to be heterozygous for the same mutation. This mutation was previously identified by Bone *et al.*, 1997.

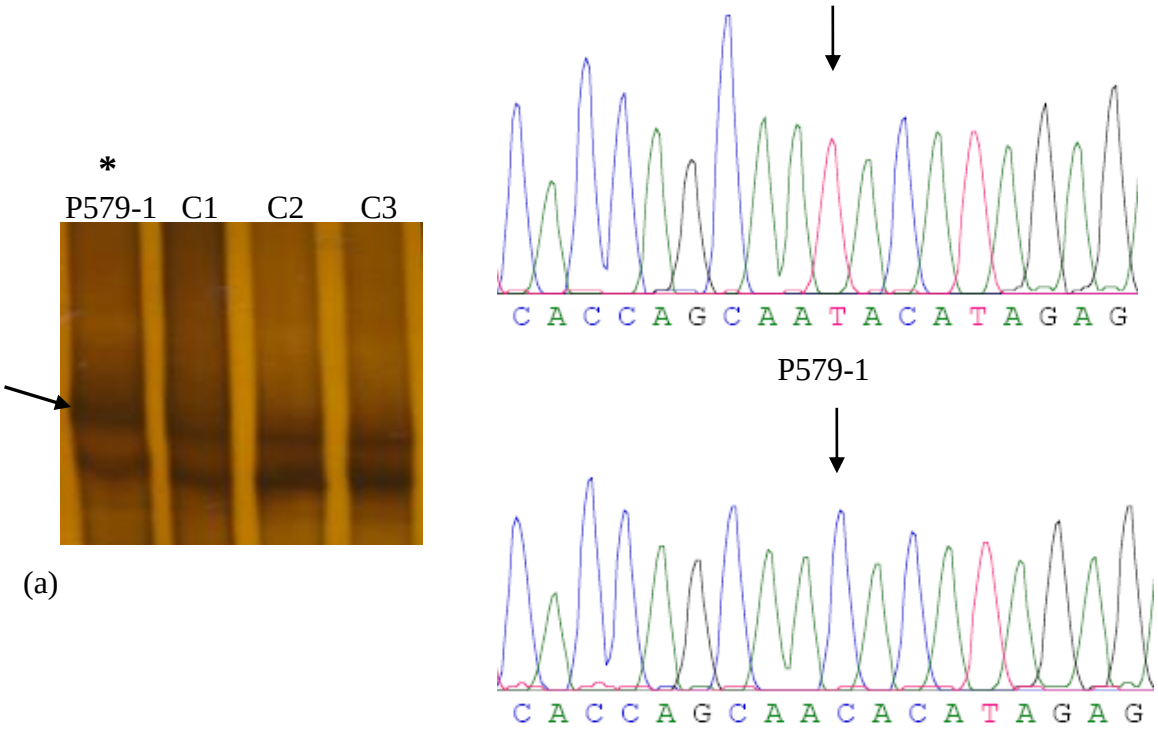

Figure 5.7 (a) 8% SSCP gels showing altered migration pattern for P579-1
(b) chromatograms showing the c.298C>T alteration and the control sequence

Patient P617 showed an aberrant band shift in fragment 2 of *Cx32* gene, and sequencing revealed a hemizygous missense mutation c.490C>T (R164W) which was previously described by Ionasescu *et al.*, 1996. This mutation was found to abolish one of the three AciI restriction site in fragment 2 (Figure 5.8).

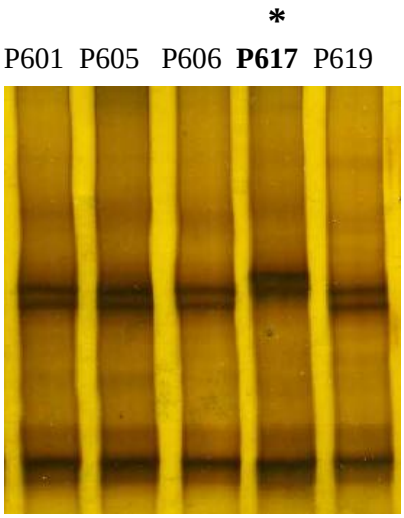

(a)

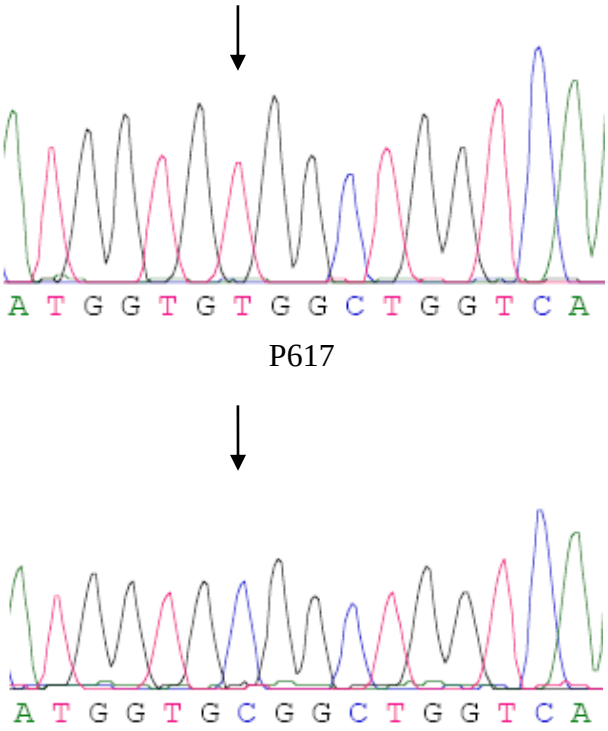

(b)

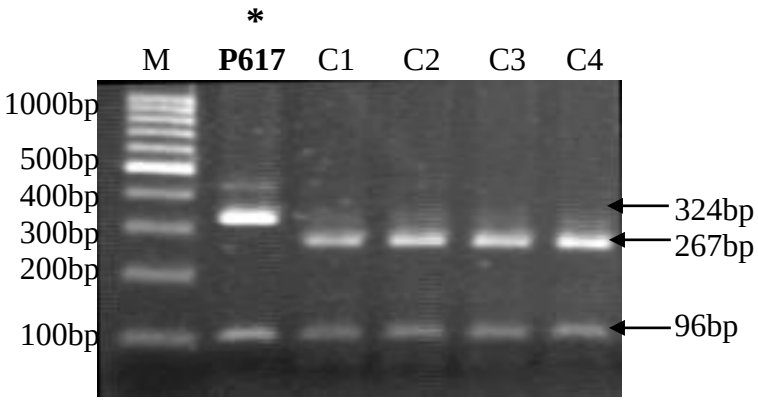

(c)

Figure 5.8 (a) 8% SSCP gel showing altered migration pattern for patient P617 (b) chromatograms showing the c.490C>T alteration and control sequence (c) AciI restriction digestion showing the 324bp and 96bp PCR product in the patient vs 267bp and 96bp products in the controls (57bp additional product in the control and 12bp product in both samples can not be seen on the gel)

5.1.1.2.HRM Analysis. HRM analysis was used to validate the sensitivity and specificity of mutation screening in the cohort with SSCP. Therefore SSCP negative patients were re-screened using HRM analysis. Patient samples with aberrant melting curves, that suggested the presence of a sequence variant in the amplicon were further analyzed by DNA sequencing.

An additional variation was found in fragment 1 of *Cx32* gene for patient P573 that could not be observed by SSCP analysis (Figure 5.9a and 5.9b). Sequencing of the sample DNA revealed missense mutation c.44G>A (R15Q) in hemizygous condition that was previously described by Fairweather *et al.*, 1994 (Figure 5.9c).

A novel hemizygous nonsense mutation was identified in amplicon 3 of *Cx32* for patient P425 which has the same c.763C>T (Q255X) change as P571 (Figure 5.10a and 5.10b). This variation could not been detected by SSCP analysis in the previous studies.

In summary, mutation analysis of *Cx32* gene identified six mutations from 72 analyzed isolated CMT patients and four mutations from 23 X-linked CMT families. All the mutations were previously reported except for I127L and Q255X that are novel sequence variations. The frequency of *Cx32* mutations in our patient cohort was found to be nearly 10% (10/95).

5.1.2. Mutation Analysis of PRPS1 Gene

From the remaining 19 *Cx32* negative familial CMTX cases, we select ten families that were suitable for haplotype analysis with the criteria of having more than one affected individual, and a complete clinical data. These 10 families were subsequently screened for the identified gene for CMTX5 (*PRPS1*- NM_002764). No variation was observed in the screening of the coding sequences and intron-exon boundaries of *PRPS1* either with SSCP (Figure 5.12) or HRM analysis (Figure 5.11). Seven exons of *PRPS1* gene showed identical or similar melting curves for all patient samples and controls, hence no sequence variations.

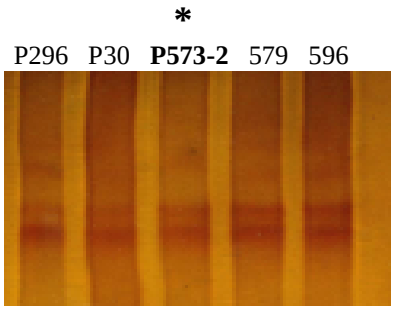

(a)

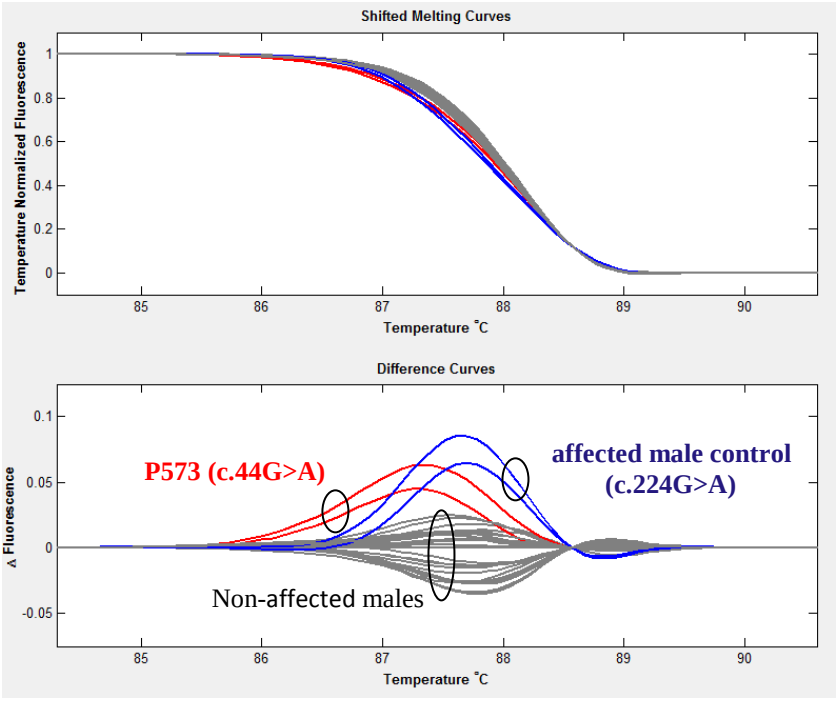

(b)

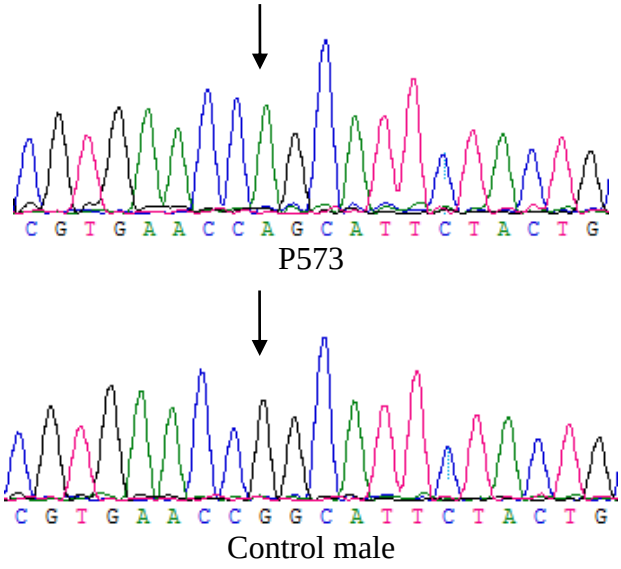

(c)

Figure 5.9 (a) 8% SSCP gel showing fragment 1 of *Cx32* (b) HRM analysis showing the melting curves for fragment 1 of *Cx32* (c) chromatograms showing the c.44G>A change and the control sequence

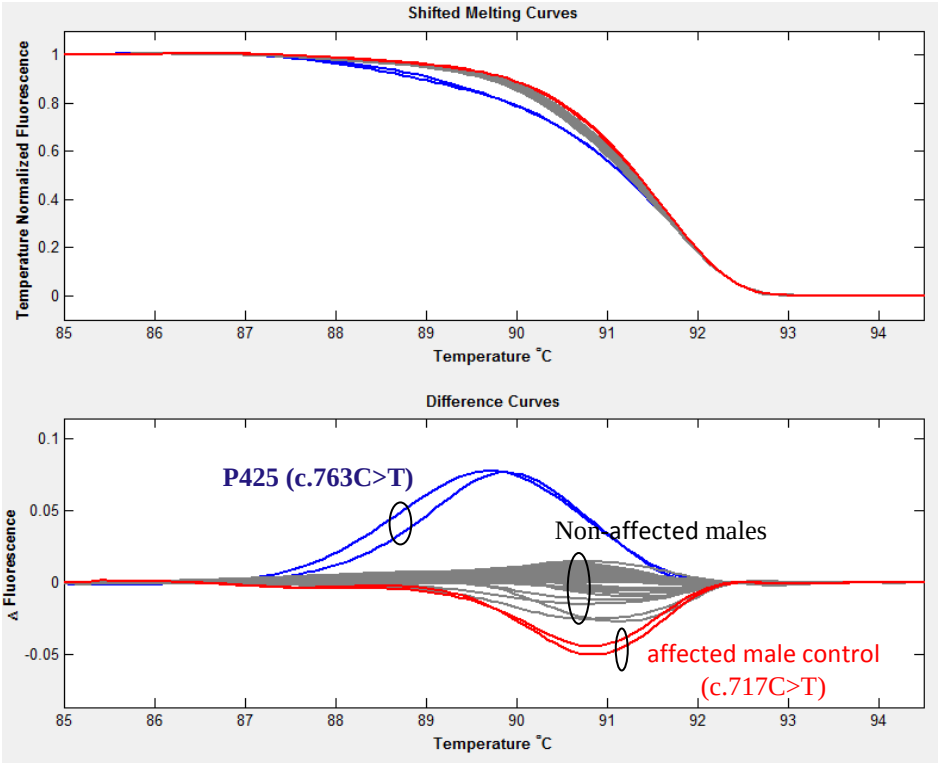

(a)

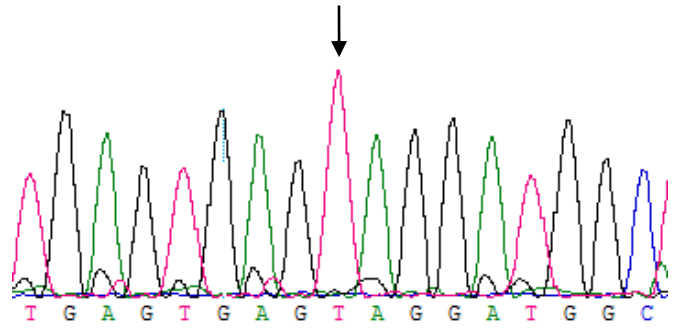

P425

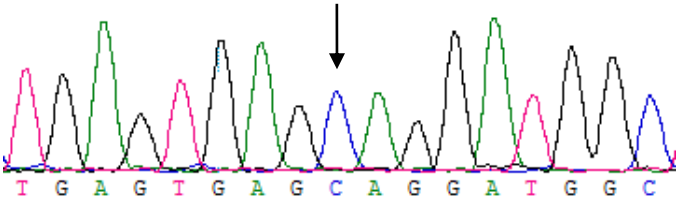

Control male

(b)

Figure 5.10 (a) HRM analysis showing melting curves for fragment 3 of *Cx32* (b) chromatograms showing the c.763C>T change and the control sequence.

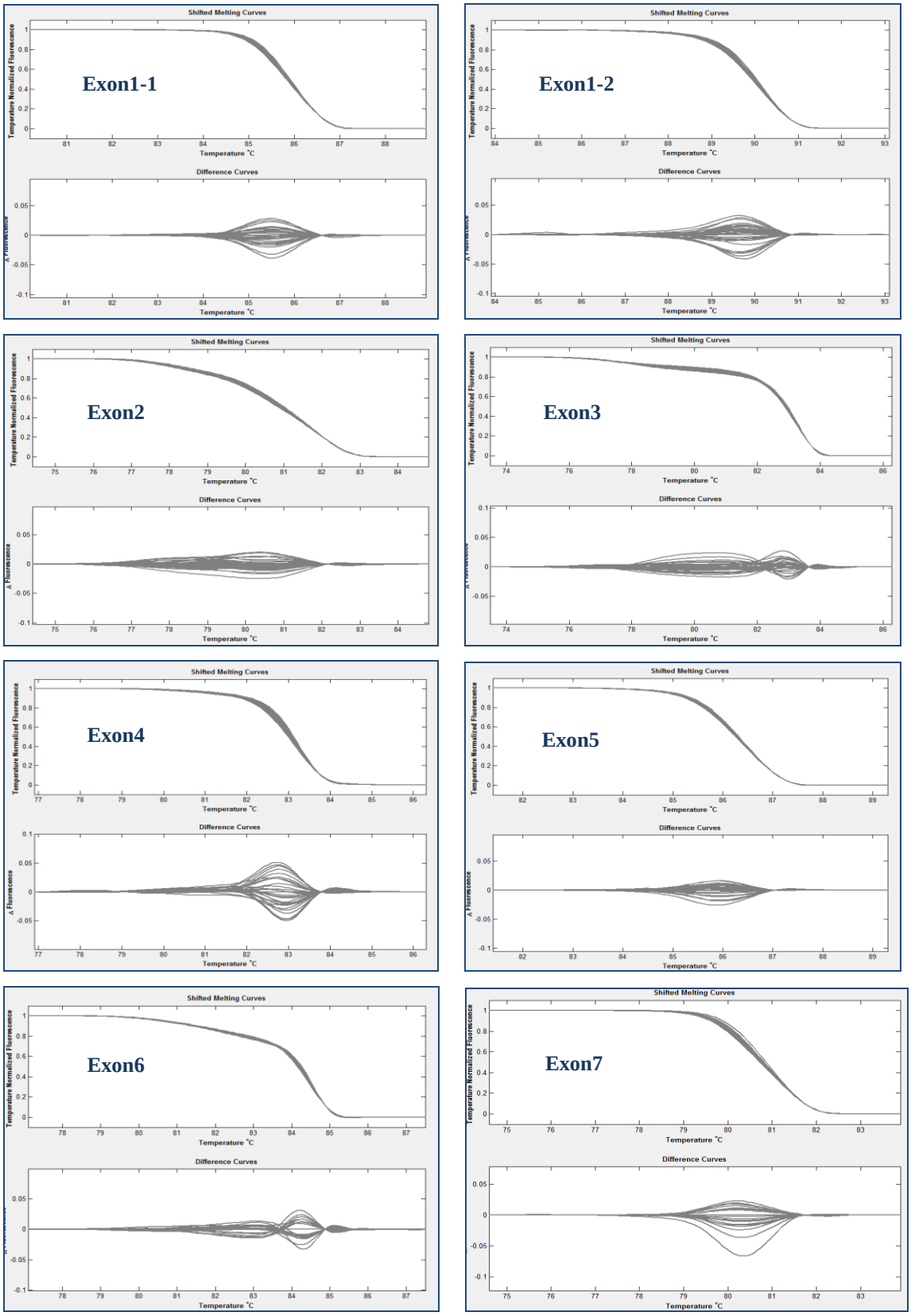

Figure 5.11. Melting curves for seven exons of *PRPS1* gene. For each exon a normalised melt transition (top) and subtractive melting curve (bottom) is shown for patients and control samples

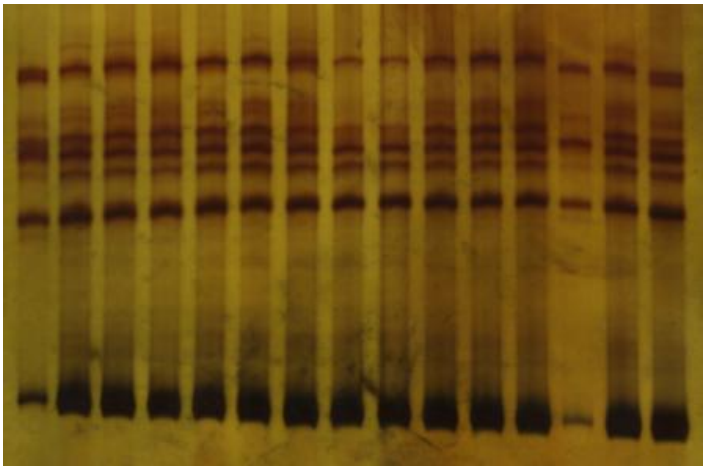

(a)

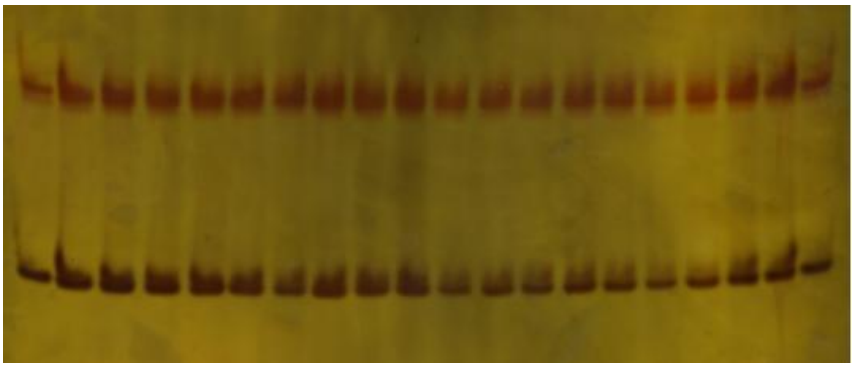

(b)

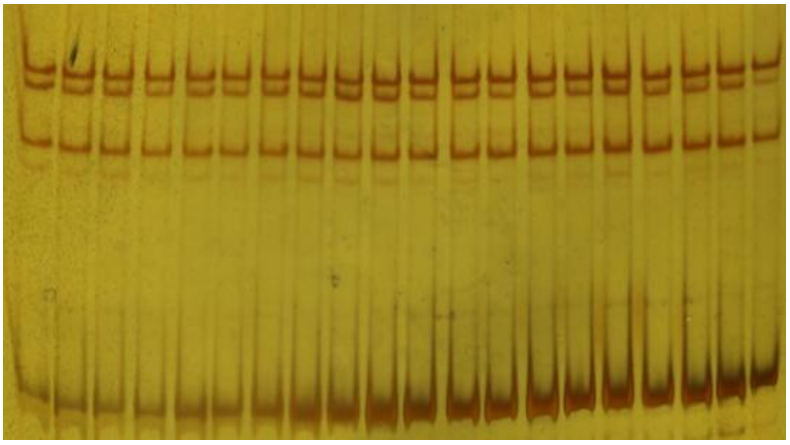

(c)

Figure 5.12. 8% SSCP gels for (a) exon2 (b) exon3 (c) exon5 of PRPS1 gene

5.1.3. Mutation Analysis of PRPS2 Gene

PRPS2 gene (NM_002765) was selected as the highest priority candidate causative gene for CMTX2 in our study since this gene is located in the candidate region and it is related to the CMTX5 causing *PRPS1* gene. Families with a CMTX2 haplotype (P224 and P727) underwent mutation screening for *PRPS2* by using HRM. An aberrant melting difference curve was observed in the patient P727-3.4 in exon 1 and sequencing of this exon reveals a c.45G>A variation (Figure 5.13). This alteration does not change the leucine residue at position 15 and was reported as a polymorphism in the database with the reference number rs1731469.

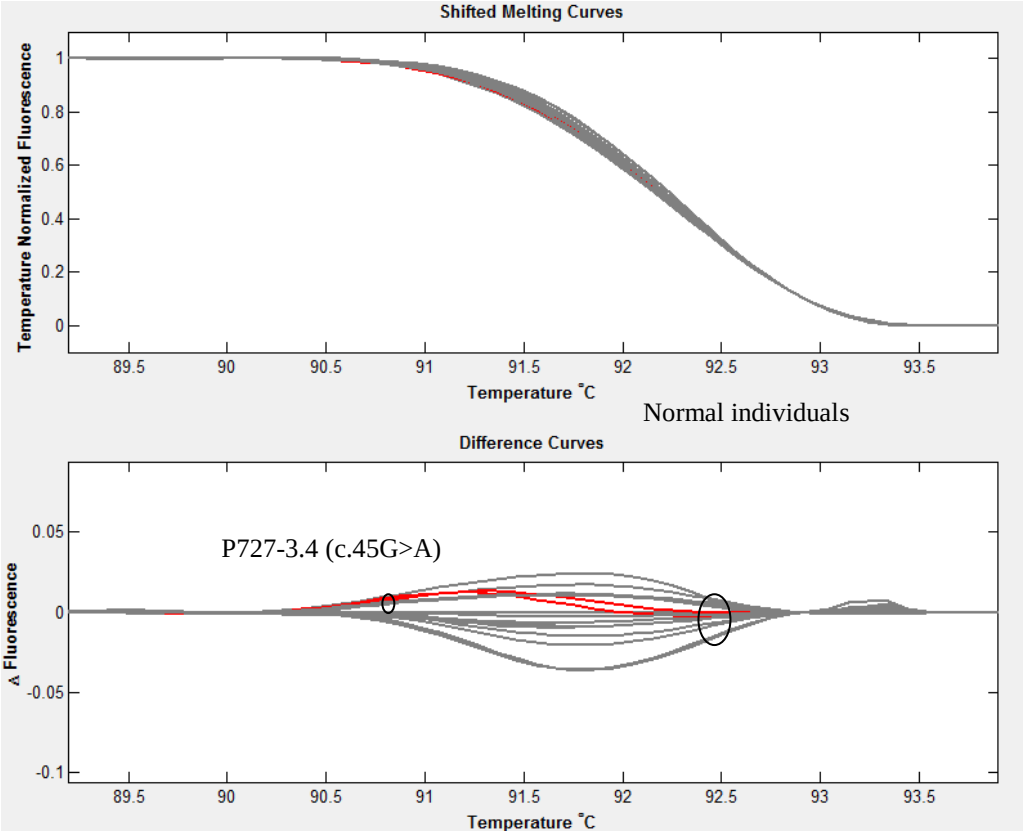

(a)

Figure 5.13. (a) HRM analysis showing the aberrant melting curve of P727-3.4 for *PRPS2* gene exon 1

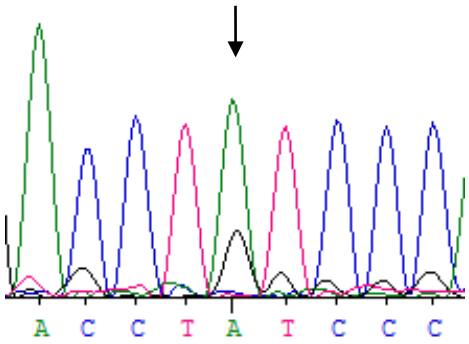

P727-3.4
(b)

Sequence analysis was performed directly on spiked HRM amplicon product. Therefore the wildtype hemizygous allele from the control patient is observed on the sequence analysis as well as the variant allele

Figure 5.13. (b) chromatogram showing the c.45G>A change in P727-3.4

In *PRPS2* gene Exon 6, a different melting profile was observed in 4 out of 11 individuals, which didn't segregate with the disease. Sequencing of individual P224-3.3 revealed a hemizygous c.864+12A>G variation in the non-coding region after exon six (Figure 5.14). This alteration was previously reported as a polymorphism by the reference number rs917580.

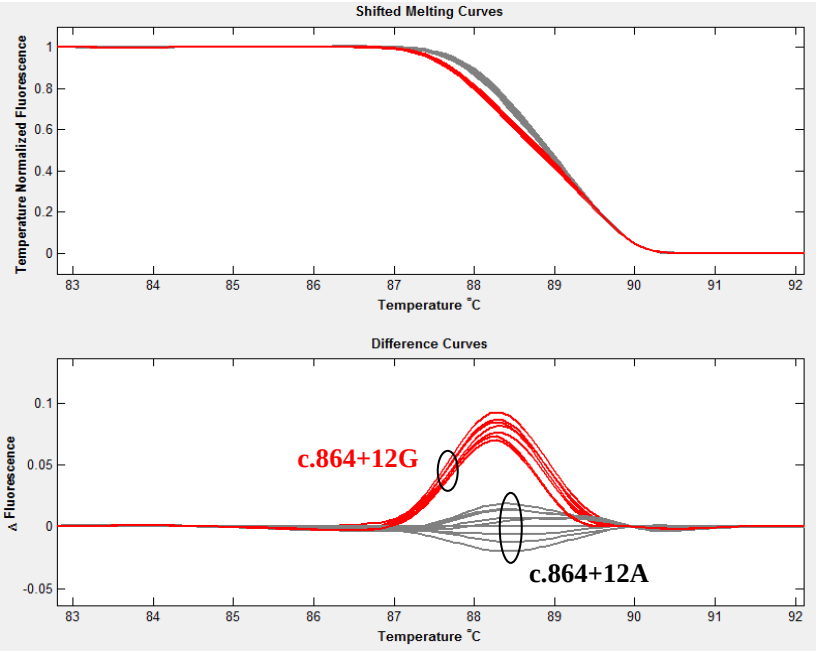

(a)

Figure 5.14. (a) HRM analysis showing the melting curves for *PRPS2* gene exon 6

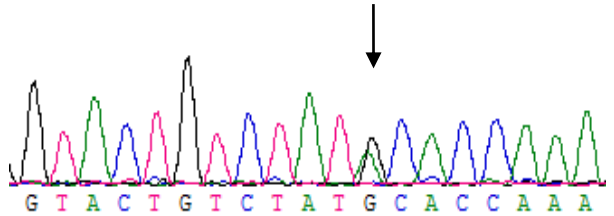

P224-3.3

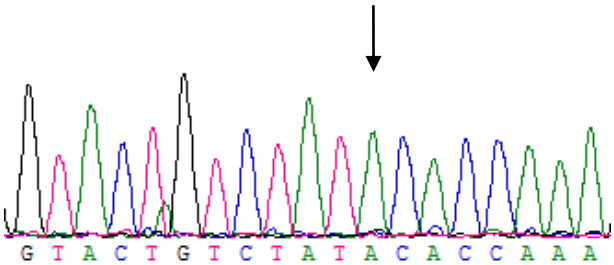

P727-3.5

(b)

Figure 5.14. (b) chromatograms showing the c.864+12A>G and the control sequence

Sequence analysis was performed directly on spiked HRM amplicon product. Therefore the wildtype hemizygous allele from the control patient is observed on the sequence analysis as well as the variant allele.

5.2. Haplotype Analysis

Haplotype analyses for the X-linked recessive loci, CMTX2, CMTX3, and CMTX4 (Cowchock Sendrome) were performed for ten X-linked families that were found to be negative for the known CMTX genes *Cx32* and *PRPS1*. The haplotypes of the family members that were excluded for linkage were given in the Appendix of this thesis.

5.2.1. Haplotype Analysis of CMTX2 Loci

For CMTX2 locus we identified two families (P224 and P727) segregating a CMTX2 haplotype for the seven markers analyzed (Figure 5.16 and 5.17 respectively). Linkage to the locus was excluded in the remaining eight families (Figure 5.15). For family P727, individuals 2.7 and 2.8 showed recombination between markers DXS7108 and DXS8022.

Table 5.1. Summary of variants identified in this study

Index Patient	Gene	Nucleotide Change	Mutation Type	Amino Acid Change
P31	*Cx32*	c.271G>A	Missense	**V91M**
P280	*Cx32*	c.224G>A	Missense	**P75Q**
P527	*Cx32*	c.379A>C	Missense (Novel)	**I127L**
P550	*Cx32*	c.43C>T	Missense	**R15W**
P560	*Cx32*	c.283G>A	Missense	**V95M**
P571	*Cx32*	c.763C>T	Nonsense (Novel)	**Q255X**
P579-1 **P579-2**	*Cx32*	c.298C>T	Missense	**H100Y**
P617	*Cx32*	c.490C>T	Missense	**R164W**
P573	*Cx32*	c.44G>A	Missense	**R15Q**
P425	*Cx32*	c.763C>T	Nonsense (Novel)	**Q255X**
P727-3.4	*PRPS2*	c.45G>A	Polymorphism	**rs1731469**
P224-2.5 **P224-3.3** **P224-3.4** **P470-2.4**	*PRPS2*	c.864+12A>G	Polymorphism	**rs917580**

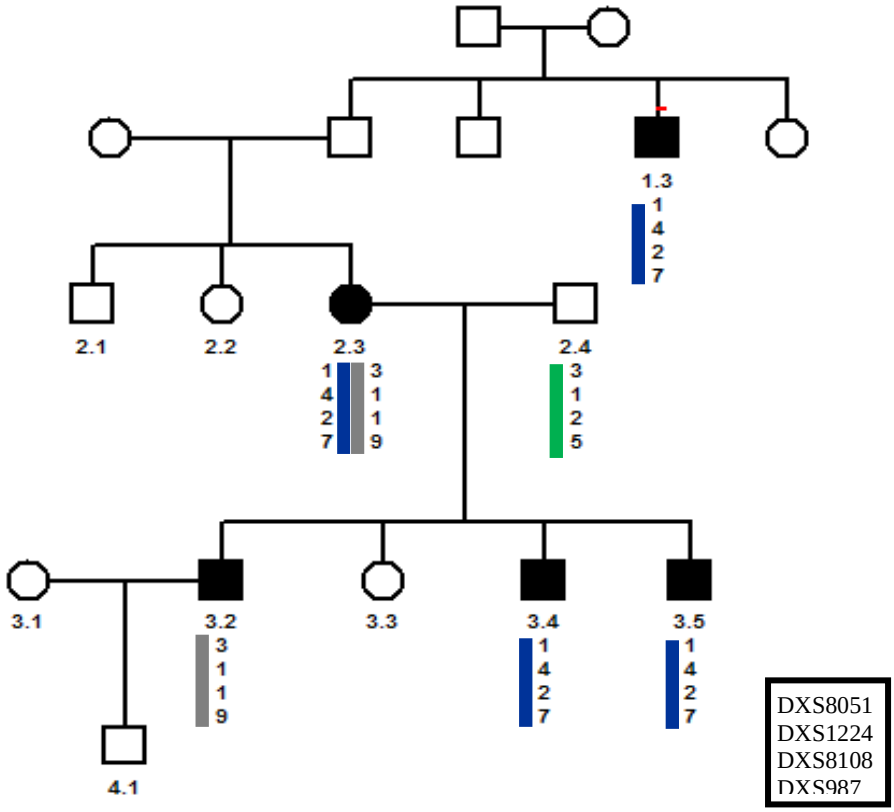

Figure 5.15. Haplotype analyses for family P158, which is excluded for CMTX2 locus. Males are represented by squares, females as circles. Black squares and circles show the affected males and females, respectively. Different colored bars show different haplotypes. The box on the right shows the order of the microsatellites used in the CMTX2 interval from telomere (top) to centromere (bottom)

5.2.2. Haplotype Analysis of CMTX3 Loci

Linkage to CMTX3 locus was excluded in eight of the 10 CMTX families (Figure 5.18). One family (P155) found to have a CMTX3 haplotype segregating with the disease for eight markers defining the CMTX3 interval (Figure 5.19). The haplotype in this family was different from the founder haplotype (5-1-7-1-1-2-4-5) described previously (Brewer *et al*., 2008). One family showed an inconclusive result (Figure 5.20), since we don't have the clinical information about the father of the individual 1.5.

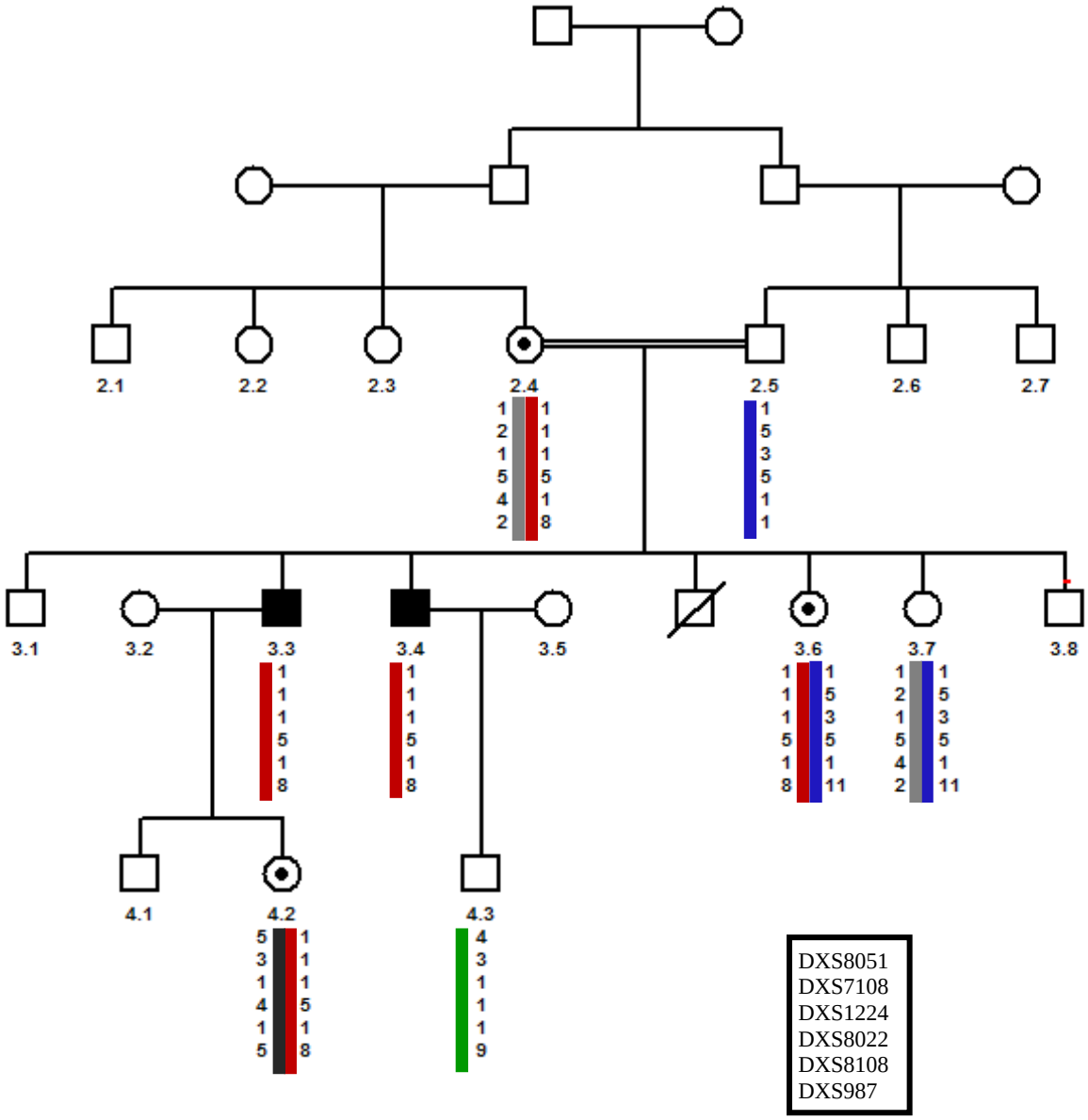

Figure 5.16. Haplotype analyses for family P224 for markers spanning the CMTX2 locus. Males are represented by squares, females as circles. Black squares and circles with central dots show the affected males and female carriers, respectively. Red bars indicate the haplotype segregating with the disease phenotype. The box on the right shows the order of the microsatellites used from telomere (top) to centromere (bottom)

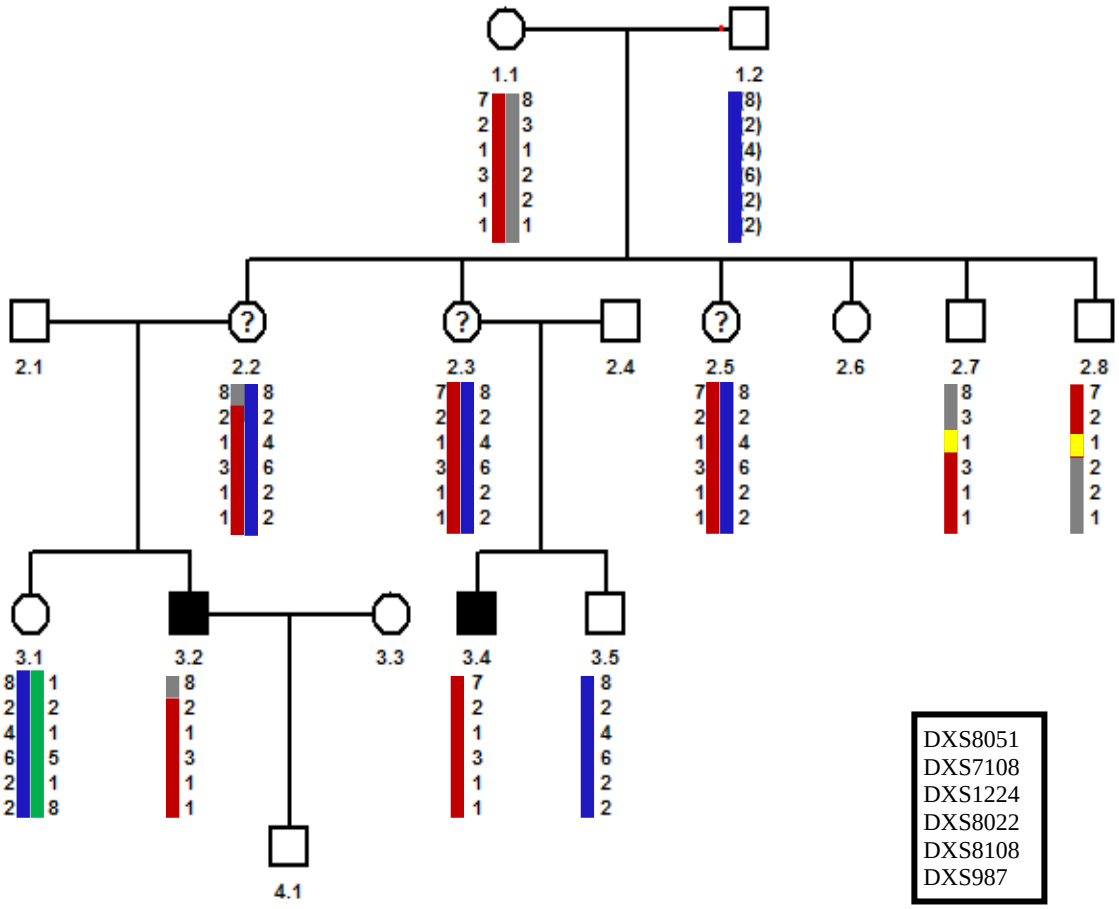

Figure 5.17. Haplotype analyses for family P727 for markers spanning the CMTX2 locus. Males are represented by squares, females as circles. Black squares show the affected males and circles with question mark show possibly affected females. Red bars indicate the haplotype segregating with the disease phenotype. Yellow bar shows the uninformative marker for this family (DXS1224). Brackets indicate the infered haplotypes. The box on the right shows the order of the microsatellites used from telomere (top) to centromere (bottom)

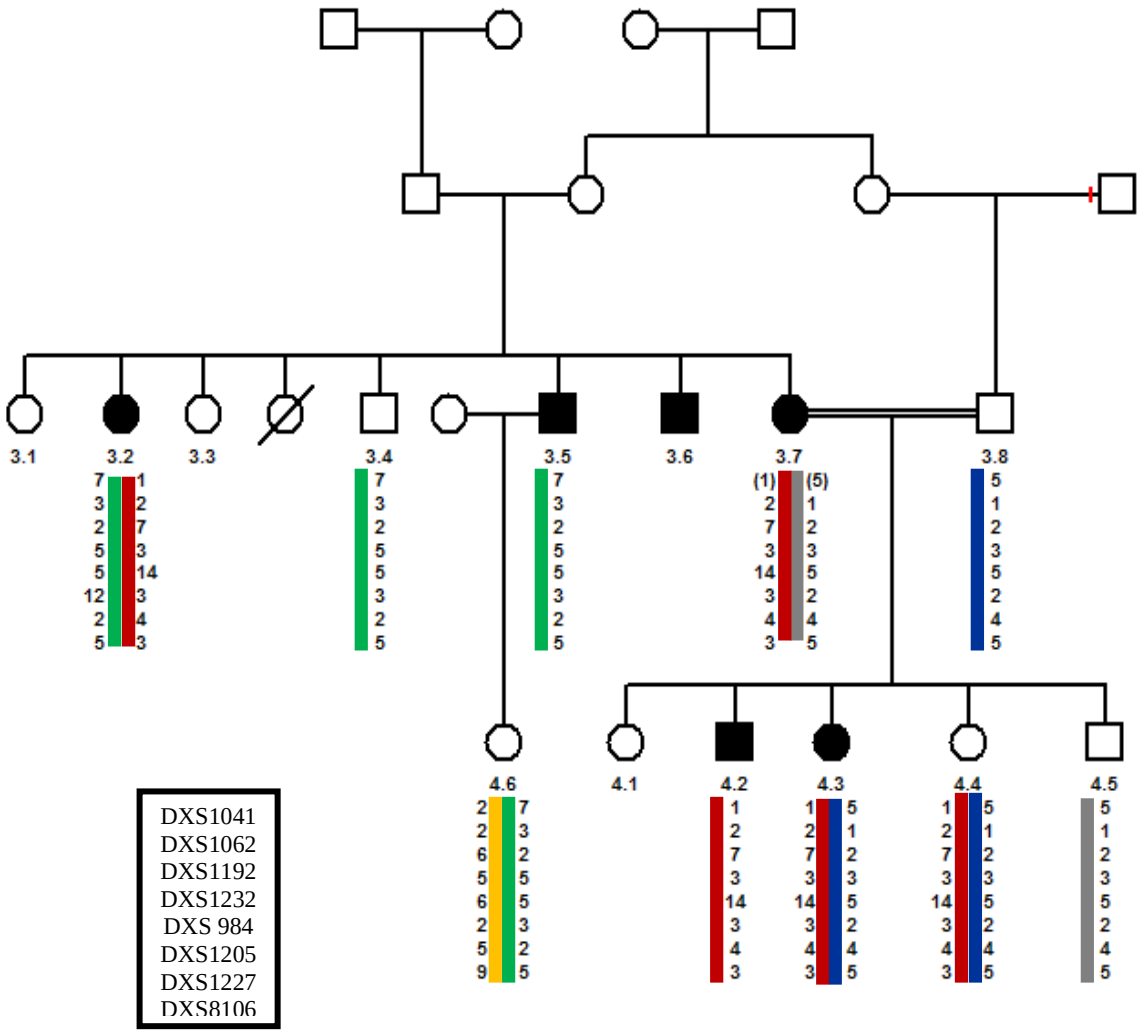

Figure 5.18. Haplotype analyses for family P444 for markers spanning the CMTX3 locus. Males are represented by squares, females as circles. Black squares and circles show the affected males and females, respectively. Different colored bars indicate different haplotypes. The box on the left shows the order of the macrosatellites used from centromere (top) to telomere (bottom)

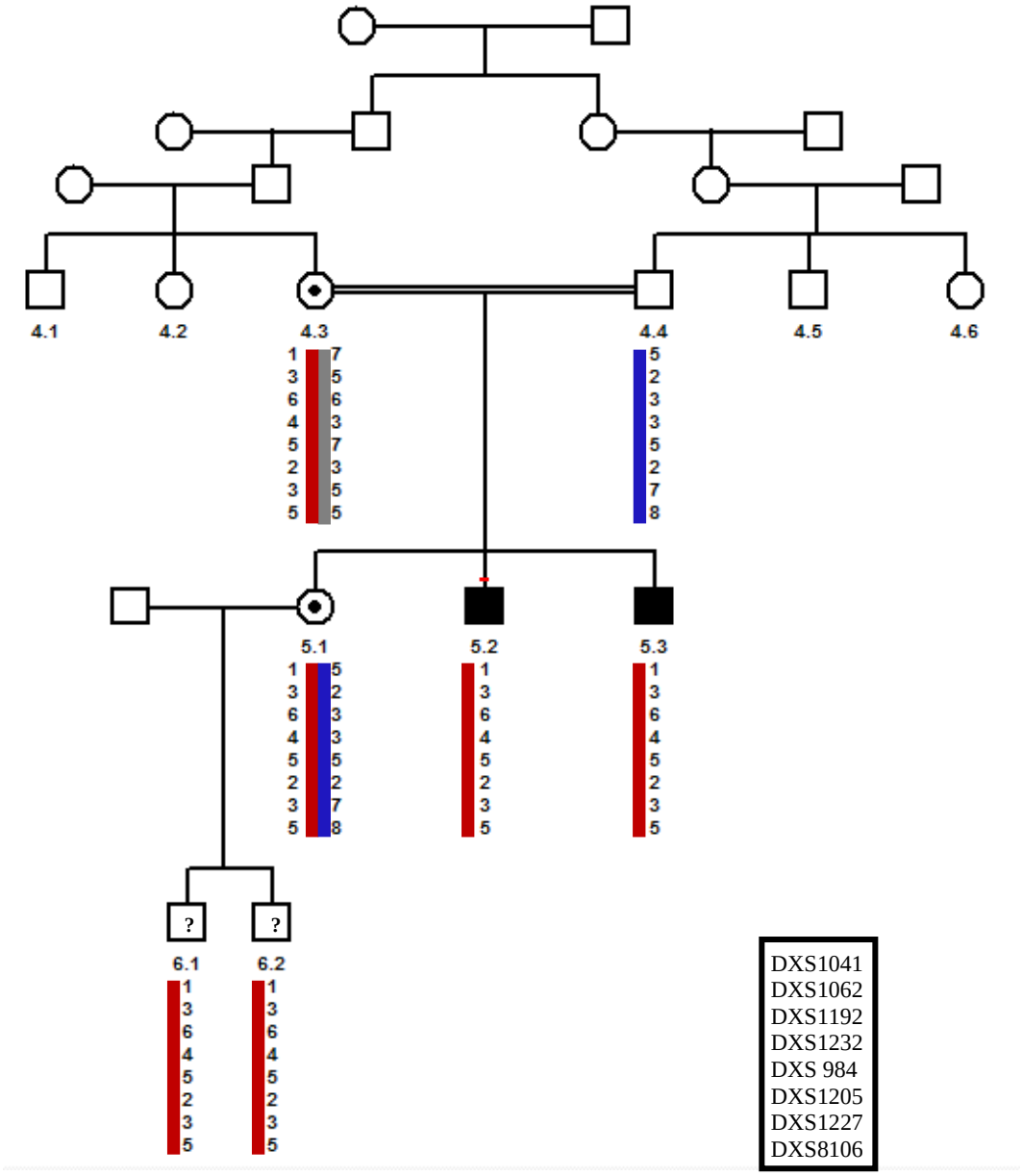

Figure 5.19. Haplotype analyses for family P155 for markers spanning the CMTX3 locus. Males are represented by squares, females as circles. Black squares and circles with central dots show the affected males and female carriers, respectively. Red bars indicates the haplotype segregating with the disease phenotype. The box on the right shows the order of the macrosatellites used from centromere (top) to telomere (bottom)

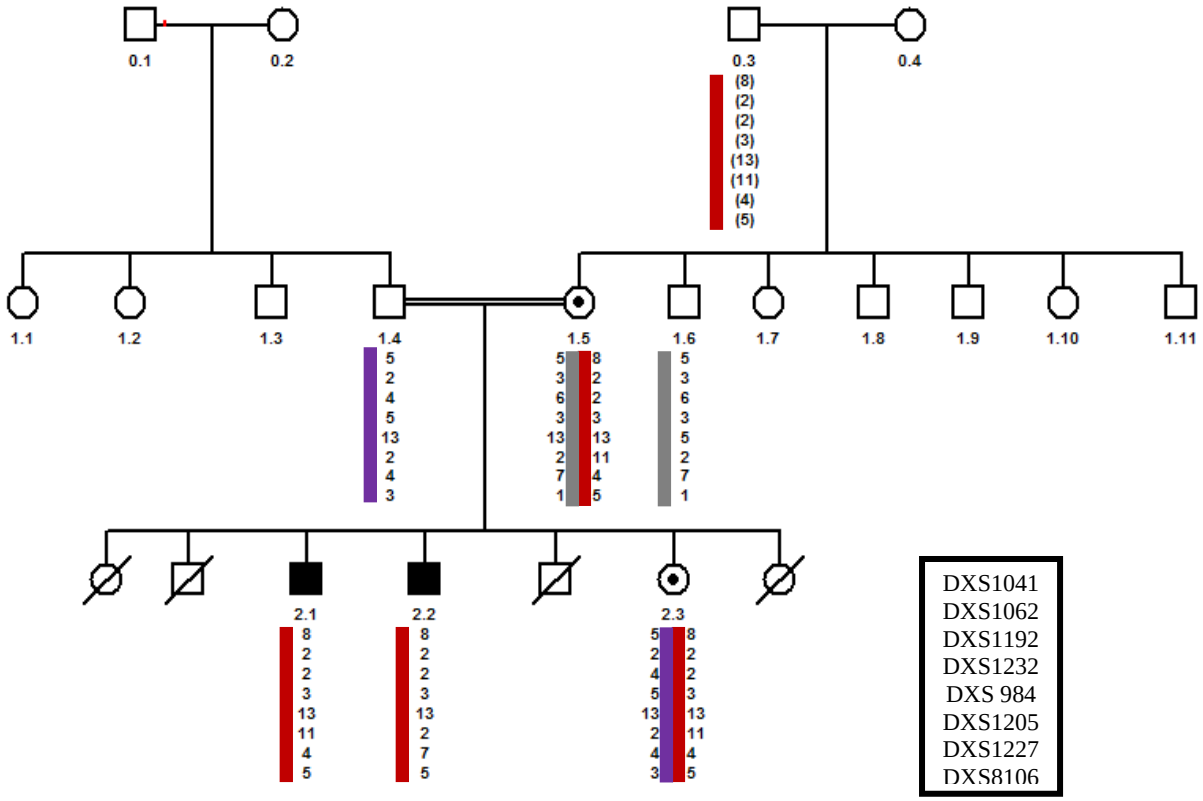

Figure 5.20. Haplotype analyses for family P408 which is inconclusive for CMTX3 locus. Males are represented by squares, females as circles. Black squares and circles with central dots show the affected males and female carriers, respectively. Different colored bars indicate different haplotypes. Question mark shows the individual with unknown clinical information. Bracket indicates the infered haplotype. The box on the right shows the order of the macrosatellites used from centromere (top) to telomere (bottom)

5.2.3. Haplotype Analysis of CMTX4 (Cowchock Disease) Loci

One family (P408) showed a CMTX4 haplotype segregating with the disease phenotype for the three markers analyzed in CMTX4 interval and linkage to this locus was excluded in nine families (Figure 5.21).

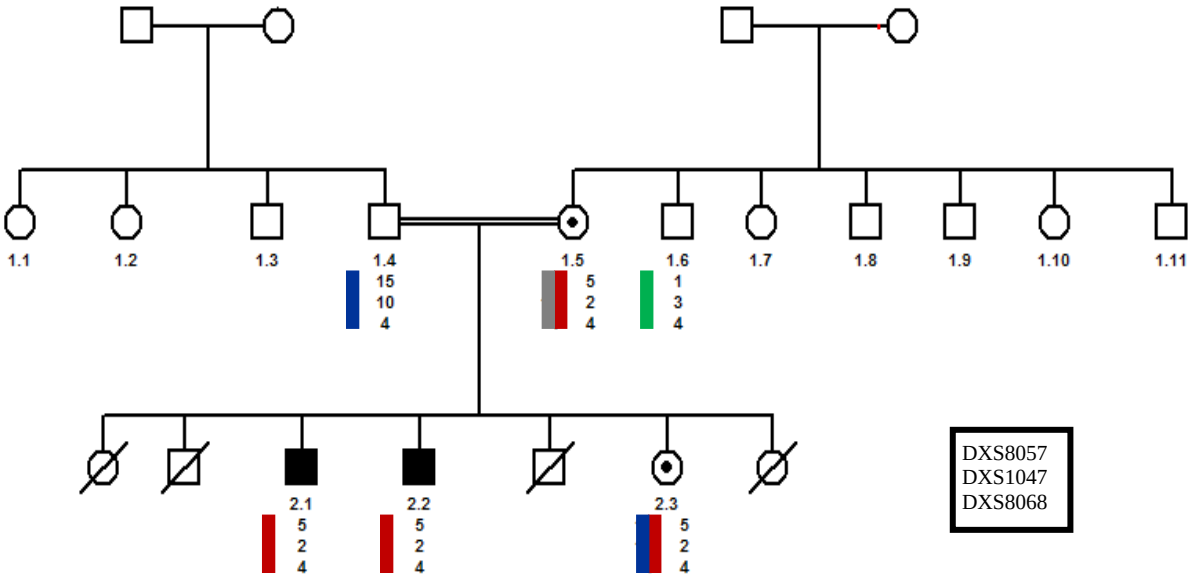

(a)

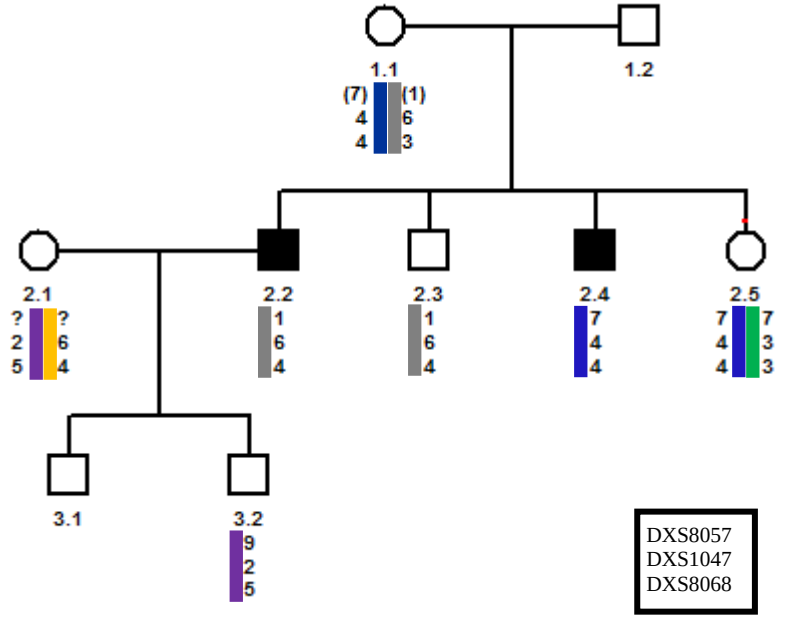

(b)

Figure 5.21. (a) Haplotype analyses for family P408 for markers spanning the CMTX4 locus. (b) Haplotype analyses for family P192 for markers spanning the CMTX4. Males are represented by squares, females as circles. Black squares and circles with central dots show the affected males and female carriers, respectively. Red bars indicates the haplotype segregating with the disease phenotype. The box on the right shows the order of the macrosatellites used from centromere (top) to telomere (bottom)

6. DISCUSSION

In this study, genetic loci known to be responsible for X-linked form of Charcot-Marie-Tooth (CMT) disease were investigated in 95 patients and their relatives for mutations and linkage. The cohort was a mixture of familial (N=23) and isolated (N=72) cases. All patients presented with a CMT diagnosis having moderately reduced nerve conduction velocities and deymelinating or axonal symptoms. The patients were found to be negative for the CMT1A duplication as well as *PMP22* and *MPZ* point mutations in our previous studies.

6.1. Mutation Analysis of *Cx32* Gene

CMTX accounts for up to 15% of all CMT cases, making it the second most common form of CMT after the CMT1A duplication (Dubourg *et al.*, 2001). There are five known loci for X-linked CMT (CMTX1, CMTX2, CMTX3, Cowchock Syndrome and CMTX5). CMTX1 accounts for almost 90% of all X-linked CMT cases (Ressot and Bruzzone, 2000) and is caused by mutations in the *Cx32* gene on Xq13.

In this study, 10% of the patients were found to be positive for *Cx32* gene mutations suggesting that the gene represent a major cause of the X-linked CMT also in our patient cohort although the prevalence is slightly lower than that of other reports. This low prevalence might be due to the possibility of presence of misdiagnosed cases in our cohort since CMTX cannot be distinguished from CMT2 and CMT1 phenotypically. Besides, we had only screened the coding region and exon-intron boundries of *Cx32* gene, but the pathogenic variations could reside in the regulatory regions, promotors or in the introns introducing novel splice sites. However, our data supports the hypothesis that X-linked CMT is a genetically heterogeneous disorder.

Cx32 is a member of highly conserved proteins that form gap junctions (Bruzzone *et al.*, 1996). Gap junctions are formed by docking of two hemichannels in the neighbouring cells and each hemichannel is made from six connexin molecules (Bruzzone *et al.*, 1996) In myelinating Schwann cells, Cx32 is localized to noncompact myelin in the incisures

and the paranodes (Bergoffen *et al.*, 1993), and allows the diffusion of ions and small molecules across the myelin sheath (Paul, 1995) which is important for their maintanence and communication. The protein composed of four transmembrane segments, two extracellular loops, and three cytoplasmic domains (Bennett *et al.*, 1991) (Figure 6.1).

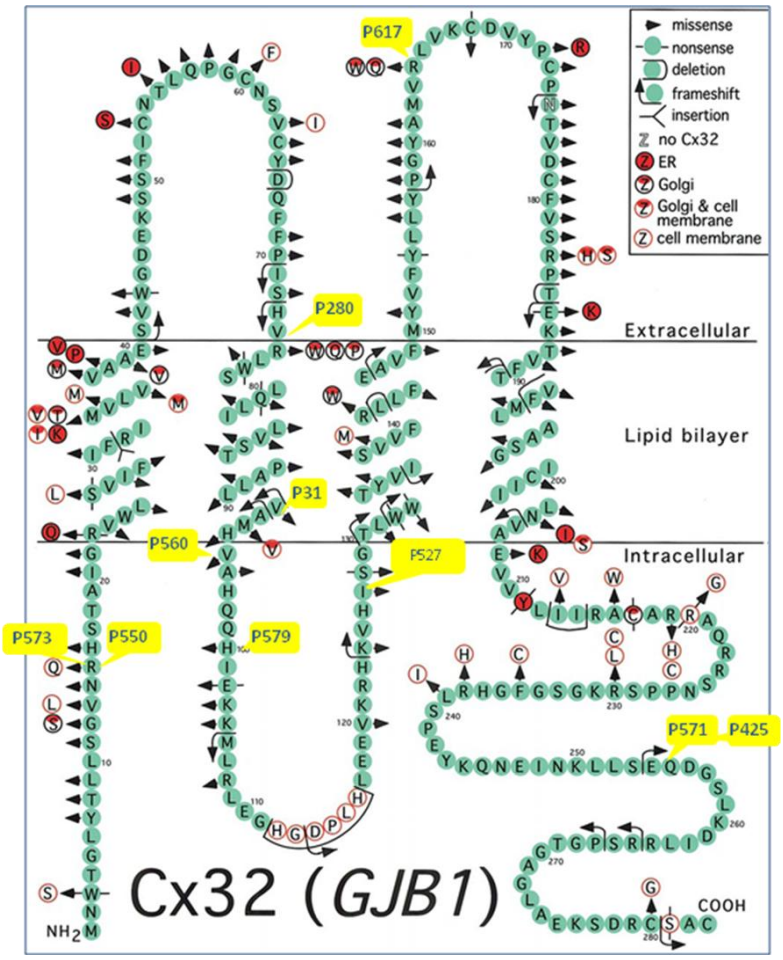

Figure 6.1 Cx32 protein and locations of the mutations identified in this study. (Diagram of Cx32 protein is taken from Yum *et al.*, 2002)

More than 260 different CX32 mutations were identified up to date. All different types of mutations including missense, frameshift, deletion and nonsense mutations were present. Cx32 mutations can have different affects on the function of the protein. Some mutations have a loss-of-function effect in which there is no expression of functional channels. On the other hand, some mutations can cause a dominant negative effect in which abnormal accumulation of Cx32 proteins in the cytoplasm, ER and Golgi apparatus prevents the trafficking of the wild type proteins to the membrane. In some cases the

connexin protein can be normally transported to the cell membrane but can not form functional cell–cell channels because they are unable to dock with hemichannels in the opposing membrane. Lastly, many mutant forms of Cx32 can form functional channels, but the electrophysical properties of these channels are altered. (Ressot *et al.*, 1998).

We screened Cx32 mutations in 23 CMT families with X-linked inheritance and 72 isolated CMT patients. We identified eight missense and two nonsense mutations in ten patients. Six of these mutations were found in isolated CMT patients and four of the mutations were identified in CMTX families indicating that Cx32 mutations were common in familial rather than isolated cases.

Patient P31 is a 46 years old male, who has abnormal mobility, distal weakness in his upper limbs and *pes cavus.* His motor nerve conduction velocity is 36.5 m/s, which is slower than normal. In the screening of Cx32 gene we identified a c.271G>A change which results in V91M substitution. Although a nonpolar amino acid is substituted by another nonpolar residue, the location of this mutation is in the 2nd transmembrane domain that is important for close packing of the channel (Figure 6.1). It is known that the second and the fourth transmembrane domains of the Cx32 protein share a degree of structural symmetry with similar amino acids in equivalent positions that is important for the packing of four helices (Tadmouri *et al.* 2000). Replacement of the conserved valine by methionine (Figure 6.2) in the middle of the fourth helix might disrupt the structural symmetry and functional channel formation.

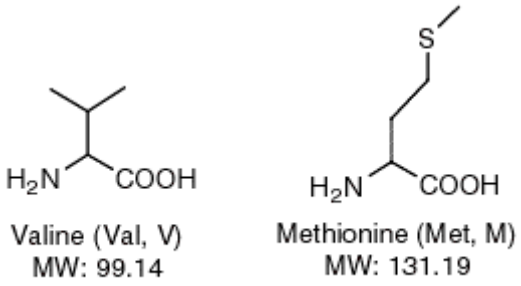

Figure 6.2 Structure of Valine and Methionine amino acids.

In patient P280 who has abnormal mobility, distal weakness in the upper limbs and *pes cavus* we identified a missense mutation c.224G>A that leads to the replacement of an

arginine with a glutamine at position 75 which is located in the 2nd transmembrane domain (Figure 6.1). There is a salt bridge network between Arg75 and Glu41 in the extracellular loop which is important for the folding of the protein (Figure 6.3). Neutralization of the positive charge of the arginine residue in this network may impair the formation of a functional protein. (Silander *et al.*, 1997)

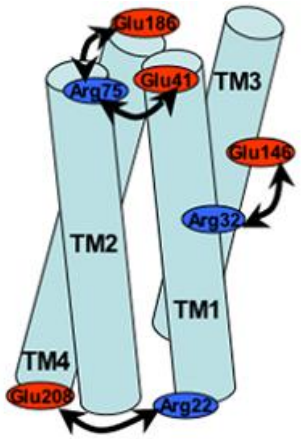

Figure 6.3. Salt bridge network in the 1st extracellular domain is Cx32 protein

Patient 527 has distal weakness and atrophy in all limbs. He was found to carry a novel missense c.379A>C alteration, which results in the substitution of a isoleucine into a leucine at position 127. Since the amino acid substitution occurs at a highly conserved residue (Figure 5.3c) and the same migration pattern wasn't observed in the SSCP analysis of 25 normal individuals, it is unlikely that this change is a common polymorphism. Although both residues are nonpolar and neutral, the mutation is located in the cytoplasmic domain which is important in the chemical gating response (Figure 6.1). There is another mutation located in the same residue shown to cause CMTX previously (Vondracek *et al.*, 2005).

Patient P550 was found to carry a hemizygous missense mutation (c.43C>T). This mutation results in arginine to tryptophan change and previously reported (Nelis *et al.*, 1996). This variation was absent in 25 healthy individuals in the restriction analysis, which shows it is not a common polymorphism. The same aminoacid change is also observed in patient P573, which changes the arginine to glutamine (Figure 6.1). Both mutations result in the neutralization of the negative charge at the N terminal tail of the

Cx32 protein that brings the polypeptide chain to the endoplasmic reticulum and have a role in the voltage gating properties (Falk *et al.,* 1994).

Patient P560 is a 48 years old male, he has abnormal mobility, distal weakness in all limbs, *pes cavus* and sensory ataxia. His motor NCV is 35 m/s. Mutation screening of P560 revealed a c.283G>A change, which leads to substitution of a valine into methionine at position 95. It is the first residue in the cytoplasmic loop (Figure 6.1) and in vitro studies of the same mutation showed loss of function (Bone *et al.*, 1995).

In patient P571 and P425 we identified a novel nonsense mutation c.763C>T (Q255X) which causes a premature stop codon (Figure 6.1). It is known that nonsense mutations that cause truncations after codon 211 form functional gap junctions, but these channels may be biophysically different from the wild-type channels. (Castro *et al.,* 1999; Rabadan-Diehl *et al.,* 1994; Ressot *et al.,* 1998). They may cause altered trafficking in myelinating Schwann cells or they may not reach to the incisures or paranodes of the myelinating Schwann cells, instead remain in some other areas of the Schwann cell membrane.

Patient P579-1 is a 18 years old male and his 14 years female cousin also affected. They both have slow motor NCVs. The female cousin has tremor and cerebellar dysfunction and the male has *pes cavus* and tremor. We identified a c.298C>T substitution which changes a polar charged histidine into a nonpolar neutral tyrosine at position 100. His female affected cousin has the same change in heterozygous state. The mutation is located in the cytoplasmic loop (Figure 6.1) and affects the ion permeability of the channel (Bone *et al.*, 1997).

Patient P617 has CNS involvement in addition to typical CMTX features and was found to carry a missense mutation, c.490C>T. This mutation changes the arginine at position 164 to tryptophan. Arg164 were found to be mutated in more than one family and described as a hot spot for mutations (Ionasescu *et al.*, 1996, Oterino *et al.*, 1996, Bort *et al.*, 1997, Haites *et al.*, 1998, Mostacciuolo *et al.*, 1999, Dubourg *et al.*, 2001,Young *et al.*, 2001,Casasnovas *et al.*, 2006, Mandich *et al.*,2008). The substitution of the basic arginine

to a non-polar tryptophan in extracellular domain 2 (Figure 6.1) results in poor hemichannel interaction and the mutated protein showed to be retarded in Golgi.

6.1.1. Comparison of SSCP and HRM analysis for mutation detection

Single strand conformation polymorphism (SSCP) is based on the conformation difference that occurs during renaturation of single stranded DNA with differences in the nucleotide sequence (Orita *et al.*, 1989; Hayashi, 1992). It is a cost efficient method for the screening of multiexon genes, however it is time consuming and requires post PCR processes. The PCR products must be denatured by heat and chemicals, allowed to renature, and must be loaded to acrylamide gels that should run overnight. Results can be obtained in a three days time. In addition, sensitivity of SSCP analysis is known to be about 80% if fragments are shorter than 300 bp (Glavac and Dean, 1993; Hayashi and Yandell, 1993). It is shown that addition of glycerol solutions to SSCP gels will lower the pH and can increase the sensitivity (Kukita *et al.*, 1997).

Alternative mutation screening methods such as high resolution melting (HRM) analysis offers a modern age technology that is rapid, sensitive, and cost-efficient. HRM analysis is based on the melting of the DNA double helix that has been amplified in the presence of a saturating fluorescence double-stranded DNA binding dye. As DNA becomes single stranded, the dye is released and the fluorescence signal decreases. HRM technology is possible because of the dye chemistry and the high resolute acquisition of fluorescent data over many temperature points. Mutation detection sensitivity was found to be 100% for the amplicons under 400 bp and up to 80% GC content in previous studies (Zhou *et al.*, 2004). Tm difference increases as the amplicon size decreases, which allows better detection.

In HRM analysis both amplification and analysis can be performed in the same tube without requirements of any post-PCR procedures. This also reduces the possibility of contamination and errors. Analysis will take 10 min after PCR amplification. Another advantage is that the method does not require labeling of primers. The same primers used in normal PCR amplification can also be used in HRM analysis.

The only problem of HRM analysis is its sensitivity in the detection of homozygous mutations. Although most of the homozygous sequence changes produce a Tm shift compared to the wild type some of them do not change the Tm at all and cannot be detected. Approximately 84% of human SNPs involve a base exchange between A::T and G::C base pairs, and these homozygotes can easily be detected by melting temperature shifts. However, in 16% of the SNPs the bases only switch strands and preserve the base pair, which produces a very small Tm differences and 4% of total SNPs show nearest-neighbor symmetry in which the adjacent bases to SNPs are identical on both strands and these homozygotes have the identical melting temperatures (Liew *et al*, 2004- Figure 6.4). In order to prevent this problem, samples should be mix with a reference wild type DNA to allow the hetero-duplex formation.

Heterozygous samples can be identified by differences in melting curve shape. Heterozygous samples produce heteroduplexes that melt at lower temperatures than homoduplexes. Melting curves of amplified heterozygotes include both homoduplexes and heteroduplexes which results in a skewed melting curve that can be easily differentiated (Liew *et al*, 2004 and Graham *et al*, 2005).

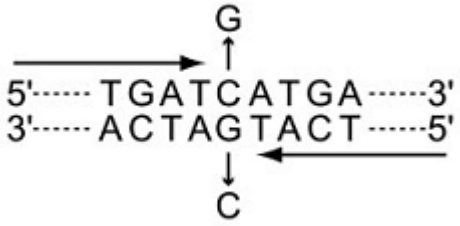

Figure 6.4. Nearest neighbour symetry (Liew et al, 2004)

The fluorescence dye used is a significant factor affecting the efficiency of HRM. The dye should be a saturating dye like LC Green plus. Conventional dsDNA dyes like SYBR Green 1 cannot be used at high concentrations since they inhibits PCR at 50% saturation and causes dye redistribution during melting analysis. Saturation of dsDNA binding sites eliminates potential for dye redistribution during melting curve acquisition. It was shown that LC green doesn't inhibit or adversely affect the PCR amplification at high amounts (Wittwer *et al.*, 2003).

Another advantage of HRM analysis is its efficiency in detection of deletion and duplications. Other mutation screening methods like SSCP often fails for the detection of small deletions and duplications. (Kennerson *et al.*, 2007 and Vaughn *et al.*, 2004). HRM analysis is also sensitive in analyzing larger amplicons that carries multiple melting domains. An aberrant shape may occur in any portion of the melting curve which shows the sequence variation in one domain.

In this study, we used both SSCP and HRM analysis for mutation screening to compare sensitivity and specificity of the two methods. Two patients those are negative for SSCP analysis, showed mutations with HRM analysis. For patient P573, the mutation (c.44G>A) was located at the beginning of the exon close to the primers. And for patient P425 the mutation (c.763C>T) is located at the 3' end of the exon close to the primers again. This might be the reason for the escape of those variations from SSCP detection; however, mutations in the same location were detected in patients P550 and P579-1 by SSCP analysis. These results show the inconsistency of SSCP and prove that HRM analysis is also sensitive for the detection of mutations close to the primers which was previously reported (Kennerson et al, 2007).

HRM analysis is especially suitable for screening multi-exon genes that can reduce the sequencing cost in a significant amount. It allows the analysis of samples that may carry the same common mutation at once without any need for sequencing. This is not the case for CX32 mutations since more than 200 different mutations have been identified up to date. But we can conclude that HRM is a very efficient method for mutation screening.

6.2. Mutation Analysis of *PRPS1* Gene

From 23 familial CMTX cases, 19 were found to be negative for *Cx32* gene after both SSCP and HRM screening. We have selected 10 of these families that have a high number of members with available DNA samples and have almost complete clinical data. Initially these 10 families were screened for the *PRPS1* gene that has been recently associated with CMTX5 in a Korean family (*Kim et al*, 2007). *PRPS1* encodes a metabolic enzyme that is critical for purine metabolism and nucleotide biosynthesis. The protein is highly conserved among different species from zebrafish to human (*Kim et al*, 2007). The

family carrying the *PRPS1* mutation showed a unique symptom triad of hearing loss, visual impairment, and peripheral neuropathy. One of our patients in family P408 had similar symptoms with peripheral neuropathy, deafness, and bilateral cataracts. This family and the remaining nine families didn't show any sequence variants when screened by both SSCP and HRM analysis. This result suggested that *PRPS1* is a very rare cause of CMTX with a special phenotype. On the other hand, no additional families other than the Korean family have been reported to have mutation in this gene so far and its involvement in CMT is still controversial.

6.3. Haplotype Analysis

Ten CMTX families negative for the most common CMT1A duplication and *PMP22* and *MPZ* point mutations were also found to be negative for the known CMTX genes *Cx32* and *PRPS1*. Segregation Analyses of haplotypes were therefore undertaken for the other known CMTX loci: CMTX2, CMTX3 and Cowchock Syndrome (CMTX4).

These ten families were not large enough to give statistically significant results in linkage analysis. Since these families are important for providing further evidence for involvement of these loci in X-linked CMT, linkage was tested only by haplotype analysis.

CMTX2 is maps Xp22.2 and characterized by infantile onset, atrophy with weakness of the lower leg muscles, areflexia, *pes cavus*, and mental retardation in two of the four affected males (Ionasescu *et al.,* 1991). No other families or further research has been published on CMTX2 since 1991. In our study, two affected brothers in Family P224 had a late onset with slowed nerve conduction velocities and distal weakness in the upper limbs (Table 6.1) and were found to have CMTX2 haplotype segregating in affected individuals (Figure 5.15).

In addition, family P727 showed a CMTX2 haplotype segregating with affected individuals and carrier females. Interestingly, two unaffected males were found to be recombinant for this haplotype. One of the unaffected males carries the proximal portion and the other unaffected male carries the distal portion of the disease haplotype. This

suggested that the disease gene may be located around this breaking point. Unfortunately the marker at the breaking point (DXS1224) was uninformative in this family (Figure 5.14) but the data suggest that the disease gene maps between markers DXS7108 and DXS8022. Additional genotyping of markers between DXS7108 and DXS8022 will be required to further narrow the region.

Table 6.1. Clinical and electrophysiological findings of families with possible linkage to CMTX2, CMTX3 and CMTX4 loci

Index Patient	Onset	Mobility	Weakness in upper limbs	Pes Cavus	Tremor	Deafness	Other Findings	MNCV
P155	2nd	W	+	+	-	-	CD	23m/s
P408	3rd	N	+	+	+	+	CD, BC	25m/s
P224	3rd	A	-	+	-	-	-	46m/s
P727	2nd	A	+	ND	-	-	SL	30 m/s

N= normal, A= abnormal, W= wheelchair, CD= cerebeller dysfunction, BC= bilateral cataract, SL= sensory loss, ND= not done

The original family reported had early onset in which two of the affected males showed mental retardation (Ionasescu *et al.*, 1991). Age of onset in these two families is late childhood. And neither family P224 nor P727 showed mental retardation in the affected males. So age of onset can be a factor affecting the severity of the disease. The evidence of a CMTX2 haplotype segregating with the disease is important for the validation of CMTX2 locus.

The original CMTX2 locus is 5.1Mb and contains 36 annotated genes (Figure 6.5). The locus was narrowed in family P727 to a 3.6 Mb region containing 27 candidate genes. One of these genes is the *PRPS2* (phosphoribosyl pyrophosphate synthetase 2) gene that is a homolog of *PRPS1*, the causative gene of CMTX5. As *PRPS2* is functionally related to *PRPS1* we screen this gene as the highest candidate for the causative gene of CMTX2. *PRPS2* codes for a subunit of five-phosphoribosyl 1-pyrophosphate (PPRibP) synthetase enzyme and is a critical regulator in the purine, pyrimidine, and pyridine nucleotide

production pathways. The protein contains 318 amino acids like *PRPS1* and is highly conserved through different species (Lizasa *et al.*, 1989).

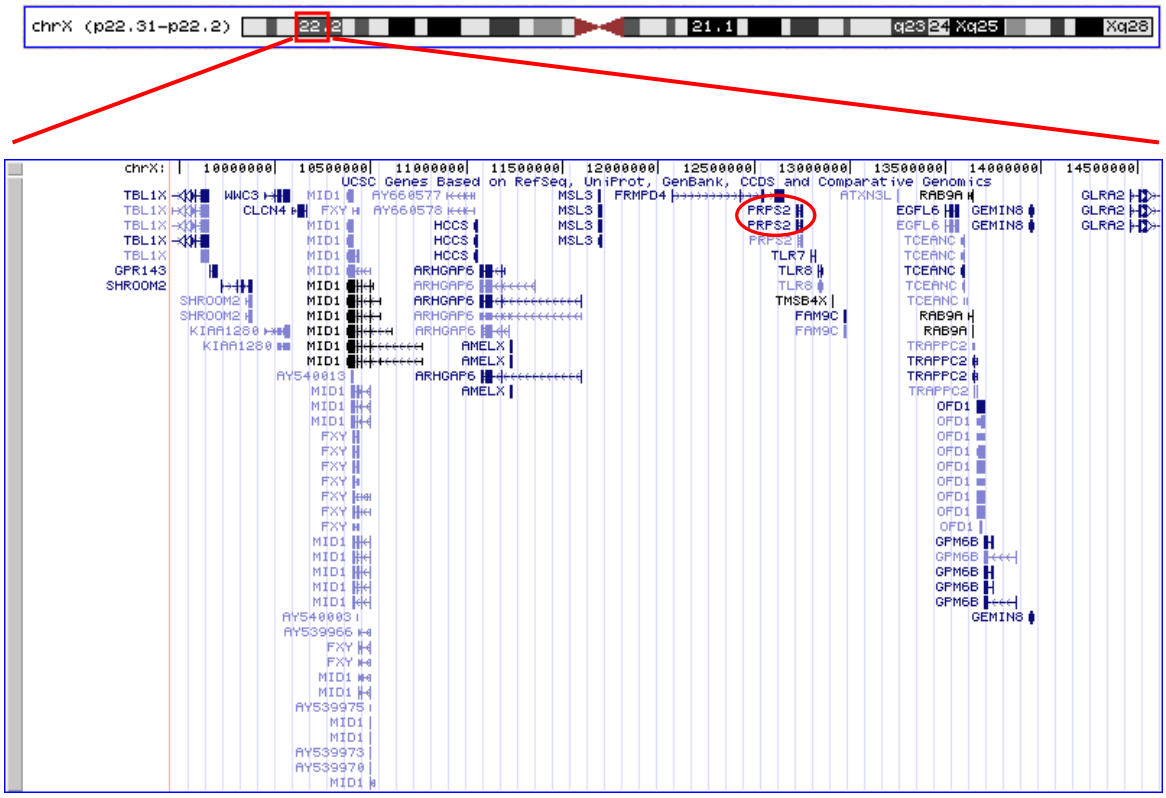

Figure 6.5. Genes located in chrX: 9,459,229bp -14,619,222bp region
(Modified from USCS Genome Browser, Human Mar. 2006 Assembly)

The coding sequence and exon-intron boundaries of the *PRPS2* gene were screened in our possible CMTX2 families and we identified two previously reported polymorphisms. In patient P727-3.4 we found a c.45G>A substitution (rs1731469) by HRM analysis. The melting curve difference plot was very subtle for this variation (Figure 5.12a). This is most likely due to the nearest neighbour symmetry in which the nucleotide change does not alter the Tm between the wild type and variant amplicon significantly (Figure 5.12b). By mixing the patient DNA with a wild type DNA prior to the PCR amplification, we allowed heteroduplex formation that makes a change in the melting curve.

The second change was in the noncoding region after exon 6 (c.864+12A>G) with reference number rs917580. It was considerably common in our cohort and for the 11

patients analyzed 4 of them found to have this change. It was not segregating with the disease showing an additional data that it was not a pathogenic variation.

Although no pathogenic variations were observed in our families, we have only excluded the coding exons and splice sites for the *PRPS2* gene. To fully rule out *PRPS2* as a causative gene, regulatory regions, promoter, intronic splice sites, 5' and 3' untranslated regions should be checked for pathogenic mutations. We cannot exclude the possibility that the disease in our families were not linked to CMTX2 locus since they were not large enough for statistical linkage analysis, the haplotypes could have been segregating with the disease by chance.

CMTX3 linked to Xq26-q28 region in two American families both with distal atrophy with weakness, and a late onset. Affected individuals were males and obligate carrier females showed no signs of the disease. In one of the families affected males presented with spastic paraparesis (*Ionescu et al.,* 1991) Confirmation of the CMTX3 locus was reported later in a New Zealand/United Kingdom family and an Australian family (Huttner *et at,*. 2006 and Brewer *et al.,* 2008 respectively). The disease haplotype in the three families reported were found to be identical, which suggested that these families may have a common ancestor and the disease is caused by a founder mutation (Brewer *et al.,* 2008).

In our study, haplotype analysis of eight markers in the CMTX3 interval for family P155 showed a CMTX3 haplotype segregating with disease (Figure 5.16). Electrophysiological findings in this family showed both demyelination and axonal involvement. Males are mildly affected and females are asymptomatic. Affected male P155-5.2 shows cerebellar dysfunction (See Table 6.1), which was also present in the original American CMTX3 family (Ionescu *et al.,* 1991).

In X-linked CMT diseases, we can not differentiate a carrier female from a normal female since the females are asymptomatic. In family P155, we assumed that individuals 4.3 and 5.1 were obligate carriers since they carried the haplotype present in all affected males in the family. In this case P155-5.1 transmitted this haplotype to both of her sons. These two sons (6.1 and 6.2) carrying the disease haplotype were normal according to

clinical examination, however, they are 13 and 9 years old, and the age of onset for this family is in the second decade of life for the affected individuals. Since the clinical data of family members 6.1 and 6.2 were not informative, yet, P155 is a candidate CMTX3 family.

The known CMTX3 locus is a 2.5 Mb region that contains 15 annotated genes and 18 expressed sequence tag (EST) clusters. Eleven of these annotated genes were excluded. (Huttner *et al*, 2006 and Brewer *et al*., 2008) Since no pathogenic mutation has been identified, characterization EST clusters is being undertaken to identify novel transcripts. The causative gene for CMTX3 will be a novel gene or in a regulatory region of a gene. (*Brewer et al,*, 2008). Linkage of additional families showing a haplotype to this locus will be important in validating potential mutations that are different to the founder mutation. A new haplotype can also be helpful to refine the locus into a narrower region.

CMTX4 (Chowchock Syndrome) is associated with deafness and mental retardation in a three-generation family which was reported by Cowchock *et al.*, 1985. Linkage analysis on the same family located the disease to Xq24-q26 (Priest *et al.* in 1995). No further linkage to this locus has been described after then. We identified a family (P408) that showed a CMTX4 haplotype segregating with disease for three markers (Figure 5.17). Affected brothers showed tremor, deafness, cerebellar dysfunction and bilateral cataracts in addition to distal weakness and *Pes cavus* (Table 6.1). Carrier females are asymptomatic. The clinical data is consistent with Cowchock Sydrome as well as the haplotype data. This family should be expanded and genotyped for additional microsatellite markers, and the candidate genes in the Xq24–q26 region should be screened for pathogenic mutations to find out the causative gene for this subtype of CMT.

7. CONCLUSION

In summary, we identified ten *Cx32* gene mutations in a cohort of 95 Turkish CMT patients. All mutations were previously reported except for I127L and Q255X, which are novel substitutions. For these novel mutations functional analyses, segregation analyses of large pedigrees, and screening of large control groups (at least 100 chromosomes) should be done to search for their pathogenicity. Haplotype analysis in 10 families revealed linkage to CMTX2 in two, CMTX3 in one, and to CMTX4 in one other family. In six families linkage to these X-linked recessive loci was excluded. We cannot exclude the possibility that these families may not have X-linked inheritance although there was no male to male transition. In addition, for some family members a more detailed clinical study should be performed to be more conclusive. The results of this study are important to show further genetic heterogeneity for X-linked CMT. For these families linkage analyses covering the whole X chromosome or genome should be performed to reveal these unknown loci.

APPENDIX A : FAMILIES EXCLUDED FOR CMTX2 LOCUS

Haplotypes of the families excluded for CMTX2 locus by using the microsatellite markers flanking the CMTX2 interval are given from Figure A.1 to Figure A.8. In all figures males are represented by squares and females are represented by circles. Black squares and circles with central dots show the affected males and female carriers, respectively.

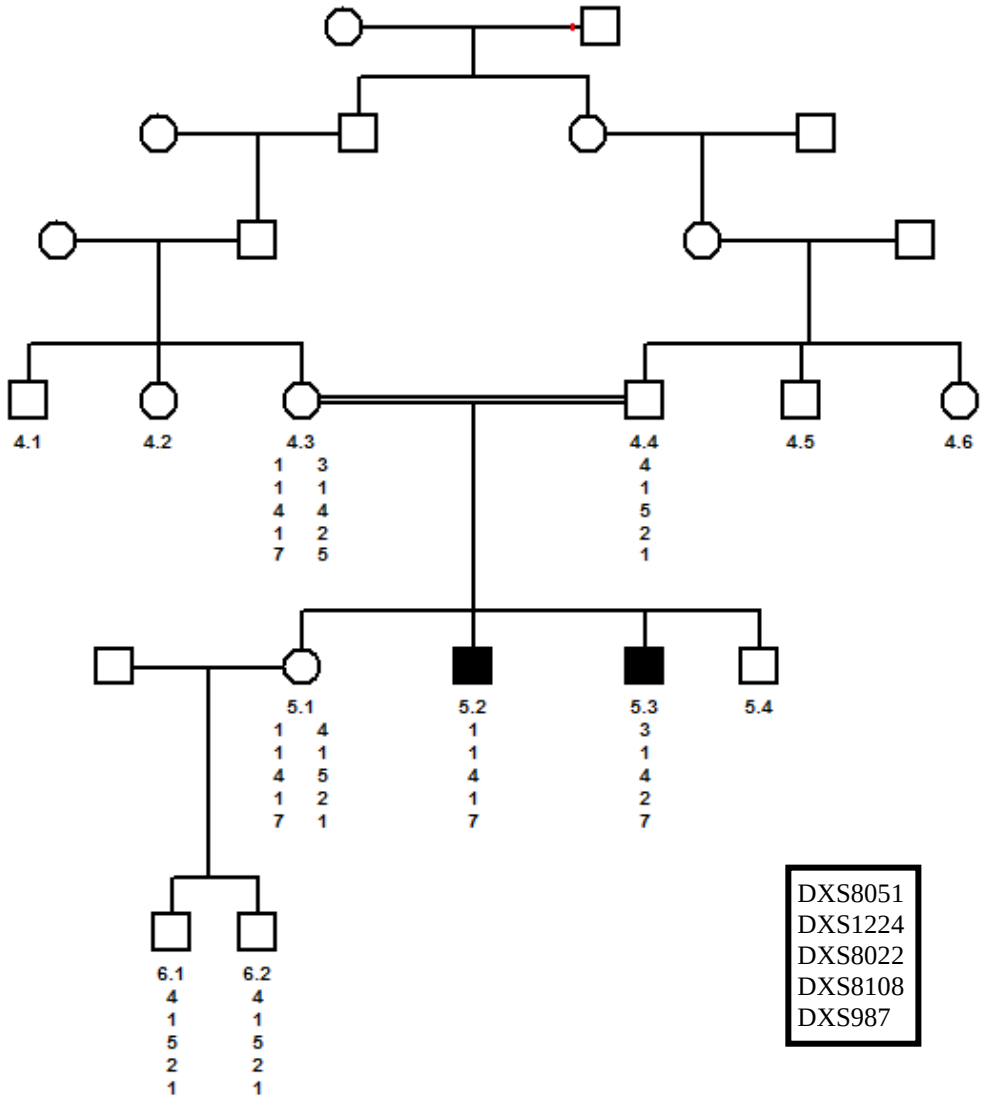

Figure A.1. Haplotype of the family P155 for the markers spanning the CMTX2 locus. The box on the right shows the order of the microsatellites used from telomere (top) to centromere (bottom)

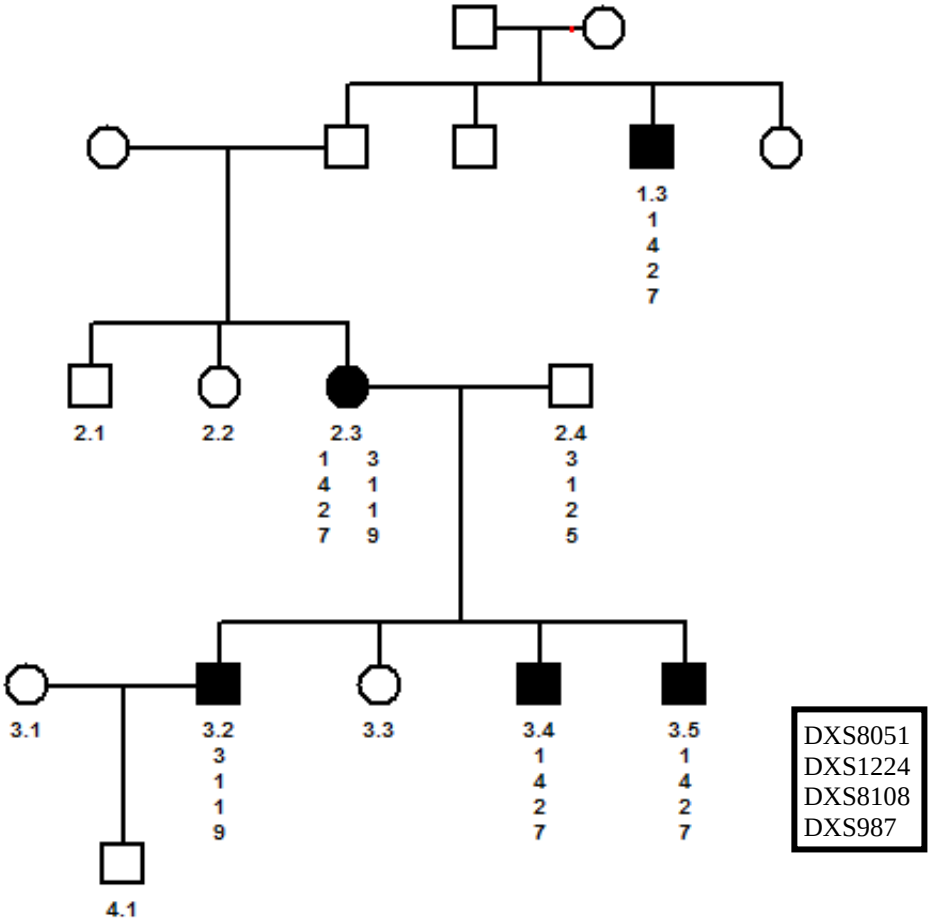

Figure A.2. Haplotype of the family P158 for the markers spanning the CMTX2 locus. The box on the right shows the order of the microsatellites used from telomere (top) to centromere (bottom)

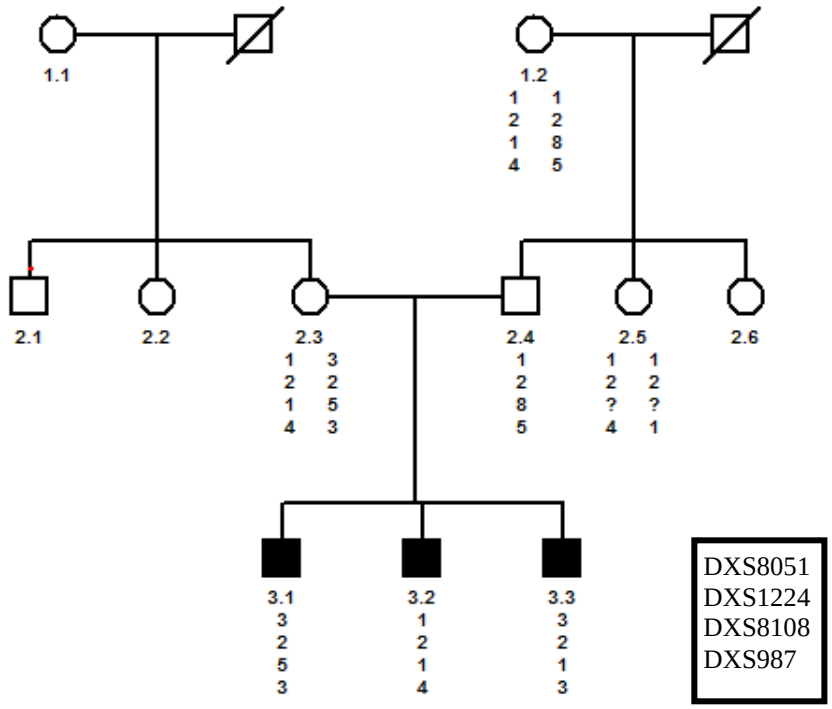

Figure A.3. Haplotype of the family P192 for the markers spanning the CMTX2 locus. The box on the right shows the order of the microsatellites used from telomere (top) to centromere (bottom)

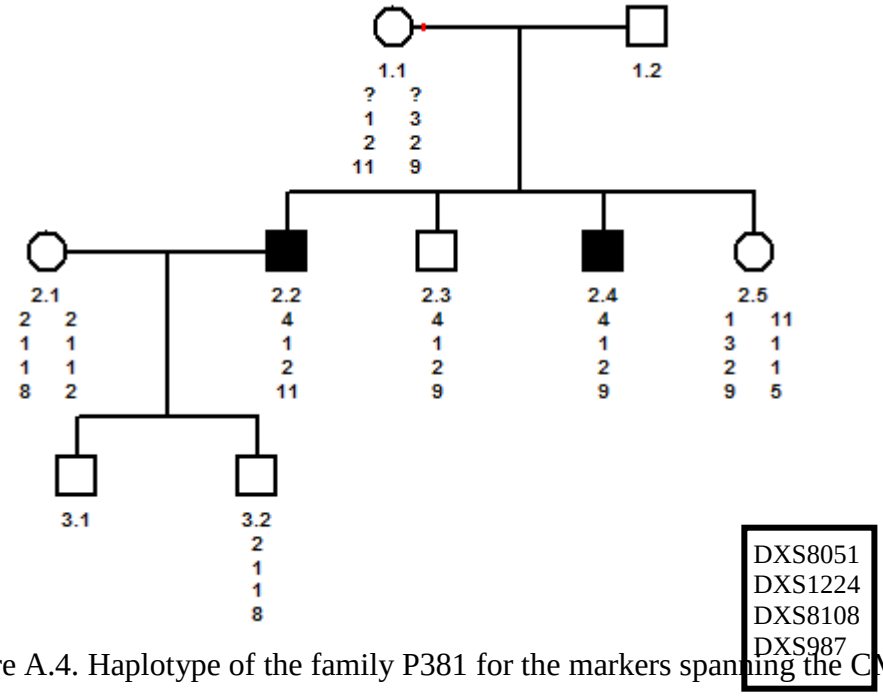

Figure A.4. Haplotype of the family P381 for the markers spanning the CMTX2 locus. The box on the right shows the order of the microsatellites used from telomere (top) to centromere (bottom)

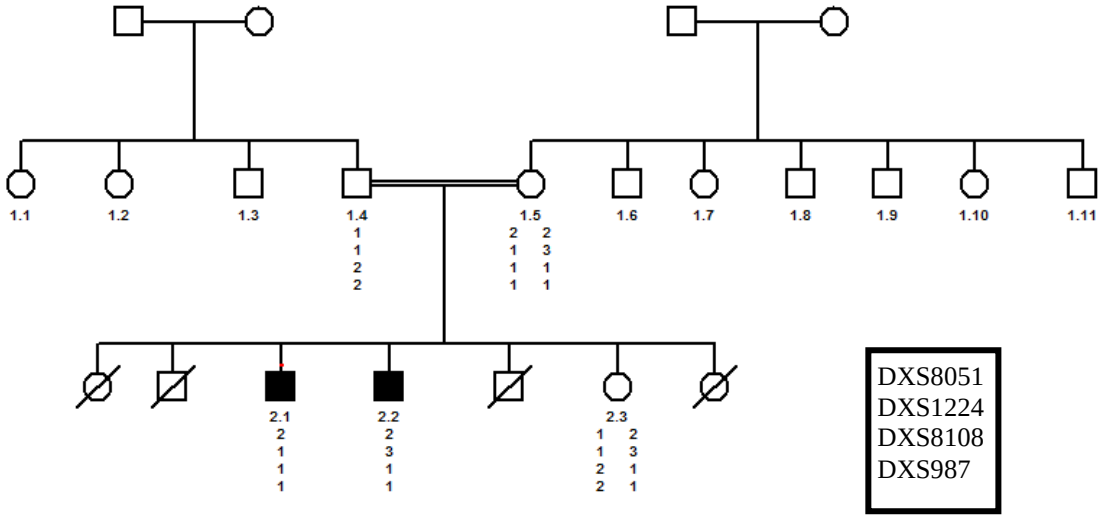

Figure A.5. Haplotype of the family P408 for the markers spanning the CMTX2 locus. The box on the right shows the order of the microsatellites used from telomere (top) to centromere (bottom)

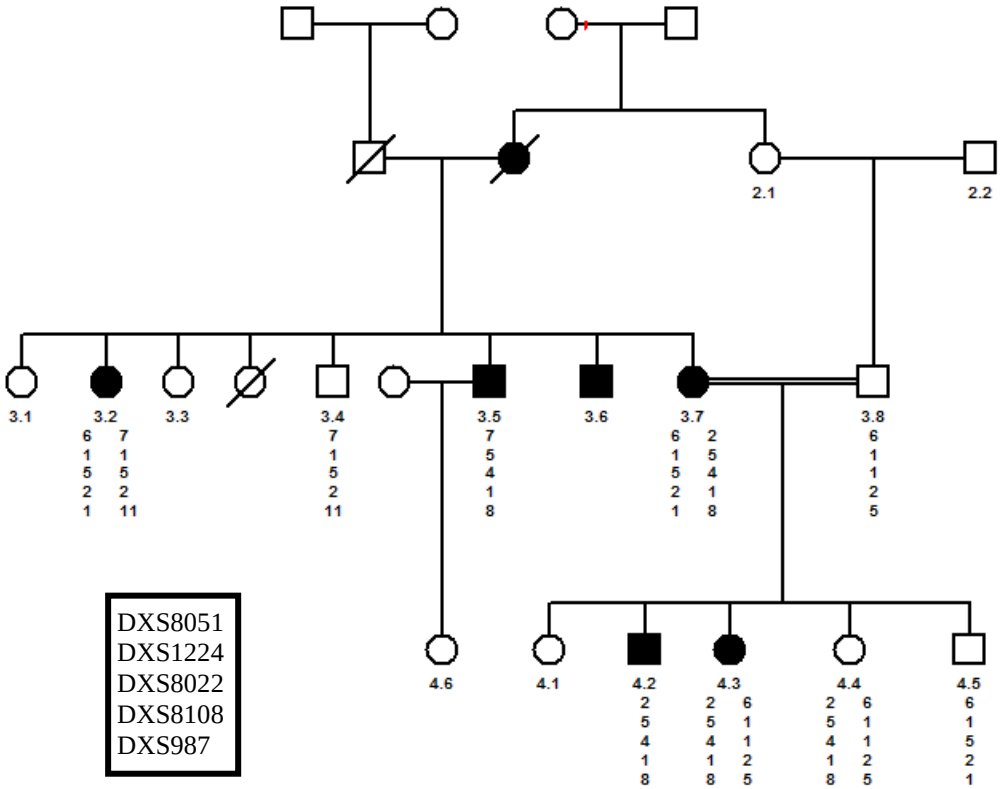

Figure A.6. Haplotype of the family P444 for the markers spanning the CMTX2 locus. The box on the left shows the order of the microsatellites used from telomere (top) to centromere (bottom)

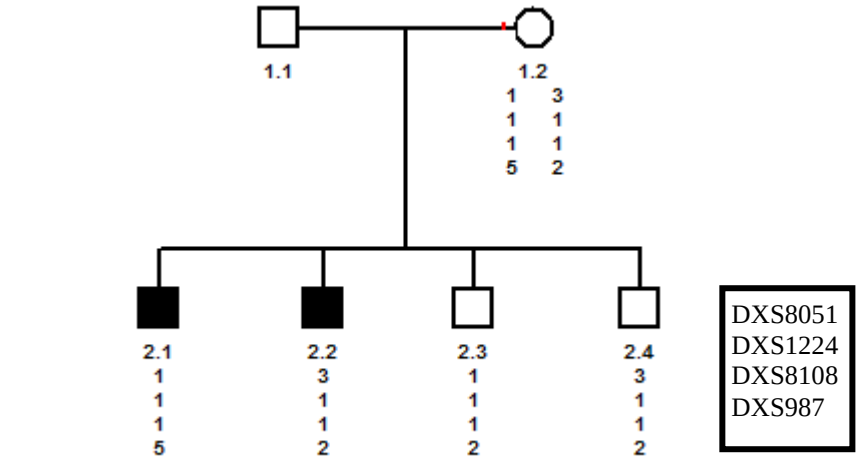

Figure A.7. Haplotype of the family P470 for the markers spanning the CMTX2 locus. The box on the right shows the order of the microsatellites used from telomere (top) to centromere (bottom)

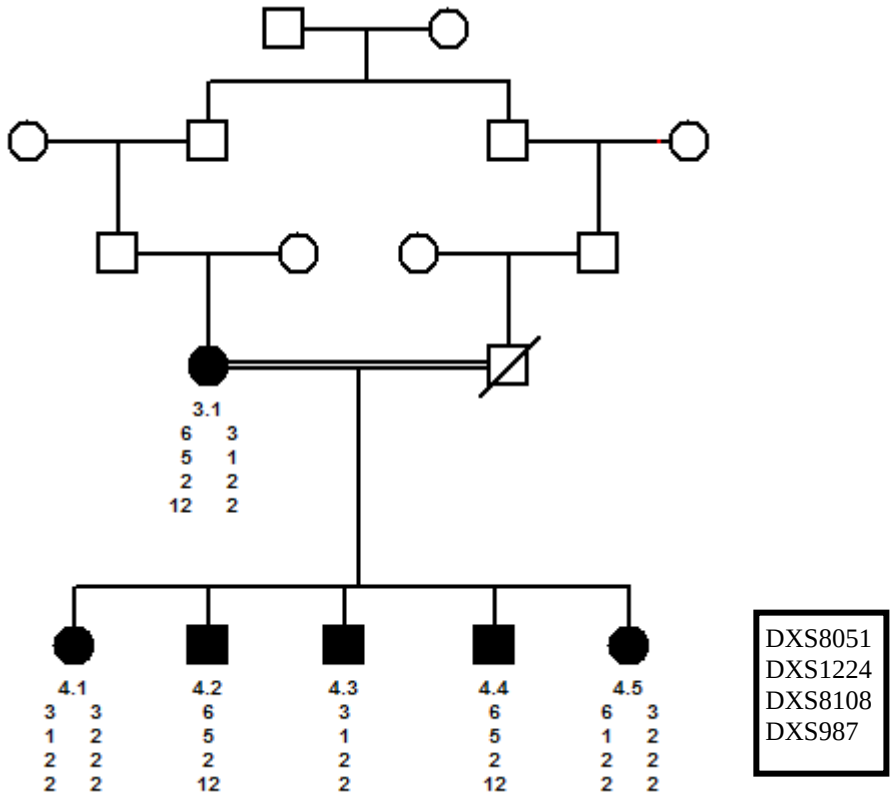

Figure A.8. Haplotype of the family P683 for the markers spanning the CMTX2 locus. The box on the right shows the order of the microsatellites used from telomere (top) to centromere (bottom)

APPENDIX B : FAMILIES EXCLUDED FOR CMTX3 LOCUS

Haplotypes of the families excluded for CMTX3 locus by using the microsatellite markers spanning the CMTX3 locus are given in Figure B.1 through Figure B.8. In all figures males are represented by squares and females are represented by circles. Black squares and circles with central dots show the affected males and female carriers, respectively.

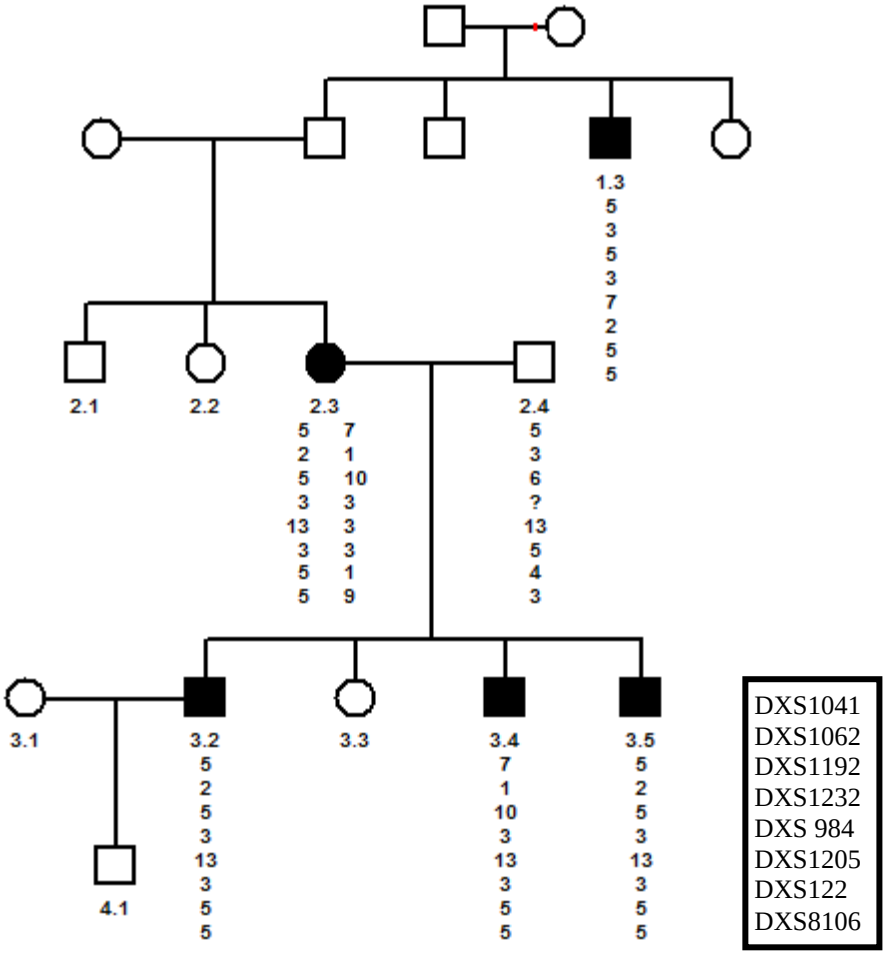

Figure B.1. Haplotype of the family P158 for the markers spanning the CMTX3 locus. The box on the right shows the order of the microsatellites used from centromere (top) to telomere (bottom)

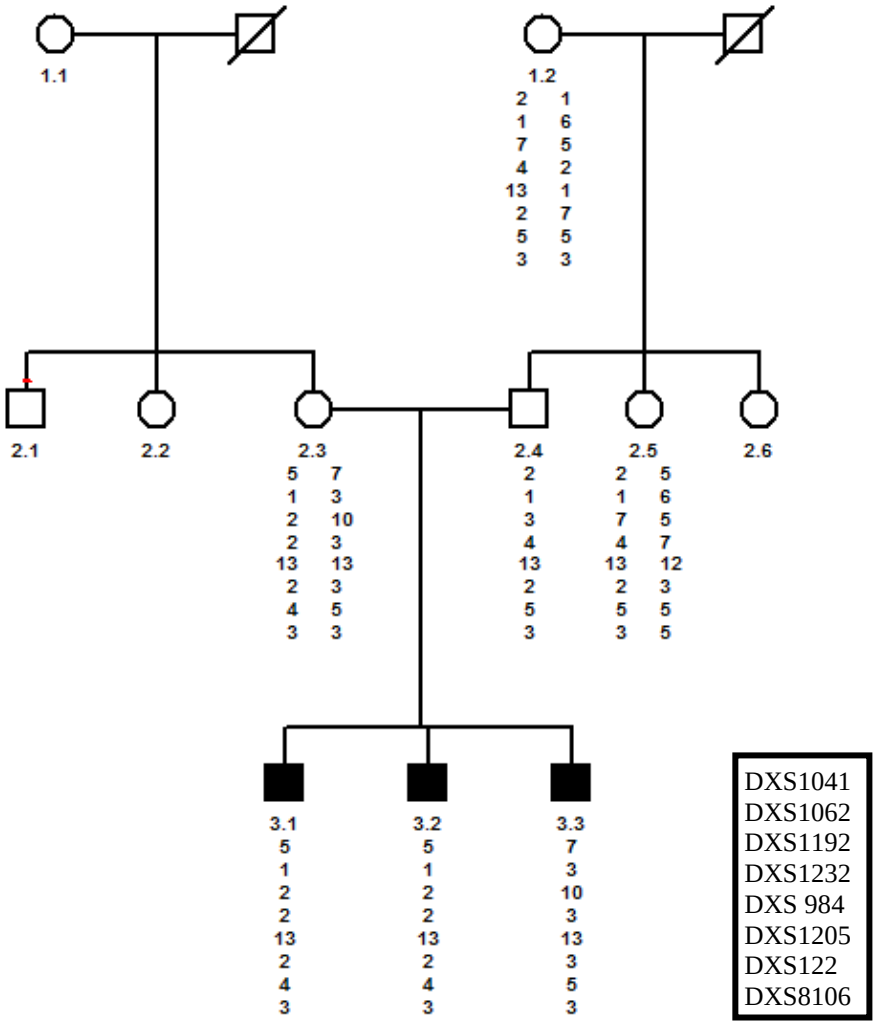

Figure B.2. Haplotype of the family P192 for the markers spanning the CMTX3 locus. The box on the right shows the order of the microsatellites used from centromere (top) to telomere (bottom)

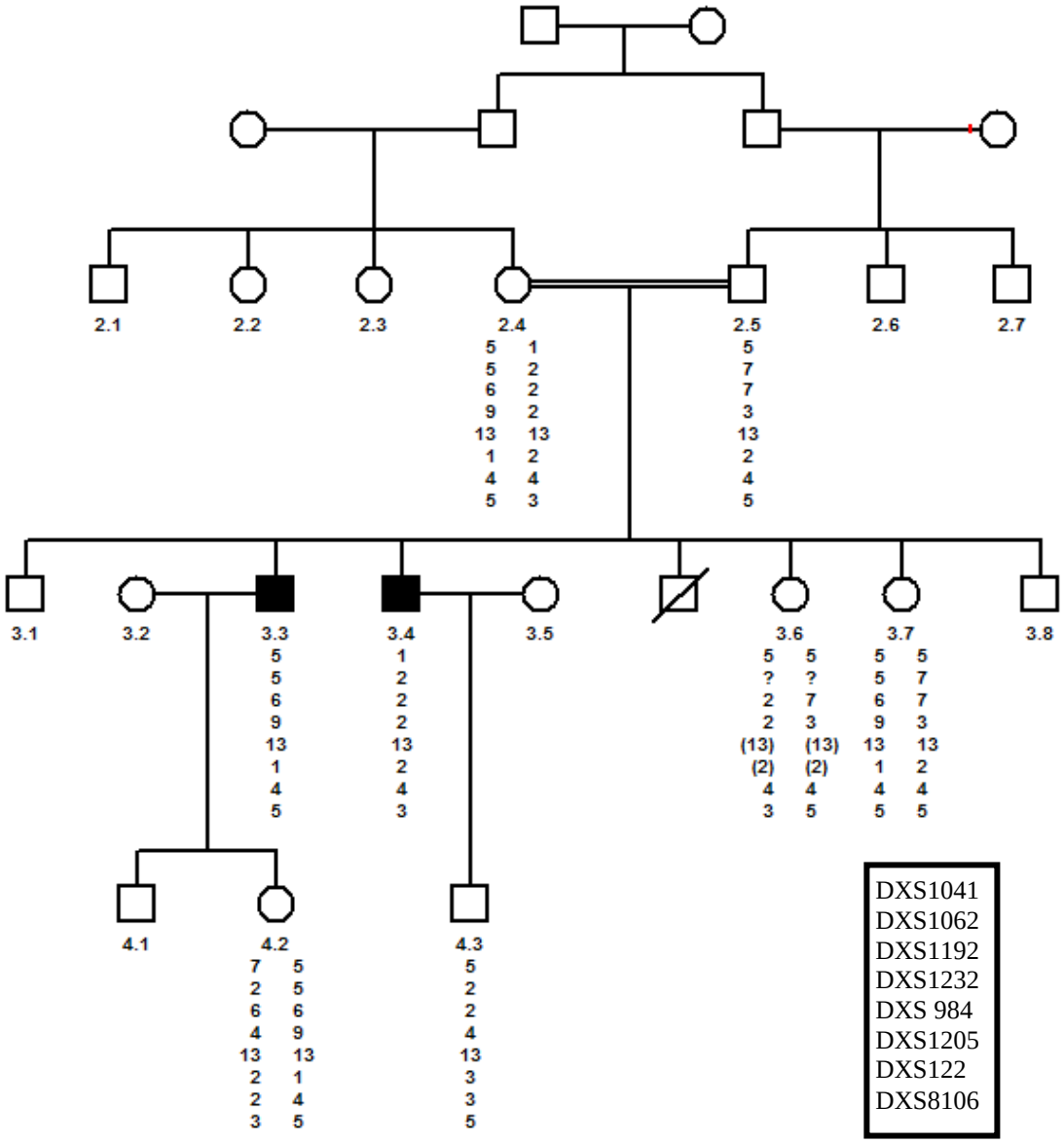

Figure B.3. Haplotype of the family P224 for the markers spanning the CMTX3 locus. The box on the right shows the order of the microsatellites used from centromere (top) to telomere (bottom)

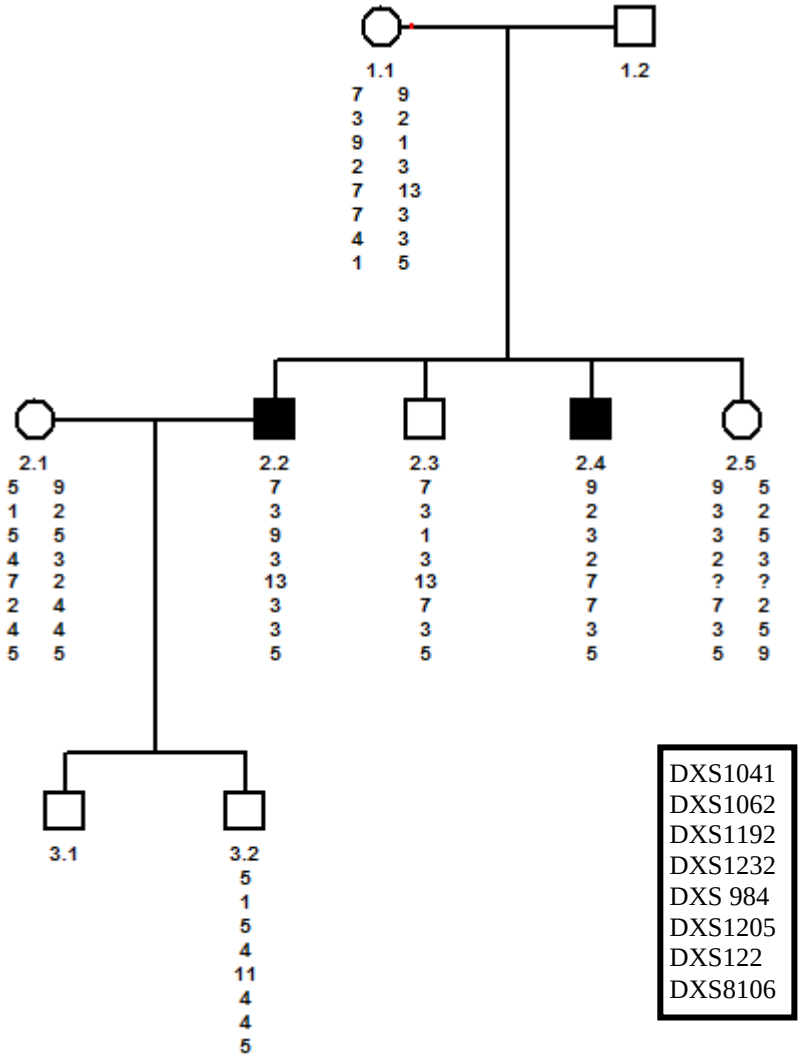

Figure B.4. Haplotype of the family P381 for the markers spanning the CMTX3 locus. The box on the right shows the order of the microsatellites used from centromere (top) to telomere (bottom)

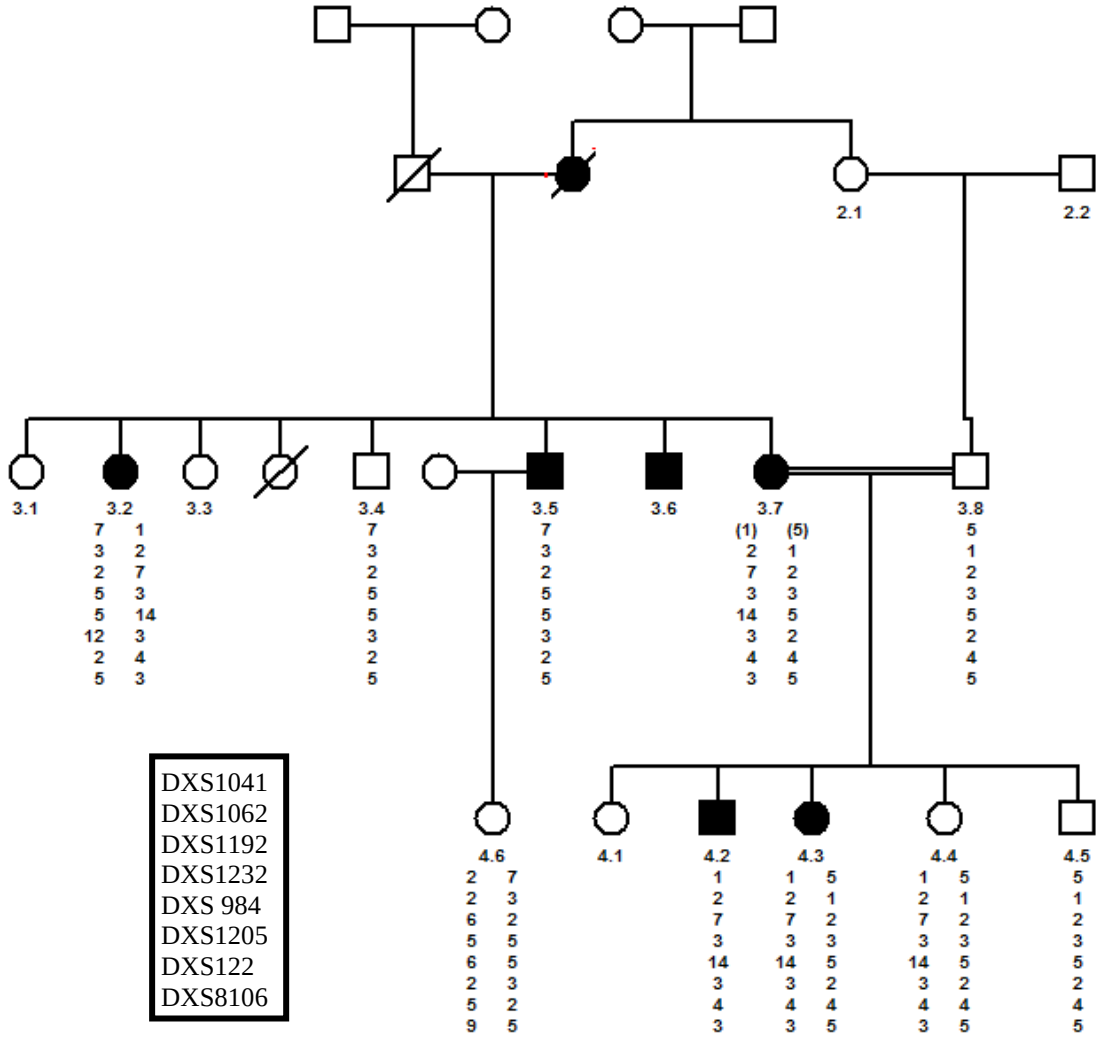

Figure B.5. Haplotype of the family P444 for the markers spanning the CMTX3 locus. The box on the left shows the order of the microsatellites used from centromere (top) to telomere (bottom)

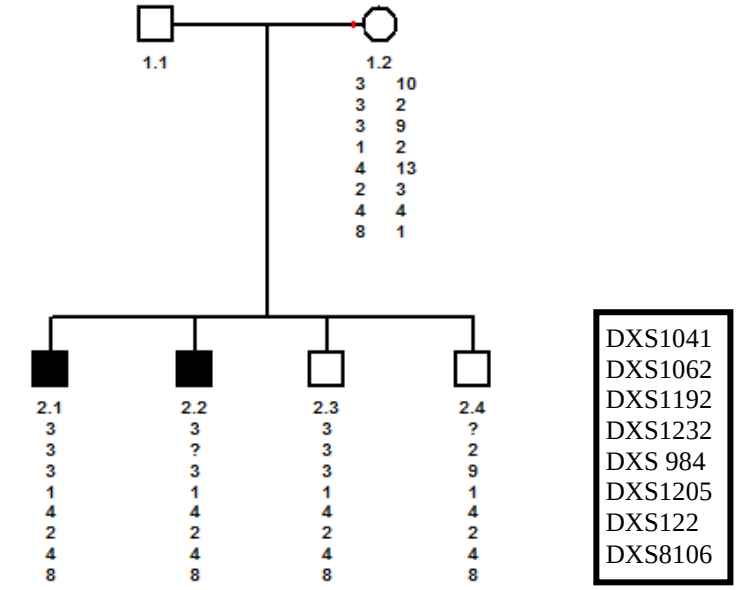

Figure B.6. Haplotype of the family P470 for the markers spanning the CMTX3 locus. The box on the right shows the order of the microsatellites used from centromere (top) to telomere (bottom)

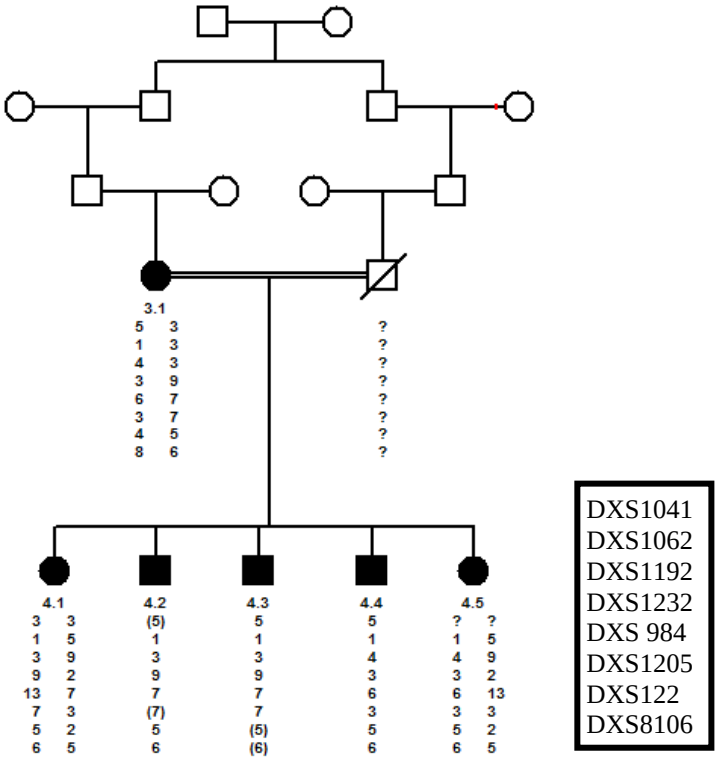

Figure B.7. Haplotype of the family P683 for the markers spanning the CMTX3 locus. The box on the right shows the order of the microsatellites used from centromere (top) to telomere (bottom)

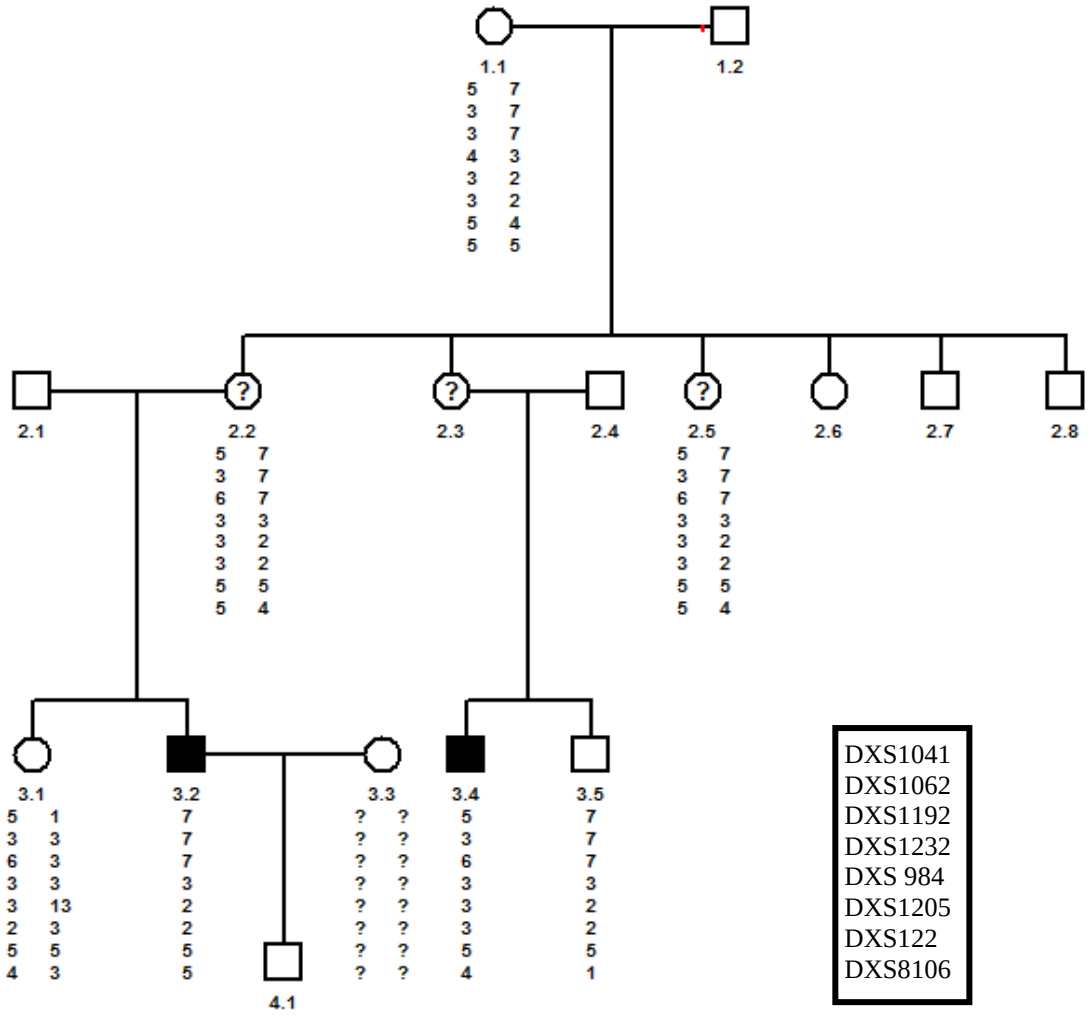

Figure B.8. Haplotype of the family P727 for the markers spanning the CMTX3 locus. The box on the right shows the order of the microsatellites used from centromere (top) to telomere (bottom)

APPENDIX C : FAMILIES EXCLUDED FOR CMTX4 LOCUS

Haplotypes of the families excluded for CMTX4 locus by using the microsatellite markers flanking the CMTX4 interval are given in Figure C.1 through Figure C.9. In all figures males are represented by squares and females are represented by circles. Black squares and circles with central dots show the affected males and female carriers, respectively.

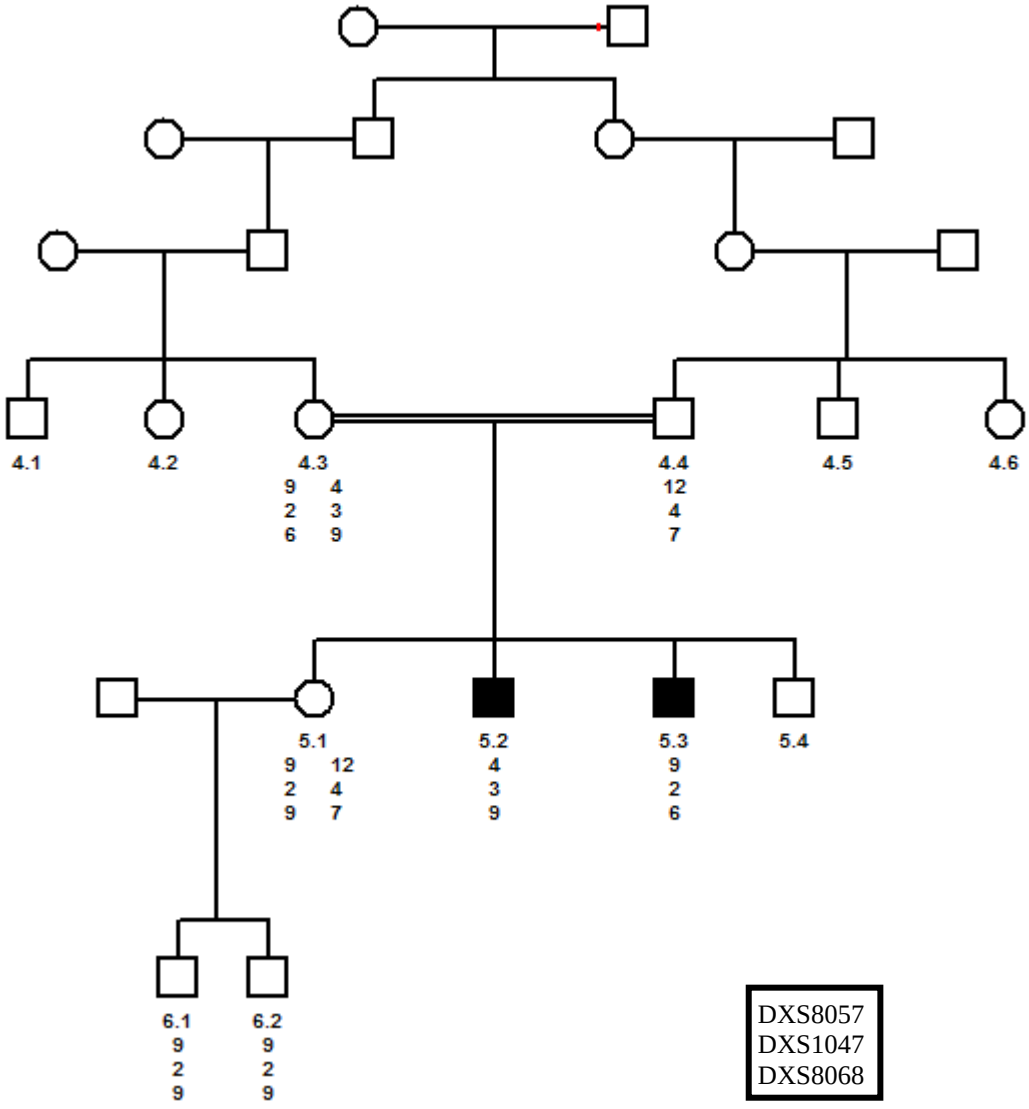

Figure C.1. Haplotype of the family P155 for the markers spanning the CMTX4 locus. The box on the right shows the order of the microsatellites used from centromere (top) to telomere (bottom)

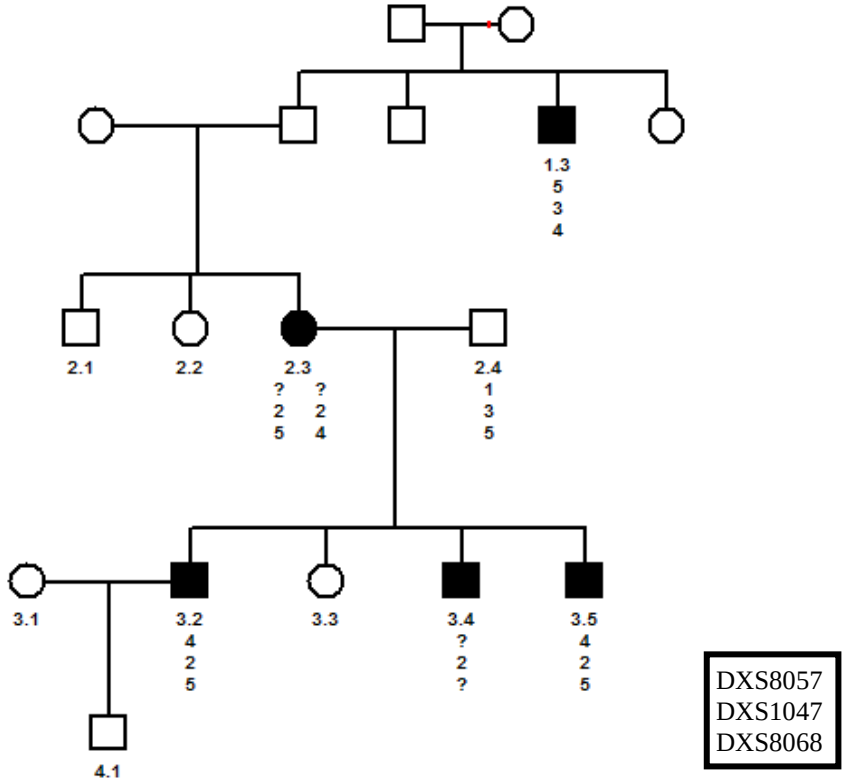

Figure C.2. Haplotype of the family P158 for the markers spanning the CMTX4 locus. The box on the right shows the order of the microsatellites used from centromere (top) to telomere (bottom)

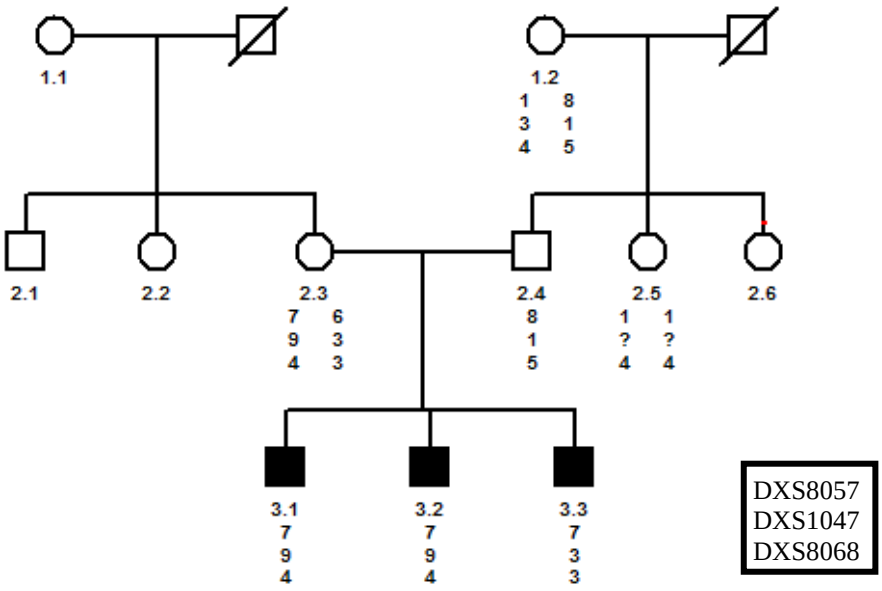

Figure C.3. Haplotype of the family P192 for the markers spanning the CMTX4 locus. The box on the right shows the order of the microsatellites used from centromere (top) to telomere (bottom)

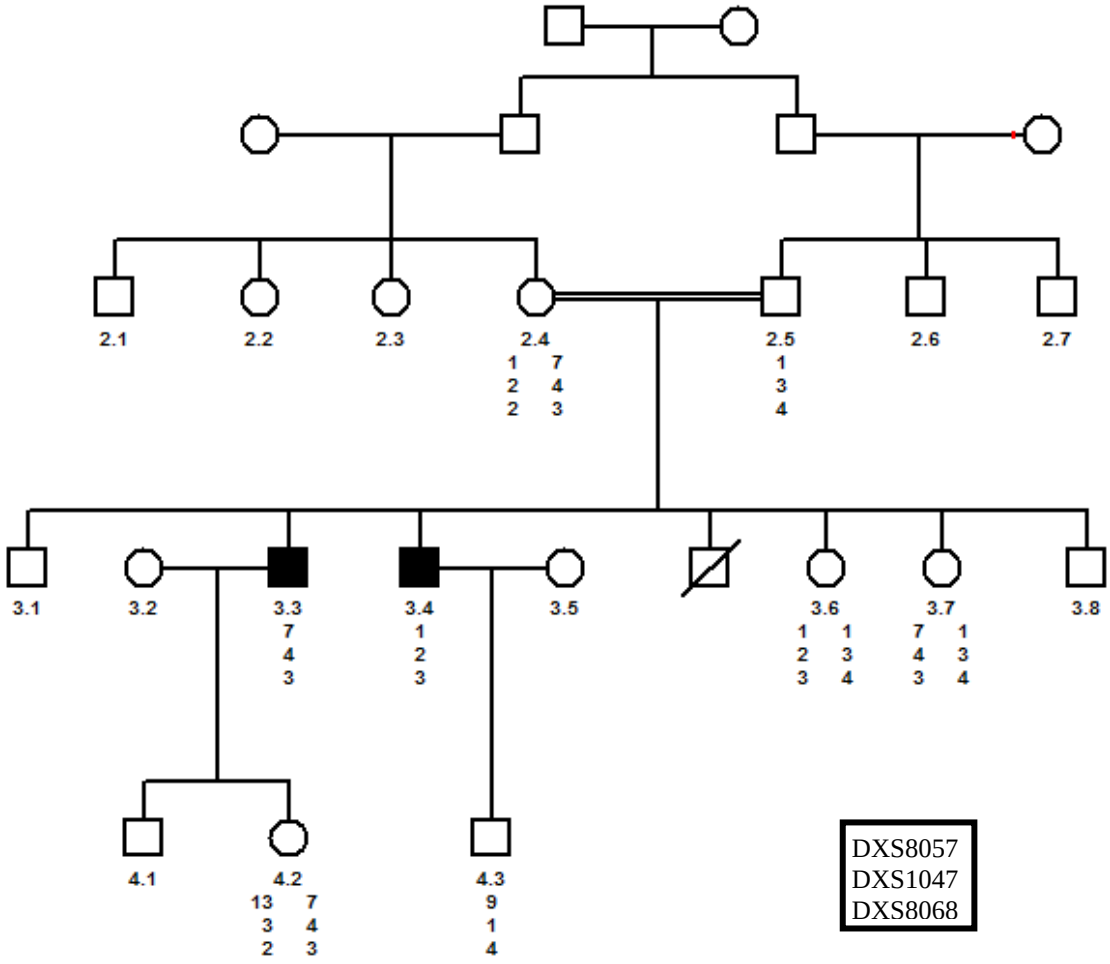

Figure C.4. Haplotype of the family P224 for the markers spanning the CMTX4 locus. The box on the right shows the order of the microsatellites used from centromere (top) to telomere (bottom)

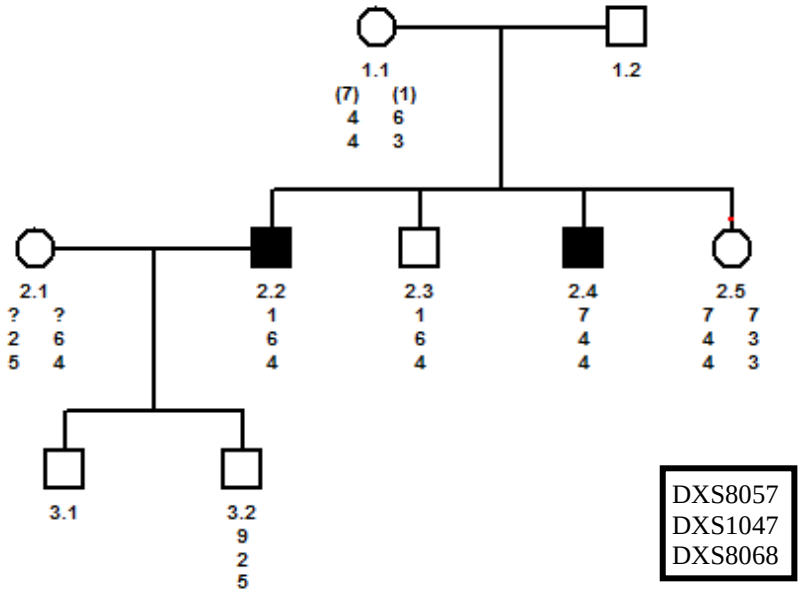

Figure C.5. Haplotype of the family P381 for the markers spanning the CMTX4 locus. The box on the right shows the order of the microsatellites used from centromere (top) to telomere (bottom)

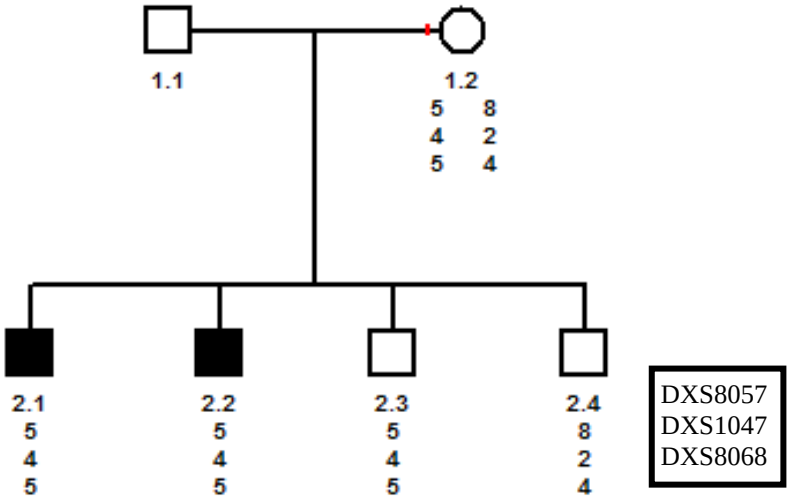

Figure C.6. Haplotype of the family P470 for the markers spanning the CMTX4 locus. The box on the right shows the order of the microsatellites used from centromere (top) to telomere (bottom)

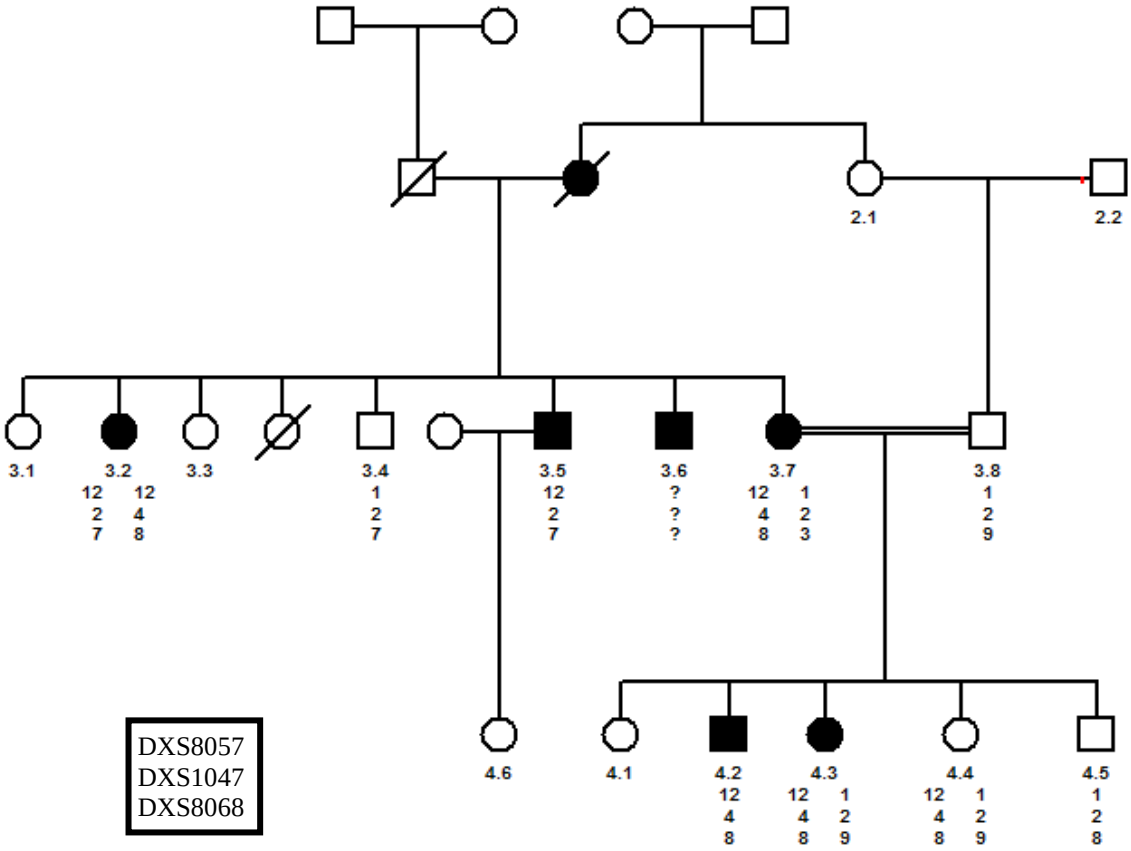

Figure C.7. Haplotype of the family P444 for the markers spanning the CMTX4 locus. The box on the left shows the order of the microsatellites used from centromere (top) to telomere (bottom)

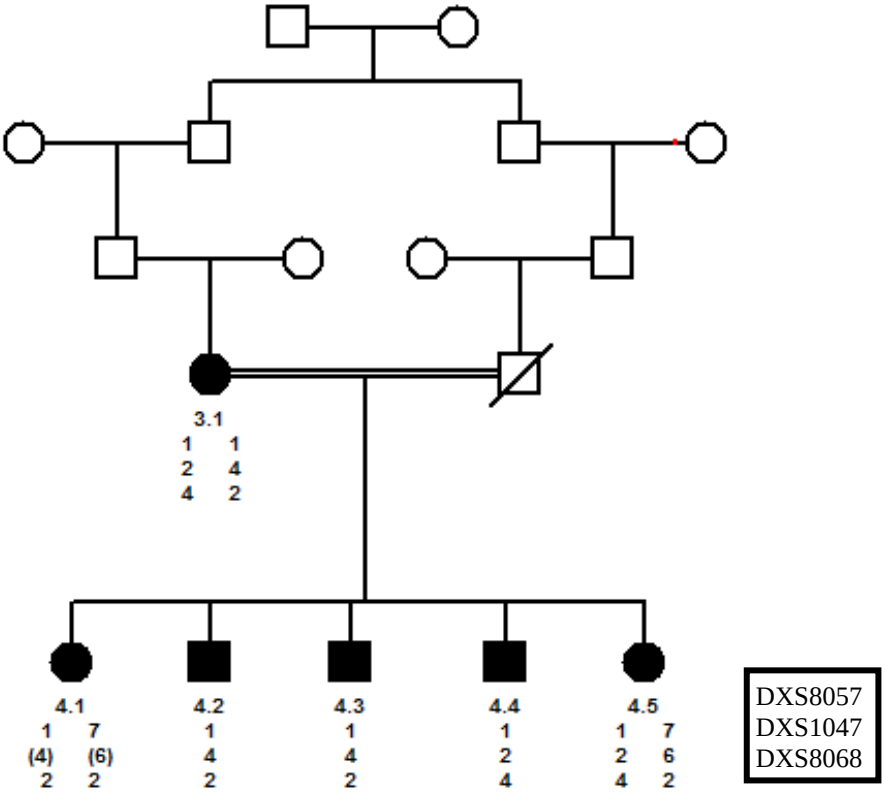

Figure C.8. Haplotype of the family P683 for the markers spanning the CMTX4 locus. The box on the right shows the order of the microsatellites used from centromere (top) to telomere (bottom)

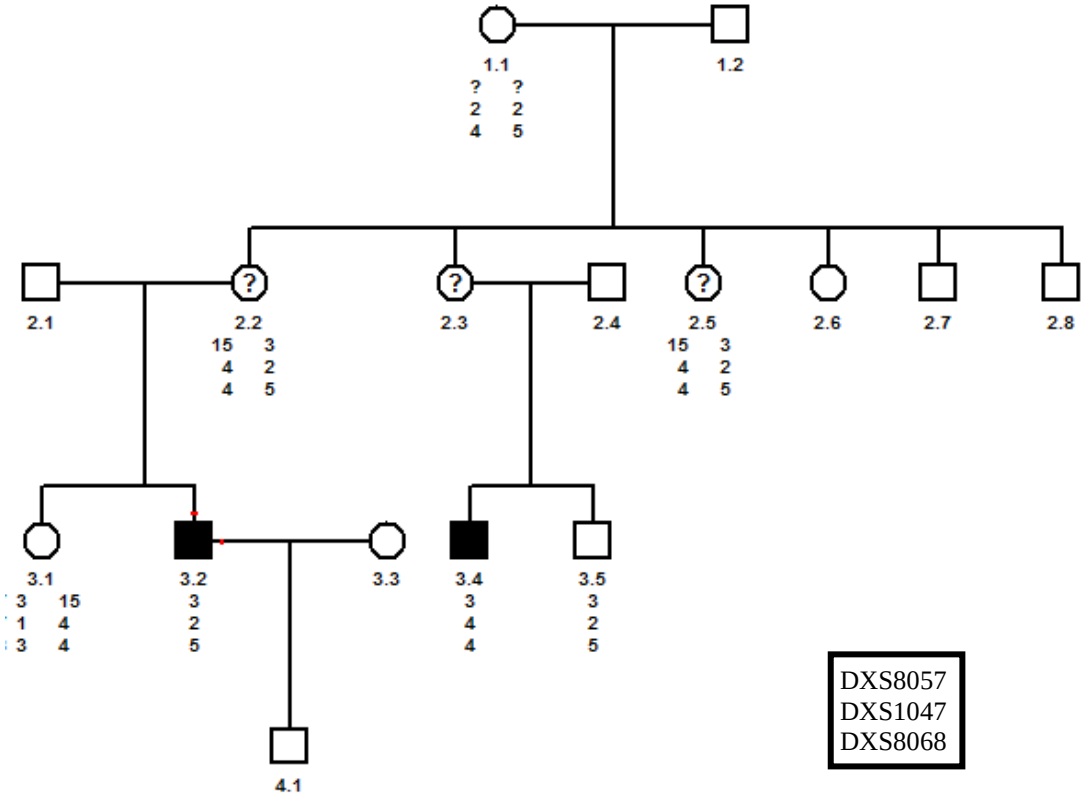

Figure C.9. Haplotype of the family P727 for the markers spanning the CMTX4 locus. The box on the right shows the order of the microsatellites used from centromere (top) to telomere (bottom)

APPENDIX D: ETHICS REPORT

Boğaziçi Üniversitesi
İnsan Araştırmaları Etik Kurulu

13 Mayıs 2008

Doç. Dr Esra Battaloğlu
Boğaziçi Üniversitesi
Moleküler Biyoloji ve Genetik Bölümü
Bebek - İstanbul

Sn. Battaloğlu,

"Charcot-Marie-Tooth (CMT) Hastalarında Otozomal Çekinik CMTX'den Sorumlu Kromozom Bölgelerine Bağlantının Araştırılması" başlıklı projeniz ile ilgili olarak Boğaziçi Üniversitesi İnsan Araştırmaları Etik Kurulu'na yapmış olduğunuz başvuru (Protokol no: 2008/15) kurulumuzun 13 Mayıs 2008 tarih ve 2008/02 sayılı toplantısında değerlendirilerek uygun bulunmuştur. Bilgilerinize sunarız.

Doç. Dr. Ali İ. Tekcan, Başkan
Boğaziçi Üniversitesi
Psikoloji Bölümü Öğretim Üyesi

Prof. Dr. Yekta Ülgen, Üye
Boğaziçi Üniversitesi
Biyomedikal Mühendisliği Enstitüsü Müdürü

Prof. Dr. Diane Sunar, Üye
İstanbul Bilgi Üniversitesi
Psikoloji Bölümü Başkanı

Doç. Dr. Şemsa Özar, Üye
Boğaziçi Üniversitesi
Ekonomi Bölümü Öğretim Üyesi (izinli)

Doç. Dr. Yeşim Atamer, Üye
İstanbul Bilgi Üniversitesi
Hukuk Fakültesi Öğretim Üyesi

REFERENCES

Abrams, C. K., S. Oh, Y. Ri, and T. A. Bargiello, 2000, "Mutations in connexin 32: the molecular and biophysical bases for the X-linked form of Charcot-Marie-Tooth disease", *Brain Research Brain Research Reviews*, Vol. 32, No. 1, pp. 203-214

Adolkofer, K., R. Naef and U. Suter, 1997, "Analysis of compound heterozygous mice reveals that the trembler mutation can behave as gain-of-function allele", *Journal of Neuroscience Research*, Vol. 49, No. 6, pp. 671-680.

Balice-Gordon, R. J., L. Bone, and S. S. Scherer, 1998, "Functional gap junctions in the schwann cell myelin sheath", *Journal of Cell Biology*, Vol. 142, No.4, pp. 1095-1104

Barhoumi, C., R. Amouri, C. Ben Hamida, M. Ben Hamida, S. Machghoul and M. Gueddiche, 2001, "Linkage of a new locus for autosomal recessive axonal form of Charcot-Marie-Tooth disease to chromosome 8q21.3", *Neuromuscular Disorders*, Vol. 11, No. 1, pp. 27–34.

Barisic, N., K. G. Claeys, M. Sirotkovic´-Skerlev, A. Löfgren, E. Nelis, P. De Jonghe and V. Timmerman, 2008, "Charcot-Marie-Tooth Disease: A Clinico-genetic confrontation", *Annals of Human Genetics*, Vol. 72,No. 3, pp. 416–441.

Baxter, R. V., K. Ben Othmane, J. M. Rochelle, J. E. Stajich, C. Hulette and S. Dew-Knight, 2002, "Ganglioside-induced differentiation-associated protein-1 is mutant in Charcot-Marie- Tooth disease type 4A/8q21", *Nature Genetics*, Vol. 30, No. 1, pp. 21–22.

Ben Othmane, K., F. Hentati, F. Lennon, C. Ben Hamida, S. Blel and A. D. Roses, 1993, "Linkage of a locus (CMT4A) for autosomal recessive Charcot-Marie-Tooth disease to chromosome 8q", *Human Molecular Genetics*, Vol. 2, No.10, pp. 1625–1628.

Bennett, M.V., L.C. Barrio, T.A. Bargiello, D.C. Spray, E. Hertzberg and J.C. Sáez, 1991,"Gap junctions: new tools, new answers, new questions", *Neuron*, Vol. 6, No. 3, pp. 305-320.

Bergoffen, J., S. S. Scherer, S. Wang, M. O. Scott, L. J. Bone, D. L. Paul, K. Chen, M. W. Lensch, P. F. Chance and K. H. Fischbeck, 1993, "Connexin mutations in X-linked Charcot–Marie–Tooth disease", *Science,* Vol. 262, No. 5142, pp. 2039–2042.

Bertorini, T., P. Narayanaswami and H. Rashed, 2004, "Charcot- Marie-Tooth disease (hereditary motor sensory neuropathies) and hereditary sensory and autonomic neuropathies", *Neurologist,* Vol. 10, No. 6, pp. 327–337.

Birouk, N., H. Azzedine, O. Dubourg, M. P. Muriel, A. Benomar and T. Hamadouche, 2003, "Phenotypical features of Maroccan family with autosomal recessive Charcot-Marie-Tooth disease associated with S194X mutation in the GDAP1 gene", *Archives of Neurology,* Vol. 60, No. 4, pp. 598–604

Bissar-Tadmouri N., Y. Parman, L. Boutrand, F. Deymeer, P. Serdaroglu, A. Vandenberghe and E. Battaloglu, 2000, "Mutational analysis and genotype:phenotype correlation in Turkish Charcot–Marie–Tooth Type 1 and HNPP patients", *Clinal Genetics,* Vol:58, No. 5 ,pp. 396–402.

Bolino, A., M. Muglia, F. L. Conforti, E. LeGuern, M. A. Salih and D. M. Georgiou, 2000, "Charcot-Marie-Tooth type 4B is caused by mutations in the gene encoding myotubularin related protein 2", *Nature Genetics,* Vol. 25, No. 1, pp. 17–19

Bone L. J., S. M. Deschênes, R.J. Balice-Gordon, K. H. Fischbeck and S. S. Scherer, 1997, "Connexin32 and X-linked Charcot–Marie–Tooth disease", *Neurobiology of Disease,* Vol. 4, No. 3-4, 221–230

Bouhouche, A., A. Benomar, N. Birouk, A. Mularoni, F. Meggouh and J. Tassin, 1999, "A locus for an axonal form of autosomal recessive Charcot-Marie-Tooth disease maps to chromosome 1q21.2- q21.3", *American Journal of Human Genetics,* Vol. 65, No. 3, pp. 722–727.

Bradbury, J., 2004, "Mitochondrial fusion protein mutated in CMT2A", *The Lancet Neurology* Vol. 3 No. 6 pp. 326.

Brewer, M., F. Changi, A. Antonellis, K. Fischbeck, P. Polly, G. Nicholson and M. Kennerson, 2008, "Evidence of a founder haplotype refines the X-linked Charcot–Marie-Tooth (CMTX3) locus to a 2.5 Mb region", *Neurogenetics*, Vol. 9, No. 3, pp. 191-195.

Bronstein, J. M., 2000, "Function of tetraspan proteins in the myelin sheath", *Current Opinion in Neurobiology*, Vol. 10, No. 5, pp. 552-557.

Bruzzone, R., T. W. White, and D. L. Paul, 1996, "Connections with connexins: The molecular basis of direct intercellular signaling", *European Journal of Biochemistry*, Vol. 238, No. 1, pp. 1–27.

Charcot, J.-M. and P. Marie, 1886, "Sur une forme particuliére d`atrophie musculaire progressive, souvent familiale, debutant par les pieds et les jambes et atteignant plus tard les mains", *Revue Médicale*, Vol. 6, pp. 97-138.

Cowchock, F. S., S. W. Duckett, L. J. Streletz, L. J. Graziani, and L. G. Jackson, 1985, " X-Linked motor-sensory neuropathy Type-II with deafness and mental retardation: A new disorder", *American Journal of Medical Genetics*, Vol. 20, No. 2, pp. 307-315.

Cuesta, A., L. Pedrola, T. Sevilla, J. Garcia-Planells, M. J. Chumillas and F. Mayordomo, 2002, "The gene encoding gangliosideinduced differentiation associated protein 1 is mutated in axonal Charcot-Marie-Tooth type 4A disease", *Nature Genetics*, Vol. 30, No. 1, pp. 22–25.

Dahl, G., R. Werner, E. Levine and C. Rabadan-Diehl and 1992, "Mutational analysis of gap junction formation", *Biophysical Journal*, Vol. 62, No. 1, pp. 172-182.

De Jonghe, P., V. Timmerman, C. Ceuterick, E. Nelis, E. De Vriendt and A. Lofgren, 1999, "The Thr124Met mutation in the peripheral myelin protein zero (MPZ) gene is associated with a clinically distinct Charcot-Marie-Tooth phenotype", *Brain*, Vol. 122, No. 2, pp. 281–290.

De Jonghe, P., I. V. Mersiyanova, E. Nelis, J. Del Favero, J. J. Martin and C. Van Broechoven, 2001, "Further evidence that neurofilament light chain gene mutations can cause Charcot-Marie-Tooth disease type 2E", *Annals of Neurology*, Vol. 49, No. 2, pp. 245–249.

Dermietzel, R. and D.C. Spray, 1993, "Gap junctions in the brain: where, what type, how many and why?", *Trends in Neurosciences*, Vol. 16, No. 5, pp.186-192.

Dermietzel, R., M. Farooq, J. A. Kessler, H. Althaus, E. L. Hertzberg, and D. C. Spray, 1997, "Oligodendrocytes express gap junction proteins connexin32 and connexin45", *Glia*, Vol. 20, No. 2, pp. 101–114.

Dobrowolski, S. F., J. T. McKinney, C. Amat di San Filippo, K. G. Sim, B. Wilcken and N. Longon, 2005, "Validation of dye-binding/high-resolution thermal denaturation for the identification of mutations in the SLC22A5 gene", *Human Mutation*, Vol. 25, No. 3, pp. 306-313.

Dubourg, O., S. Tardieu, N. Birouk, R. Gouider, J. M. Leger, T. Maisonobe, A. Brice, P. Bouche and E. LeGuern, 2001, "Clinical, electrophysiological and molecular genetic characteristics of 93 patients with X-linked Charcot–Marie–Tooth disease", *Brain*, Vol. 124, No. 10, 1958–1967.

Dyck, P. J., P. Chance, R. Lebo and J. A. Carney, 1993, "Hereditary motor and sensory neuropathy", in P. J. Dyck and P. K. Thomas (eds), *Peripheral Neuropathy*, pp. 1094-1136, W. B. Saunders, Philadelphia.

Dyck, P. J., W. J. Litchy, S. Minnerath, T. D. Bird, P. F. Chance, D. J. Schaid and A. E. Aronson, 1994, "Hereditary motor and sensory neuropathy with diaphragm and vocal cord paresis", *Annals of Neurology*, Vol. 35, No. 5, pp. 608-615.

Edgar, J. M. and J. Garbern, 2004, "The myelinated axon is dependent on the myelinating cell for support and maintenance: molecules involved", *Journal of Neuroscience Research*, Vol. 76, No. 5, pp. 593-598.

Erwin, W.G., 1944, “A pedigree of sex-linked recessive peroneal atrophy”, *Journal of Heredity*, Vol. 35, pp. 24-26.

Evgrafov, O. V., I. Mersiyanova, J. Irobi, L. Van Den Bosch, I. Dierick, C. L. Leung, 2004, “Mutant small heat-shock protein 27 causes axonal Charcot-Marie-Tooth disease and distal hereditary motor neuropathy” *Nature Genetics*, Vol. 36, No. 6, pp. 602–606.

Falk, M. M., N. M. Kumar, and N. B. Gilula, 1994, “Membrane insertion of gap junction connexins: polytopic channel forming membrane proteins”, *The Journal of Cell Biology*, Vol. 127, No. 2, pp. 343–355.

Feng, Y., B. Pres and A. Wandinger-Ness, 1995, “Rab 7: an important regulator of late endocytic membrane traffic”, *The Journal of Cell Biology*, Vol. 131 No. 6, pp. 1435–1452.

Fischbeck, K.H., N. ar-Rushdi, M. Pericak-Vance, M. Rozear, A.D. Roses and J.P. Fryns, 1986, “X-linked neuropathy: Gene localization with DNA probes”, *Annals of Neurology*, Vol. 20, No. 4, pp. 527-532.

Fryns J.P. and H.Van den Berghe, 1980, “Sex-linked recessive inheritance in Charcot-Marie-tooth disease with partial clinical manifestations in female carriers”, *Human Genetics*, Vol. 55, No. 3, pp. 413-415.

Glavac, D., and M. Dean, 1993, “Optimization of the single-strand conformation polymorphism (SSCP) technique for detection of point mutations”, *Human Mutations*, Vol. 2, No. 5, pp. 404-414.

Griffin, J. W and P. N. Hoffman, 1993, “Degeneration and regeneration in the peripheral nervous system”, *Peripheral Neuropathy*, Third Edition, WB Saunders, Philedelphia, pp 361-367,

Harding, A. E. and P. K. Thomas, 1980, "Hereditary distal spinal muscular atrophy. A report on 34 cases and a review of the literature", *Journal of the Neurological Sciences*, Vol. 45, No. 2-3, pp. 337-348.

Hayasaka, K., M. Himoro, W. Sato, G. Takada, K. Uyemura and N. Shimizu, 1993, "Charcot-Marie-Tooth neuropathy type 1B is associated with mutations of the myelin P0 gene", *Nature Genetics*, Vol. 5, No. 1, pp. 31–34.

Hayashi, K., 1992, "PCR-SSCP:a method for detection of mutations", *Genetic analysis, techniques and applications*, Vol.9, No. 3, pp. 73-79.

Hayashi K. and D.W. Yandell, 1993, "How sensitive is PCR-SSCP?", Human Mutation, Vol.2, No. 5, pp. 338–346.

Herrmann, M. G., J. D. Durtschi, L. K. Bromley, C. T. Wittwer and K. V. Voelkerding, 2006, "Amplicon DNA melting analysis for mutation scanning and genotyping: cross-platform comparison of instruments and dyes", *Clinical Chemistry*, Vol. 52, No. 3, pp. 494-503.

Huttner I.G., M.L. Kennerson, S.W. Reddel, D. Radovanovic and G.A. Nicholson, 2006, "Proof of genetic heterogeneity in X-linked Charcot-Marie-Tooth disease", Neurology, Vol. 67, No. 11, pp. 2016-2021.

Ionasescu, V. V., J. Trofatter, J. L. Haines, A. M. Summers, R. lonasescu, and C. Searby, 1991, "Heterogeneity in X-linked recessive Charcot-Marie-Tooth neuropathy", American Journal of Human Genetics, Vol. 48, No. 6, pp. 1075-1083.

Ismailov, S. M., V. P. Fedotov, E. L. Dadali, A. V. Polyakov, C. Van Broeckhoven and V. I. Ivanov, 2001, "A new locus for autosomal dominant Charcot-Marie-Tooth disease type 2 (CMT2F) maps to chromosome 7q11–q21", *European Journal of Human Genetics*, Vol. 9, No. 8, pp. 646–650.

Jessen, K. R., L. Morgan, H. J. Stewart and R. Mirsky, 1990, "Three markers of adult non-myelin-forming Schwann cells, 217c(Ran-1), A5E3 and GFAP: development and regulation by neuron-Schwann cell interactions", *Development*, Vol. 109, No. 1, pp. 91-103.

Jordanova, A., J. Irobi, F. P. Thomas, P. Van Dijck, K. Meerschaert and M. Dewil, 2006, "Disrupted function and axonal distribution ofmutant tyrosyl-tRNA synthetase in dominant intermediate Charcot-Marie-Tooth neuropathy", *Nature Genetics*, Vol. 38, No. 2, pp. 197–202.

Joseph, L. J., M. M. Le Beau, GA. Jr. Jamieson, S. Acharya, T. B. Shows and J. D. Rowley, 1988, "Molecular cloning, sequencing, and mapping of EGR2, a human early growth response gene encoding a protein with "zinc-binding finger" structure", *The Proceedings of the National Academy of Sciences*, Vol. 85, No. 19, pp. 7164–7168.

Fischbeck K.H., N. ar.-Rushdi, M. Pericak-Vance, M. Rozear, A.D. Roses and J.P. Fryns, 1986, "X-linked neuropathy: gene localization with DNA probes", *Annals of Neurology*, Vol. 20, No. 4, pp. 527–532.

Kamholz, J., D. Menichella, A. Jani, J. Garbern, R. A. Lewis, K. M. Krajewski, J. Lilien, S. S. Scherer and M. E. Shy, 2000, "Charcot-Marie-Tooth disease type 1 molecular pathogenesis to gene therapy", *Brain*, Vol. 123, No. 2, pp. 222-233.

Kelsell, D. P., J. Dunlop, H. P. Stevens, N. J. Lench, J. N. Liang, G. Parry, R. F. Mueller and I. M. Leigh, 1997, "Connexin 26 mutations in hereditary non-syndromic sensorineural deafness", *Nature*, Vol. 387, No. 6628, pp. 80-83.

Kennerson, L., T. Warburton, E. Nelis, M. Brewer, P. Polly, P. De Jonghe, V. Timmerman, and G. A. Nicholson, 2007, "Mutation scanning the GJB1 gene with high-resolution melting analysis: implications for mutation scanning of genes for Charcot-Marie-Tooth disease", *Clinical Chemistry*, Vol. 53, No. 2, pp. 349-352.

Kim, H. J., S. H. Hong, C. S. Ki, B. J. Kim, J. S. Shim, S. H. Cho, J. H. Park, and J. W., 2005, "A novel locus for X-linked recessive CMT with deafness and optic neuropathy maps to Xq21.32-q24", *Neurology*, Vol. 64, No. 11, pp. 1964-1967.

Kim, H. J., K. M. Sohn, M. E. Shy, K. M. Krajewski, M. Hwang, J. H. Park, S. Y. Yang, H. H. Won, B. O. Choi, S. H. Hong, B. J. Kim, Y. L. Suh, C. S. Ki, S. Y. Lee, S. H. Kim, and J. W. Kim, 2007, "Mutations in *PRPS1*, which encodes the phosphoribosyl pyrophosphate synthetase enzyme critical for nucleotide biosynthesis, cause hereditary peripheral neuropathy with hearing loss and optic neuropathy (CMTX5)", *American Journal of Human Genetics*, Vol. 81, No. 3, pp. 552-558.

Kirchhoff, S., E. Nelles, A. Hagendorff, O. Kruger, O. Traub and K. Willecke, 1998, "Reduced cardiac conduction velocity and predisposition to arrhythmias in connexin40-deficient mice", *Current Biology*, Vol. 8, No. 5, pp. 299–302.

Kleopa, K. A., and S. S. Scherer, 2002, "Inherited neuropathies". *Clinical Neurology and Neurosurgery*, Vol. 20, No. 3, pp. 679–709.

Kochanski, A., 2006, "How to asses the pathogenicity of mutations in Charcot-Marie-Tooth disease and other diseases", *Journey of Applied Genetics*, Vol. 47, No. 3, pp. 255-260.

Kuhlenbaumer, G., P. Young, G. Hunermund, B. Ringelstein and F. Stogbauer, 2002, "Clinical features and molecular genetics of hereditary peripheral neuropathies", *Journal of Neurology*, Vol. 249, No. 12, pp. 1629–1650.

Kukita, Y., T. Tahira, S. S. Sommer, and K. Hayashi, 1997, "SSCP analysis of long DNA fragments in low pH gel", Human Mutation, Vol. 10, No. 5, pp. 400-407.

Kumar, N. M. and N. B. Gilula, 1996, "The gap junction communication channel", *Cell*, Vol. 84, No. 3, pp. 381-388.

Kunzelmann, P., I. Blumcke, O. Traub, R. Dermietzel, and K. Willecke, 1997, "Coexpression of connexin45 and -32 in oligodendrocytes of rat brain", *Journal of Neurocytology*, Vol 26, No. 1, pp.17–22.

Kwon, J. M., J. L. Elliott, W. C. Yee, J. Ivanovich, N. J. Scavarda and P. J. Moolsintong, 1995, "Assignment of a second Charcot- Marie-Tooth type II locus to chromosome 3q", *The American Journal of Human Genetics*, Vol. 57, No. 4, pp. 853–858.

Le Douarin, N. M. and E. Dupin, 1993, "Cell lineage analysis in neural crest ontogeny", *Journal of Neurobiology*, Vol. 24, No. 2, pp. 146-161.

Liew, M., R. Pryor, R. Palais, C. Meadows, M. Erali, E. Lyon and C. Wittwer, 2004, "Genotyping of single-nucleotide polymorphisms by high-resolution melting of small amplicons", *Clinical Chemistry*, Vol. 50, No. 7, pp. 1156-1164.

Loewenstein, W. R., 1981, "Junctional intercellular communication: the cell-to-cell membrane channel", *Physiological Reviews*, Vol. 61, No. 4, pp. 829- 913.

lonasescu, V. V., T. Jonathan, J. L. Haines, A. M. Summers, R. Lonasescu and C. Searby, 1991, "Heterogeneity in X-linked recessive Charcot-Marie-Tooth neuropathy", *American Journal of Human Genetics*, Vol. 48, No. 6, pp. 1075-1083.

Luming, Z., L. Wang, R. Palais, R. Pryor and C. T. Wittwer, 2005, "High-resolution DNA melting analysis for simultaneous mutation scanning and genotyping in solution", *Clinical Chemistry*, Vol. 51, No. 10, pp. 1770-1777.

Mackay, D., A. Ionides, Z. Kibar, G. Rouleau, V. Berry, A. Moore, A. Shiels and S. Bhattacharya, 1999, "Connexin46 mutations in autosomal dominant congenital cataract", *American Journal of Human Genetics*, Vol. 64, No. 5, pp. 1357-1364.

Maier, M., P. Berger and U. Suter, 2002, "Understanding Schwann cell-neurone interactions: the key to Charcot-Marie-Tooth disease?", *Journal of Anatomy*, Vol. 200, No. 4, pp. 357-366.

Marrosu M.G, S. Vaccargiu, G. Marrosu, A. Vannelli, C. Cianchetti and F. Muntoni, 1998, "Charcot-Marie-Tooth disease type 2 associated with mutation of the myelin protein zero gene", *Neurology*, Vol. 50, No. 5, pp. 1397-1401.

Martini, R. and M. Schachner, 1997, "Molecular bases of myelin formation as revealed by investigations on mice deficient in glial cell surface molecules", *Glia*, Vol. 19, No. 4, pp. 298-310.

Mastaglia, F. L., K. J. Nowak, R. Stell, B. A. Phillips, J. E. Edmondson and S. M. Dorosz, 1999, "Novel mutation in the myelin protein zero gene in a family with intermediate hereditary motor and sensory neuropathy", *The Journal of Neurology, Neurosurgery, and Psychiatry*, Vol. 67, No. 2, pp.174– 179.

Matsunami, N., B. Smith, L. Ballard, M.W. Lensch, M. Robertson, H. Albertsen, C.O. Hanemann, H.W. Müller, T.D. Bird and R. White, 1992, "Peripheral myelin protein-22 gene maps in the duplication in chromosome 17p11.2 associated with Charcot-Marie-Tooth 1A", *Nature Genetics*, Vol.1 No. 3, pp. 176-179.

Mersiyanova, I. V., A. V. Perepelov, A. V, Polyakov, V. F. Sitnikov, E. L. Dadali and R. B. Oparin, 2000, "A new variant of Charcot-Marie-Tooth disease type 2 is probably the result of a mutation in the neurofilament-light gene", *The American Journal of Human Genetics*, Vol. 67, No. 1, pp. 37–46.

Milks, L.C., N. M. Kumar, R. Houghten, N. Unwin and N. B. Gilula, 1988, "Topology of the 32-kd liver gap junction protein determined by site-directed antibody localizations", *The EMBO Journal*, Vol. 7, No. 10, pp. 2967-2975.

Nagarajan, R., J. Svaren, N. Le, T. Araki, M. Watson and J. Milbrandt, 2001, "EGR2 mutations in inherited neuropathies dominantnegatively inhibit myelin gene expression", *Neuron*, Vol. 30, No. 2, pp. 355–368.

Nelis, E., C. Van Broeckhoven, P. De Jonghe, A. Lofgren, A. Vandenberghe and P. Latour, 1996, "Estimation of the mutation frequencies in Charcot-Marie-Tooth disease type 1 and hereditary neuropathy with liability to pressure palsies: a European collaborative study", *European Journal of Human Genetics*, Vol. 4, No. 1, pp. 25–33.

Nelis, E., J. Berciano, N. Verpoorten, K. Coen, I. Dierick and V. Van Gerwen, 2004, "Autosomal dominant axonal Charcot-Marie-Tooth disease type 2 (CMT2G) maps to chromosome 12q12–q13.3", *Journal of Medical Genetics*, Vol. 41, No. 3, pp. 193–197.

Nicholson, G., and J. Nash, 1993, "Intermediate nerve conduction velocities define X-linked Charcot–Marie–Tooth neuropathy families", *Neurology***,** Vol.43, No. 12, pp. 2558–2564.

Niemann A, P. Berger, U. Suter, 2006, "Pathomechanisms of mutant proteins in Charcot-Marie-Tooth Disease", *NeuroMolecular Medicine*, Vol. 8, No. 1-2, pp. 217–242.

Orita, M., H. Iwahana, H. Kanazawa, K. Hayashi, and T. Sekiya, 1989, "Detection of polymorphisms of human DNA by gel electrophoresis as single-strand conformation polymorphisms", *Proceedings of the National Academy of Sciences of the USA*, Vol. 86, No. 8, pp. 2766-2770.

Palais, R., M. A. Liew and C. T. Wittwer, 2005, "Quantitative heteroduplex analysis for single nucleotide polymorphism genotyping", *Analytical Biochemistry*, Vol. 346, No. 1, pp. 167-175.

Patel, P.I., B.B. Roa, A.A. Welcher, R. Schoener-Scott, B.J. Trask, L. Pentao, G.J. Snipes, C.A. Garcia, U. Francke, E.M. Shooter, J.R. Lupski and U. Suter, 1992, "The gene for the peripheral myelin protein PMP-22 is a candidate for Charcot-Marie-Tooth disease type 1A", *Nature Genetics*, Vol. 1, No. 3, pp. 159-165.

Paul D.L., K. Yu, R. Bruzzone, R.L. Gimlich and D.A. Goodenough, 1995, "Expression of a dominant negative inhibitor of intercellular communication in the early Xenopus embryo causes delamination and extrusion of cells", *Development*, Vol. 121, No. 2, pp. 371-381.

Pedrola, L., A. Espert, X. Wu, R. Claramunt, M. E. Shy and F. Palu, 2005, "GDAP1, the protein causing Charcot-Marie-Tooth disease type 4A, is expressed in neurons and is associated with mitochondria", *Human Molecular Genetics*, Vol. 14, No. 8, pp. 1087–1094.

Poliak S and E. Peles, 2003, "The local differentiation of myelinated axons at nodes of Ranvier", *Nature Reviews Neuroscience*, Vol. 4, No. 12, pp. 968-980.

Priest, J. M., K. H. Fishbeck, N. Nouri, and B.J. Keats, 1995, "A Locus for axonal motor-sensory neuropathy with deafness and mental retardation maps to Xq24-q26", *Genomics*, Vol. 29, No. 2, pp. 409-412.

Raeymaekers, P, V. Timmerman, P. De Jonghe, L. Swerts, J. Gheuens, J.J. Martin, L. Muylle, G. De Winter, A. Vandenberghe and C. Van Broeckhoven, 1989, "Localization of the mutation in an extended family with Charcot-Marie-Tooth neuropathy (HMSN I)", *The American Journal of Human Genetics*, Vol. 45, No. 6, pp. 953-958.

Rautenstrauss, B., A. Leal, K. Huehne, F. Bauer, H. Sticht and P. Berger, 2005, "Positional cloning of the CMT2B2 gene and its implications for CMT1A", Meeting of the peripheral Nerve Society, Tuscany, Italy. *Journal of the Peripheral Nervous System*, Vol.10, No.1, pp. 77.

Reaume, A.G., P.A. De Sousa, S. Kulkarni, B. L. Langille, D. Zhu, T. C. Davies, S. C. Juneja, G. M. Kidder and J. Rossant, 1995, "Cardiac malformation in neonatal mice lacking connexin43", *Science*, Vol. 267, No. 5205, pp. 1831–1834.

Ressot, C., D. Gome` s, A. Dautigny, D. Pham-Dinh and R. Bruzzone, 1998, "Connexin32 mutations associated with X-linked Charcot–Marie–Tooth disease show two distinct behaviors: loss of function and altered gating properties", *The Journal of Neuroscience*, Vol. 18, No. 11, pp. 4063-4075.

Ressot, C., and R. Bruzzone, 2000, "Connexin channels in Schwann cells and the development of the X-linked form of Charcot-Marie-Tooth disease", *Brain Research Brain Research Reviews*, Vol. 32, No.1, pp. 192-202.

Roa, B. B., C. A. Garcia, U. Suter, D. A. Kulpa, C. A. Wise, J. Mueller, A. A. Welcher, G. J. Snipes, E. M. Shooter, P. I. Patel and J. R. Lupski, 1993, "Charcot-Marie-Tooth disease type 1A. Association with a spontaneous point mutation in the PMP22 gene" *The New England Journal of Medicine*, Vol. 329, No. 2, pp. 96-101.

Rosenberg, R. N., and A. Chutorian, 1967, "Familial opticoacoustic nerve degenaration and polyneuropathy", *Neurology*, Vol. 17, pp. 827-832

Rummler, L. S., P. T. Dihn and R. Gupta, 2004, "The anatomy and biochemistry of myelin and myelination", *Operative Techniques in Orthopaedics*, Vol. 14, No. 3, pp. 146-152.

Sanders, S., G. A. Nicholson, R. A. Ouvrier, J. G. McLeod and J. D. Pollard, 1998, **"**Charcot-Marie-Tooth Disease: Histopathological features of the peripheral myelin protein (PMP22) duplication (CMT1A) and Connexin32 mutations (CMTX1)", *Muscle and Nevre*, Vol. 21, pp. 217-225.

Scherer, S. S., S. M. Deschenes, Y. T. Xu, J. B. Grinspan, K. H. Fischbeck and D.L. Paul, 1995, "Connexin32 is a myelin-related protein in the PNS and CNS", *The Journal of Neuroscience*, Vol. 15, No. 12, pp. 8281– 8294.

Scherer, S. S., 1997(A), "The biology and pathobiology of Schwann cells", *Current Opinion in Neurology*, Vol. 10, pp. 386-397.

Scherer, S. S., Y. T. Xu, E. Nelles, K. Fischbeck, K. Willecke and L. J. Bone, 1997(B), "Connexin32-null mice develop a demyelinating peripheral neuropathy", *Glia*, Vol. 24, No. 1, pp. 8-20.

Scherer, G., M. Held, M. Erdel, D. Meschede, J. Horst, R. Resniewicz and A. T. Midro, 1998, "Three Nnovel SRY mutations in XY gonadal dysgenesis and the enigma of XY gonadal dysgenesis cases without SRY mutations", *Cytogenetics and Cell Genetics*, Vol. 80, No. 1-4, pp. 188-192.

Scherer, S. S. and J. L., Salzer, 2001, "Axon-Schwann cell interactions during peripheral nevre degeneration", *Glial Cell Development*, Oxford, Oxford University Pres,

Shiels, A., D. Mackay, A. Ionides, V. Berry, A. Moore and S. Bhattacharya, 1998, "A missense mutation in the human connexin50 gene (GJA8) underlies autosomal dominant 'zonular pulverulent' cataract, on chromosome 1q", *American Journal of Human Genetics*, Vol. 62, No. 3, pp. 526-532.

Simon, A. M., D. A. Goodenough and D. L. Paul, 1998, "Mice lacking connexin 40 have cardiac conduction abnormalities characteristic of atrioventricular block and bundle branch block", *Current Biology*, Vol. 8, No. 5, pp. 295–298.

Simon, A.M., D. A. Goodenough, E. Li and D. L. Paul, 1997, "Female infertility in mice lacking connexin 37", *Nature*, Vol. 385, No. 6616, pp. 525–529.

Sivakumar, K., T., Kyriakides, I., Puls, G. A Nicholson, B. Funalot and A. Antonellis, 2005, "Phenotypic spectrum of disorders associated with glycyl-tRNA synthetase mutations", *Brain*, Vol. 128, No.10, pp. 2304–2314.

Street, V. A., C. L. Bennett, J. D. Goldy, A. J. Shirk, K. A. Kleopa, B. L. Tempel, H. P. Lipe, S. S. Scherer, T. D. Bird and P. F. Chance, 2003, "Mutation of a putative protein degradation gene LITAF/SIMPLE in Charcot-Marie-Tooth disease 1C", *Neurology*, Vol. 60, No. 1, pp. 22-26.

Suter U and S. S. Scherer, 2003. "Disease mechanisms in inherited neuropathies", *Nature Reviews Neuroscience*, Vol. 4, No. 9, pp. 714–726.

Taira, M., T. Lizasa, K. Yamada, H. Shimada, and M. Tatibana, 1989, "Tissue-differential expression of two distinct genes for phosphoribosyl pyrophosphate synthetase and existence of the testis-specific transcript", *Biochimica et Biophysica Acta*, Vol. 1007, No.2, pp. 203-208

Tang, B. S., W. Luo, K. Xia, J. F. Xiao, H. Jiang and L. Shen, 2004, "A new locus for autosomal dominant Charcot-Marie-Tooth disease type 2 (CMT2L) maps to chromosome 12q24", *Human Genetics*, Vol. 114, No. 6, pp. 527–533.

Taylor, C. F., M. Harland, R. Charlton and G. R. Taylor, 2003, "Evaluation of high-resolution melting curve analysis as a high-throughput mutation scanning tool", *Clinical Chemistry*, Vol. 49, No. 6, pp. 853-860.

Timmerman, V., E. Nelis, W. Van Hul, B.W. Nieuwenhuijsen, K.L. Chen, S. Wang, K. Ben Othman, B. Cullen, R.J. Leach and C.O. Hanemann, 1992, "The peripheral myelin protein gene PMP-22 is contained within the Charcot-Marie-Tooth disease type 1A duplication", *Nature Genetics*, Vol. 1, No. 3, pp. 171-175.

Tooth, H. H., 1886, *The peroneal type of progressive muscular atrophy*, Ph.D Thesis, H. K. Lewis, London.

Topilko, P., S. Schneider-Maunoury, G. Levi, A. Baron-Van Evercooren, A. B. Chennoufi and T. Seitanidou, 1994, "Krox- 20 controls myelination in the peripheral nervous system", *Nature*, Vol. 371, No. 6500, pp. 796–799.

Valentijn, L. J., F. Baas, R. A. Wolterman, J. E. Hoogendijk, N. H. Van Den Bosch, I. Zorn, A. W. Gabreels-Festen, M. De Visser and P. A. Bolhuis, 1992, "Identical point mutations of PMP22 in trembler-j mouse and Charcot-Marie-Tooth type 1A ", *Nature Genetics*, Vol. 2, No. 4, pp. 288-291.

Vance, J. M., G. A. Nicholson, L. H. Yamaoka, J. Stajich, C. S. Stewart, M. C. Speer, W. Y. Hung, A. D. Roses, D. Barker and M. A. Pericak-Vance, 1989, "Linkage of Charcot-Marie-Tooth neuropathy type 1A to chromosome 17", *Experimental Neurology*, Vol. 104, No. 2 pp. 186-189.

Vaughn, C. P. and K. S. Elenitoba-Johnson, 2004, "High-resolution melting analysis for detection of internal tandem duplications", *The* Journal *of molecular diagnostics: JMD*, Vol. 6, No. 3, pp. 211-216.

Verhoeven, K., M. Villanova, A. Rossi, A. Malandrini, P. De Jonghe and V. Timmerman, 2001, "Localization of the gene for the intermediate form of Charcot-Marie-Tooth to chromosome 10q24.1– q25.1", *The American Journal of Human Genetics*, Vol. 69, No. 4, pp. 889–894.

Verhoeven, K., P. De Jonghe, K. Coen, N. Verpoorten, M. Auer-Grumbach and J. M. Kwon, 2003, "Mutations in the small GTP-ase late endosomal protein RAB7 cause Charcot-Marie-Tooth type 2B neuropathy", American Journal of Human Genetics, Vol. 72, No. 3, pp. 722-727.

Warner, L. E., P. Mancias, I. J. Butler, C.M. McDonald, L. Keppen, K. G. Koob and J. R. Lupski, 1998, "Mutations in the early growth response 2 (EGR2) gene are associated with hereditary myelinopathies", *Nature Genetics*, Vol. 18, No. 4, pp. 382-384.

Webster, H. de F., P. J. Dyck, P. K. Thomas, J. W. Griffin, P. A. Low and J. F. Poduslo (eds.), 1993, "Development of peripheral nerve fibers", in, *Peripheral Neuropathy*, pp. 243-266.

Wise, C. A., C. A. Garcia, S. D. Davis, Z. Heju, L. Pentao, P. I. Patel and J. R. Lupski, 1993, "Molecular analysis of unrelated Charcot-Marie-Tooth Disease patients suggest a high frequency the CMT1A duplication", *American Journal of Human Genetics*, Vol. 53, No. 4, pp. 853-863.

Wittwer, C. T., G. H. Reed, C. N. Gundry, J. G. Vandersteen and R. J. Pryor, 2003, "High-resolution genotyping by amplicon melting analysis using LCGreen", *Clinical Chemistry*, Vol. 49, No. 6, pp. 853-860.

Xia, J. H., C. Y. Liu, B. S. Tang, Q. Pan, L. Huang, H. P. Dai, B. R. Zhang, W. Xie, D. X. Hu, D. Zheng, X. L. Shi, D. A. Wang, K. Xia, K. P. Yu, X. D. Liao, Y. Feng, Y. F. Yang, J. Y. Xiao, D. H. Xie and J. Z. Huang, 1998, "Mutations in the gene encoding gap junction protein beta-3 associated with autosomal dominant hearing impairment", *Nature Genetics*, Vol. 20, No. 4, pp. 370-373.

Young, P. and U. Suter, 2003, "The causes of Charcot-Marie-Tooth disease", *Cellular and Molecular Life Sciences*, Vol. 60, No. 12, pp. 2547-2560.

Yum, S. W., K. A. Kleopa, S. Shumas, and S. S. Scherer, 2002, "Diverse trafficking abnormalities of connexin 32 mutants causing CMTX", *Neurobiology of Disease*, Vol. 11, No. 1, pp. 43-52.

Zhao, C., J. Takita, Y. Tanaka, M. Setou, T. Nakagawa and S. Takeda, 2001, "Charcot-Marie-Tooth disease type 2A caused by mutation in a microtubule motor KIF1Bbeta", *Cell*, Vol. 105, No. 5, pp. 587– 597.

Züchner, S., M. Noureddine, M. Kennerson, K.Verhoeven, K. Claeys and P. De Jonghe, 2005, "Mutations in the pleckstrin homology domain of dynamin 2 cause dominant intermediate Charcot-Marie-Tooth disease", *Nature Genetics*, Vol. 37, No. 3, pp. 289– 294